Analytical Methods

Accepted Manuscript

This article can be cited before page numbers have been issued, to do this please use: E. Bolea, M. S. Jimenez, J. Perez-Arantegui, J. C. Vidal, M. Bakir, K. Ben-Jeddou, A. C. Giménez, D. Ojeda, C. Trujillo and F. Laborda, *Anal. Methods*, 2021, DOI: 10.1039/D1AY00761K.

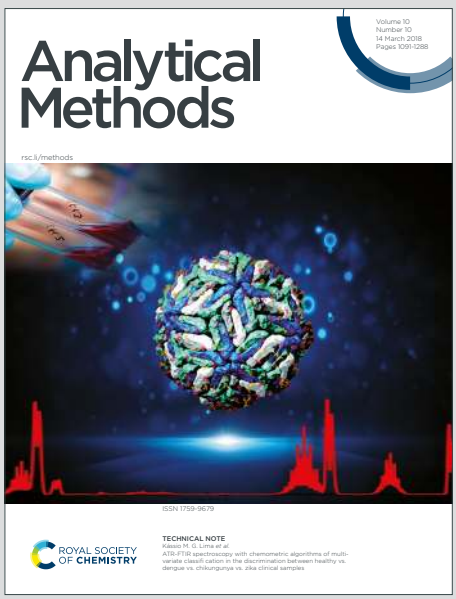

ROYAL SOCIETY OF CHEMISTRY

rsc.li/methods

View Article Online
DOI: 10.1039/D1AY00761K

Analytical applications of single particle inductively coupled plasma mass spectrometry: A comprehensive and critical review

Received 00th January 20xx,
Accepted 00th January 20xx

DOI: 10.1039/x0xx00000x

Eduardo Bolea, Maria S. Jimenez, Josefina Perez-Arantegui, Juan C. Vidal, Mariam Bakir, Khaoula Ben-Jeddou, Ana C. Gimenez-Ingalaturre, David Ojeda, Celia Trujillo and Francisco Laborda*

Single particle inductively coupled plasma mass spectrometry (SP-ICP-MS) refers to the use of ICP-MS as a particle counting technique. When ICP-MS measurements are performed at very high data acquisition frequencies, information about (nano)particles containing specific elements and their dissolved forms can be obtained (element mass per particle, size and number and mass concentrations). As a result of its outstanding performance, SP-ICP-MS has become a relevant technique for the analysis of complex samples containing inorganic nanoparticles. This review discusses the maturity level achieved by the technique through the methods developed for the detection, characterisation and quantification of engineered and natural (nano)particles. The application of these methods in different analytical scenarios is comprehensively reviewed and critically discussed, with special attention to their current technical and metrological limitations. The emergent applications of SP-ICP-MS in the field of nanoparticle-tagged immunoassay and hybridization methods are also reviewed.

SP-ICP-MS: A fast-developing technique

The use of inductively coupled plasma mass spectrometers in single particle mode has led to the emergence of a particle counting technique known as single particle inductively coupled plasma mass spectrometry (SP-ICP-MS). Although the origins of the technique can be traced back to the 1970's,[1] a series of key papers by Degueldre et al.,[2–6] published between 2003 and 2006, are considered its starting point. However, the application of SP-ICP-MS to the analysis of engineered nanomaterials,[7,8] followed by its implementation in commercial ICP-MS instruments,[9–11] became the main driving force behind the success of the technique in recent years.

Figure 1

Fig. 1 Comparison of the evolution of SP-ICP-MS with respect to ICP-MS (adapted from Horlick[12]).

The birth and evolution of SP-ICP-MS resembles that of the ICP-MS technique itself (Fig. 1). After their initial conception, it took some time to get the first ICP-MS research instrument, as well as the first application to nanomaterials in the case of SP-ICP-MS. But from then on, it took only about three years for manufacturers to launch the first commercial ICP-MS instruments, or the first dedicated instruments in the case of SP-ICP-MS. Thereafter, conventional ICP-MS evolved in a fast way, becoming a mature technique in about ten years.[12] According to Horlick, a mature technique is characterised by the fact that their methods are applied to a wide range of analytical problems and determinations, and become established as a routine tool with broad commercialisation. Before the maturity stage, a technique goes through a characterisation stage, a period of intense research activity aimed at achieving a complete picture of the technique at instrumental, metrological and methodological levels. On the other hand, during the characterisation stage the new technique seems to have no limits and to be able to solve all the problems, whereas with maturity comes the realization that not all is ideal and there are a number of problems that will not be solved. In the case of SP-ICP-MS, the question is whether the technique can be considered to have reached maturity or is still in the characterisation phase. The final aim of this comprehensive review is to gather the publications involving SP-ICP-MS and critically evaluate the current state of the technique, its limitations and its level of maturity level. Special attention is paid to the problem-solving analytical methods developed and their application under different relevant analytical scenarios.

Basic principles

When an ICP-MS instrument is used at very high reading frequencies, ICP-MS becomes a particle counting technique, being able to deliver information in a particle-by-particle basis. The basics of SP-ICP-MS measurements were established by Degueldre et al.[2] Basically, when a diluted suspension of nanoparticles is nebulized into an ICP-MS, and an isotope of the element present in the nanoparticles is measured at acquisition frequencies over ca. 100 Hz, a series of events corresponding to individual nanoparticles are recorded over a continuous baseline. The intensity of these events is related to the mass of the element

Group of Analytical Spectroscopy and Sensors (GEAS), Institute of Environmental Sciences (IUCA), University of Zaragoza, Pedro Cerbuna 12, 50009, Zaragoza, Spain.
* Corresponding author.

in the nanoparticle, and hence to its size if additional information about the composition, shape and density of the nanoparticle are available, whereas the frequency of events is proportional to the number concentration of nanoparticles. Subsequently, Laborda et al.[7] revealed that information about dissolved forms of the element measured could also be obtained from the baseline. Whereas the dissolved species are homogeneously distributed in all the aerosol droplets, the nanoparticles are present randomly in some of them. Thus, a constant signal (baseline) is produced by the dissolved species, whereas the nanoparticles give rise to individual signal events, as it can be seen in a typical time scan (Fig. 2.a).

As the SP-ICP-MS measurements are performed in time resolved mode, the data acquisition frequency (or the number of events along a fixed acquisition time), controlled through the dwell time of the instrument, is one of the most relevant parameters. Considering that the ion cloud generated in the plasma from a single nanoparticle can be detected during 300–1000 µs,[13,14] nanoparticle events can be recorded in two different forms, depending on the dwell time selected. When using dwell times in the millisecond range (3–10 ms), larger that the duration of the ion cloud in the instrument, events are recorded as one-reading signals (pulses), whereas for dwell times in the microsecond range (10–200 µs), they are recorded as peaks (transient signals), comprising several readings (see the insets in Fig. 2.a). For pulses, the intensity event is given by the reading itself, whereas for peaks, the intensity is calculated as the sum of the individual readings along it. With respect to the acquisition frequency, it is worth to mention that the commercial launch of SP-ICP-MS in 2014 was linked to quadrupole spectrometers with higher reading frequencies, allowing dwell times down to 10 µs,[10] instead of just working at milliseconds. In the meantime, time-of-flight[9] and double focussing[11] spectrometers have become commercially available with minimum dwell times of 33 and 10 µs, respectively.

Raw data from both milli- and microsecond time scans can be processed by plotting the event intensity vs. the number of events, obtaining histograms as shown in Fig. 2.b, where the first distribution is due to the background and/or the presence of dissolved forms of the element measured and the second to the nanoparticles themselves. The second distribution is further processed to convert the event intensities to mass of element per nanoparticle or size distributions (Fig. 2.c). Instrumental and metrological issues related to measurements, data acquisition and data processing have been summarized and described in detail in a number of reviews[1,15–18] and articles therein. It is worth to mention that the different types of quantitative information on nanoparticles achievable by SP-ICP-MS, and discussed in the next section, require different calibrations with nanoparticle size and number concentration standards. If size standards of the particles under study are not available, indirect calibrations based on the use of dissolved standards are usually applied. In these cases, sample introduction flow rate and the analyte nebulization efficiency have to be known to determine the mass of element per nanoparticle and hence the nanoparticle size. The analyte nebulization efficiency is commonly determined using the methods developed by Pace et al.[8] An overview of calibration issues in SP-ICP-MS can be found in Laborda et al.[19]

Figure 2

Fig. 2 (a) Time scan of suspension containing nanoparticles and dissolved forms of the same element. (b) Event intensity histogram of data from (a). (c) Mass per nanoparticle/size distribution of spherical nanoparticles calculated from the second intensity distribution in (b).

Analytical information: Analytes and measurands

The strength of SP-ICP-MS lies in the different types of analytical information that the technique can provide from very simple measurements. As we have seen above, two types of analytes are under the scope of SP-ICP-MS, namely (nano)particles and dissolved species. The term "nanoparticle" is going to be used here in a broad sense, although in most cases it will coincide with the ISO definition (nano-object with its three dimensions in the nanoscale, 1-100 nm).[20] Other nano-objects, like nanofibers/nanotubes or nanoplates (two and one dimensions in the nanoscale, respectively) may be suitable of being analysed by SP-ICP-MS, depending on the magnitude of the other dimensions that are not in the nanoscale. Thus, particles over 100 nm, even in the micrometre range, have been successfully analysed, although issues related to their nebulization and ionization must be considered.[21]

Table 1 Analytes, analytical information and measurands involved in SP-ICP-MS.

analytical information		analyte	measurand
qualitative	presence/absence	nanoparticle dissolved element	
quantitative content	concentration	nanoparticle	number concentration mass concentration of nanoparticulate element
	concentration	dissolved element	mass concentration of dissolved element
characterisation	element content	nanoparticle	element mass per particle
	size	nanoparticle	equivalent spherical diameter
	element content distribution	nanoparticle	histogram showing the number of particles for each of a number of defined element content per particle classes
	size distribution	nanoparticle	histogram showing the number of particles for each of a number of defined size classes

In any case, the information provided by SP-ICP-MS can be: (i) qualitative, about the presence of (nano)particulate and dissolved forms of specific elements; (ii) quantitative contents, as number and mass concentrations; and (iii) characterisation, about the mass of element/s per nanoparticle and nanoparticle size.

For dissolved species, the mass concentration of the element monitored is the measurand of interest, whereas for nanoparticles, the primary measurands of concern are the number concentration and the mass of element per particle. When additional information about the shape, composition and density of the particles is available, information about the size of the particles can be obtained. Nevertheless, a spherical shape is commonly assumed and the equivalent spherical diameter is the measurand usually reported. Any population of particles always exhibits more or less broad size distributions, recorded primarily by SP-ICP-MS as element content distributions, whose measurands are histograms showing the number of particles for each of a number of defined size or element content per particle classes, respectively. Table 1 summarises the quantitative and characterisation information with the corresponding measurands for each of the analytes involved in SP-ICP-MS. Qualitative information about the presence/absence of dissolved species and/or nanoparticles over a certain concentration and size cannot be disregarded because of the practical limitations of the technique when analysing complex samples, as it will be shown below. In addition, other types of information can be obtained from SP-ICP-MS measurements (e.g., porosity,[22] density,[23] aggregation,[24,25] agglomeration[26]), although they will not be discussed in detail.

Scientific production and evolution stage

Since the publication of the first article by Degueldre and Favarger in 2003, almost 400 studies directly related to SP-ICP-MS have been published in peer-reviewed journals until the end of 2020. These publications include a limited number of reviews, tutorials and divulgation articles; whereas most of them consists of articles on fundamentals and basic aspects of the technique, the development of methods, as well as their application. As it has been stated above, the analysis of engineered nanomaterials is behind the success of SP-ICP-MS, and most of the works deal with manufactured nanoparticles, although natural and incidental nanoparticles have also been analysed. SP-ICP-MS has proved its usefulness in other areas, like nanoparticle tag-based immunoassay and hybridization methods, as it will be discussed in a specific section.

The scientific production from 2003 to the end of 2020 has been organized in four fields, namely "Reviews", "Fundamentals", "Method Development" and "Applications". With respect to the "Reviews" field, one tutorial,[15] five reviews[1,16–18,27] and two divulgation articles[28,29] on the specific topic of SP-ICP-MS have been published to date. However, the technique is being included in most reviews on ICP-MS[30,31] or about the analysis of natural[32] or engineered[33–35] nanomaterials. The "Fundamentals" field covers publications whose main objective is the study of basic aspects of the technique (e.g., instrumentation, plasma processes, sample introduction, data acquisition and processing). All these studies have been performed with nanoparticle standards, although synthetic matrices have been considered in some cases, but always under controlled laboratory conditions. The "Method Development" field includes publications focused on the development of proofs-of-concept methods, based on the use of in-lab synthesized nanoparticles, nanoparticle standards or samples spiked with standards. When the method has been applied to samples containing original nanoparticles, it has been considered under the "Applications" field. Analysis of samples from laboratory tests (e.g., in vivo, in vitro, migration) involving nanoparticle standards have also been considered within this field, as it will be justified below.

Fig. 3 summarizes the distribution of publications in the four fields cited above directly related with the analysis of nanomaterials or samples containing nanomaterials, as well as their chronological evolution. The analysis of these data may give light about the maturity and the expected evolution of SP-ICP-MS. As it has been stated above, the rise of SP-ICP-MS publications started from 2011, with a constant increase in the total number of publications related to both "Fundamentals" and "Method Development" until 2016, showing some stabilization in recent years, whereas the number of publications about "Applications" is steadily growing. Following the evolution stages proposed by Horlick, and despite some overlap between them is unavoidable, the trend in publications suggests that SP-ICP-MS has passed the stage of characterisation and would be at the beginning of the maturity stage. However, other indicators than the extent of application of the technique, namely metrological indicators like method validation and traceability, should also be considered. While traceability of results is out of question in conventional ICP-MS because of the availability of validated methods, standards and reference materials,[36] this is not the case in SP-ICP-MS. As will be seen in the following sections, the number of SP-ICP-MS methods developed for the most diverse applications is increasing, although the number of validated ones is still limited. On the other hand, due to the special features of nanoparticles, the availability of standards and reference materials is still scarce, conditioning in the end the traceability of the results obtained.

Figure 3

Fig. 3 Evolution of SP-ICP-MS publications related to Reviews, Fundamentals, Method Development and Applications.

Analytical methods based on SP-ICP-MS: validation

In spite of the significant evolution of the technique discussed above, method validation in SP-ICP-MS is still at an early stage, lacking the harmonization of other fields in analytical chemistry, mainly because of the special features of nanoparticles as analytes. Whereas conventional analytes consist of identical entities (mostly atoms in ICP-MS) identified by their chemical composition (e.g., silver, titanium dioxide), identification of particles (e.g., 10 nm spherical silver or titanium dioxide nanoparticles) requires determining their chemical composition

but also their morphology (size and shape). This means that validation parameters, like limits of detection and quantification, working range, precision or trueness, must be applied to mass/number concentrations but also to particle size. With respect to size, it must keep in mind that particles always exhibit more or less broad size distributions, entailing that particles cannot be considered as truly identical entities. An additional drawback in relation to validation is the lack of certified reference materials for nanoparticles in any type of matrix, which forces to use recovery tests with matrix-free reference materials or properly characterised commercial nanoparticles for the evaluation of trueness. These recovery tests, based on the spike of nanoparticles, must test not only the recovery of the mass added, but also that the particle size and its distribution remain unchanged. For all these reasons, Linsinger at al.[37] proposed an adaptation of conventional validation schemes to the detection and quantification of engineered nanoparticles, although the number of validated methods already published is still scarce. In most cases, the scheme has been based on the addition of nanoparticles to different matrices, such as surface waters,[38] fruit juices,[39] chicken meat,[40] human liver and spleen tissues[41] or human blood.[42] In these cases, particle stability in the matrices has a strong influence on trueness and precision of the results, as it was reported for silver nanoparticles in chicken meat, since metallic nanoparticles were transformed into silver sulfide.[40] Only in a few cases, samples with nanoparticles originally present, such as Ag nanoparticles in confectionery,[43] have been described in validated methods. Finally, some methods for screening purposes have also been validated for detection of silver and gold nanoparticles in foods[44] and TiO_2 nanoparticles in confectionery products.[45]

Validation parameters commonly determined in these studies include trueness, selectivity, precision, detection limits, linearity and robustness.[37] The evaluation of trueness has been done mostly by spiking control samples with nanoparticle standards, ensuring that the particle size and size distribution remain unchanged, together with the recovery of the mass added. In general, larger bias, as high as +80% have been reported for number concentration compared to particle size, with bias around -20%.[19] Comparison with nominal median diameter and/or concentration of the standard added is the common rule, although the confirmation of the results by independent methods is highly recommended when possible. Thus, validation of the size characterisation has been performed by comparison with electron microscopy techniques (TEM or SEM), such in the characterisation of a series of TiO_2 materials used as food additives[46] or with the gold nanoparticle reference material RM8012,[47] showing differences on size distributions.

Selectivity has been evaluated considering possible (poly)atomic interferences[38,40,41] and other matrix constituents, which may cause changes in nebulization efficiency or in the ionization, affecting to particle concentration and size, respectively.[48] In any case, the effect of other nanoparticles or nanoparticles of the same composition but with different properties (size, coating...) should also be evaluated.

Respect to precision, determination of the nanoparticle number concentration is usually less precise than size determination, with reproducibility that reach up to 90% in some cases.[49] Data processing, is the driving factor in this parameter over sample preparation or sample dilution, especially at high baseline levels that make discrimination of nanoparticle readings more difficult.[43] It should be noted that satisfactory results have been obtained when comparing the repeatability and reproducibility obtained with the values predicted by the Horwitz ratio in the analysis of TiO_2 particles at concentration levels in the order of 0.01 mg Ti kg^{-1}.[41]

Despite there are not expressions widely accepted for the calculation of the limits of detection in the different domains covered by SP-ICP-MS, Laborda et al.[17] have proposed a harmonizing approach to calculated LODs for validation purposes. Most widely applied criteria for calculation of size detection limits are based on the use of multiples of the baseline standard deviation (n-sigma criterion). Multiples from 3- to 8-sigma criteria can be found in SP-ICP-MS publications,[41] although the use of 5-sigma criteria has been justified by these authors[17] on a routine basis. In general, size LODs depend on different factors, such as the concentration of the dissolved element, the strategy used for substracting the baseline signal to the particle signal or the type of mass spectrometer.[45] A comprehensive list of size LODs for metallic and oxide nanoparticles using a commercial quadrupole instrument under typical experimental conditions can be found in Laborda et al.[17] Size LODs around 10 nm and larger were obtained for most common nanoparticles at 100 µs dwell times. Incomplete vaporization of large particles in the plasma can limit the linearity of the size measurement ranges, hence larger particles, in the micrometre range, can produce signals outside the linear range of the detector.[50] For instance, a linear size range up to 150 nm has been reported for gold nanoparticles, whereas for SiO_2 it can increase up to 1000 [51] or 2000 nm.[50] Besides, particles larger than 2-5 µm are transported into the plasma with lower efficiency.

With respect to the number concentration LOD, it depends on the number of particles events detected in the blank, the sample introduction to the ICP-MS and the acquisition time. The use of conventional procedures for concentration LOD based on the blank standard deviation as in size LOD results in unrealistic values[9,42] and therefore, they cannot be used interchangeably. LOD values of 100 particles per mL have been reported[17] with acquisition times of 60 s, using a cyclonic spray chamber and a concentric nebulizer. The number concentration measurement range is limited by the occurrence of multiple particle events, which cause a progressively loss of linearity. The occurrence of events due to two or more nanoparticles is predicted by Poisson statistic and is expected to be significant, depending on the nebulization system and the range of dwell times (milli or microseconds) used.[13] Linear ranges up to 10^7 L^{-1} can be achieved with conventional nebulization systems at millisecond dwell times, which can be increased one order of magnitude working at microsecond dwell times.

Robustness has been evaluated commonly by changing different parameters that affect the measurement results, such as sample pre-treatment or dilution factor,[40] although in some cases only

the element total concentration has been considered for robustness evaluation.[41]

Other studies have included quality control procedures, such as the evaluation of trueness by spiking nanoparticles standards to natural matrix samples, considering that conventional procedures cannot be directly applied in SP-ICP-MS analysis due to the limitations described above. Thus, trueness has been evaluated by measuring recovery of the spiked nanoparticles, mainly based on number concentration, and the use of alternative techniques to confirm size results, such as for the sizing and quantification of Ag nanoparticles in food simulants,[52] moisturizing creams,[53] fish tissue,[54] or ZnO[55] and TiO_2 nanoparticles[56] in natural waters. This strategy has also been applied to the detection of naturally occurring iron oxide nanoparticles in crude oil and residual fuel oil by spiking in-lab synthesized silica-shelled Fe_3O_4 nanoparticles.[57] Alternatively, the agreement between the total element content determined by acid digestion and ICP-MS can be used for confirmation of the results, as in the determination of Ce, Cd and Pt-bearing nanoparticles in road runoff sediments[56] or Au nanoparticles in tumour cells after alkaline digestion.[58]

However, if the sample contains nanoparticles smaller than the LOD,[54–56] size information will be overestimated and number/mass concentration underestimated in consequence. In such situations, SP-ICP-MS should be restricted to confirm the presence of nanoparticles containing the element monitored over a certain equivalent diameter and concentration.

Applications of SP-ICP-MS: Analytical scenarios

In relation to the application of SP-ICP-MS to real-world analytical problems, Fig. 4 shows four different analytical scenarios that can be considered. Whereas the first one (type 0) corresponds to the analysis of pristine nanoparticles commonly produced at laboratory or industrial-scale, which just involves their characterisation, the other three correspond mainly to the needs of analytical information arising from the risk assessment of nanomaterials and nanoproducts in relation to environment, health and safety, as well as to legal regulations, which involve the detection, characterisation and/or quantification of nanoparticles in the presence of, more or less, complex matrices. Type 1 scenario includes the analysis of industrial and consumer products containing nanoparticles (e.g., cosmetics, textiles, polymers). Type 2 scenarios consider laboratory tests with pristine nanoparticles or products containing nanoparticles to assess their release, fate, and behaviour (2.1) as well as their (eco)toxicity in a variety of exposure conditions (e.g., environmental micro and mesocosms, migration in food simulants, gastrointestinal digestions, *in vitro* and *in vivo* (eco)toxicity test) (2.2). Finally, type 3 scenarios are related to the monitoring of the occurrence of nanoparticles in foods (3.1) environment (3.2) and organisms (3.3).

Leaving aside the scenario type 0, where the nanoparticles are the sample because of the lack of matrix, each of the three other scenarios involve samples containing nanoparticles and, in general terms, represent a progressive increase in analytical complexity, from the point of view of both the matrix and the decreasing concentrations.

Figure 4

Fig. 4 Analytical scenarios related to nanoparticles (adapted from Laborda et al.[59]).

The use and application of SP-ICP-MS methods has been organized according to the scenario classification presented in Fig. 4. Fig. 5 shows the distribution of the number of publications in relation to these different scenarios. The chart shows that two thirds of applications correspond to laboratory tests (scenario 2), whereas one fourth involves samples originally containing nanoparticles (scenario 3). The analysis of pristine nanomaterials (scenario 0) and products containing nanoparticles (scenario 1) account for 16%, most probably because they are usually analysed by other well-stablished techniques (e.g., electron microscopy, DLS). The following sections provide a detailed reviewing of the SP-ICP-MS application in the different scenarios considered.

Figure 5

Fig. 5 Distribution of publications (2011-2020) related to applications of SP-ICP-MS in different analytical scenarios.

View Article Online
DOI: 10.1039/D1AY00761K

Table 2 Scenario 0: Analysis of pristine nanoparticles.

sample	nanoparticle composition	sample preparation	dwell time	mass analyser	collision/ reaction cell gas	analytical information	measurands	complementary techniques	ref.
suspension	Ag	-	5 ms	Q	no	qualitative (NP)	NP size distribution	TEM DLS	60
	Ag	-	100 µs	Q	no	characterisation (NP) quantitative (NP) quantitative (DE)	NP mean size NP size distribution NP mass concentration DE mass concentration	TEM DLS	61
	Au@Ag (Ag shell)	-	50 µs	Q	no	characterisation (NP) quantitative (NP)	NP mean size NP size distribution NP number concentration	AF4-UV-vis	62
	Au-Ag alloy	-	6 ms 20 µs	Q	no	characterisation (NP)	molar ratios Au:Ag	-	63
	Au	-	100 µs	Q	no	characterisation (NP) quantitative (NP)	NP mean size NP number concentration	TEM	64
	Au (NP and nanorods)	-	6 ms 20 µs	Q	no	characterisation (NP)	NP mean size	TEM DLS UV-vis	65
	Au/polymer composite	-	100 µs	Q	no	characterisation (NP)	mean mass per NP NP mass distribution	ICP-MS TEM AF4-ICP-MS CFFF-ICP-MS	66
	CuO FeOOH	-	50 µs	DF	no	characterisation (NP)	NP mean size NP size distribution	SEM XRD DLS	67
	Ni	-	500 µs	Q	no	characterisation (NP) quantitative (NP) quantitative (DE)	NP mean size NP size distribution NP number concentration NP mass concentration DE mass concentration	SEM TEM XRD	68
	Pd	-	50 µs	Q	no	characterisation (NP)	NP mean size NP size distribution	SEM SAXS XRD	69
	$NaYF_4$ (Yb dopped) $NaYF_4$ (Er dopped) $NaGdF_4$ (Yb dopped) $NaGdF_4$ (Er dopped)	-	100 µs	Q	no	characterisation (NP)	NP size distribution	TEM XRD	70
powder	TiO_2	dispersion in 2% PVP	50 µs	Q	no	characterisation (NP) quantitative (DE)	NP mean size NP size distribution DE mass concentration	DLS TEM	71
	SiO_2/Pt	dispersion	10 ms	Q	He	characterisation (NP)	mean mass per NP	ICP-MS SEM-EDS TEM XPS	72
	CNT (trace metals)	dispersion in 1% Triton X-100	10 ms	Q	no	qualitative (NP) quantitative (NP)	- CNT number concentration	SEM-EDS NTA	73
	CNT (trace Y)	dispersion in 1% Na deoxycholate	100 µs	Q	no	qualitative (NP) quantitative (NP)	- CNT mass concentration	ICP-MS TEM	74

View Article Online
DOI: 10.1039/D1AY00761K

	TiO_2 (Mn)	-	100 µs	Q	no	characterisation (NP)	mean mass per NP NP mass distribution	NTA UV-vis SEM TEM SAM AES XPS XRD Raman	75
filters	Au	water extraction	100 µs	Q	no	characterisation (NP) quantitative (NP)	NP mean size NP size distribution NP mass concentration	HIM SEM-EDS XRD UV-vis	76

Table 3 Scenario 1: Analysis consumer and industrial products containing nanoparticles.

View Article Online
DOI: 10.1039/D1AY00761K

sample	nanoparticle composition*	sample preparation	dwell time	mass analyser	collision/ reaction cell gas	analytical information	measurands	complementary techniques	ref.
cosmetics									
sunscreen	TiO_2	dispersion in ethanol	50 µs	DF	no	characterisation (NP) quantitative (NP)	NP mean size NP size distribution NP number concentration NP mass concentration	-	77
	TiO_2	dispersion in 1% Triton X-100	100 µs	Q	no	characterisation (NP) quantitative (NP)	NP mean size NP size distribution NP number concentration NP mass concentration	ICP-MS SEM-EDS	78
	TiO_2	defatting with hexane + filtration	100 µs	Q	no	characterisation (NP) quantitative (NP) quantitative (DE)	NP mean size NP size distribution NP number concentration DE mass concentration	ICP-MS SEM TEM DLS AF4-MALS-ICP-MS	79
	TiO_2 ZnO	dispersion in 1% Triton X-100	-	-	-	characterisation (NP)	NP mean size	TEM-EDS XRD	80
	TiO_2 ZnO	dispersion in 1% Triton X-100	5 ms	Q	He	characterisation (NP) quantitative (NP)	NP mean size NP number concentration NP mass concentration	AF4-MALS-ICP-MS	81
lip balm	TiO_2	defatting with hexane + filtration	100 µs	Q	He	characterisation (NP)	NP size distribution	ICP-MS CE-ICP-MS	82
toothpaste	TiO_2	dispersion in 0.1% SDS	100 µs	Q	He	characterisation (NP)	NP size distribution	ICP-MS CE-ICP-MS	82
	TiO_2 Al_2O_3	H_2O_2 digestion + dilution in 0.1% SDS	10 ms	Q	no	characterisation (NP) quantitative (NP)	NP mean size NP size distribution NP number concentration	ICP-MS STEM-EDS DLS AF4-MALS-ICP-MS HDC-ICP-MS	83
sunscreen lip balm toothpaste creams shampoo	TiO_2	defatting with hexane dispersion in 0.1% SDS	100 µs	Q	no	characterisation (NP) quantitative (NP) quantitative (DE)	NP mean size NP size distribution NP number concentration DE mass concentration	ICP-MS ICP-OES DLS	84
moisturizing cream	Ag	dispersion in methanol	100 µs	Q	no	characterisation (NP) quantitative (NP)	NP mean size NP size distribution NP number concentration NP mass concentration	ICP-MS FESEM TEM	53
exfoliant	plastic polymers (C-)	dispersion in water	200 µs	Q	no	qualitive (NP)	-	FESEM	85
other consumer products									
antibacterial spray	Ag	-	3 ms	Q	no	qualitative (NP) qualitative (DE)	-	HPLC-ICP-MS TEM	86
	Ag	-	10 ms	Q	no	characterisation (NP)	NP mean size NP size distribution	ICP-MS	87
commercial sprays	Ag- Sn- Zn-	-	5 ms	Q	no	characterisation (NP)	NP mean size	ICP-MS DLS SEM-EDS TEM-EDS SMPS	88
food additives									

E174	Ag	ethanol wetting + dispersion in 0.05% BSA	3 ms	Q	no	characterisation (NP) quantitative (NP)	NP mean size NP size distribution NP number concentration NP mass concentration	TEM	43
E171	TiO_2	dispersion in water	3 ms	Q	NH_3	characterisation (NP) quantitative (NP)	NP mean size NP size distribution NP number concentration NP mass concentration	TEM-EDS HAADF-STEM-EDS	46
	TiO_2	dispersion in 0.05% BSA	3 ms	Q	no	characterisation (NP)	NP mean size NP size distribution	SEM NTA AF4-MALS AF4-ICP-MS	89
other materials									
steel	NbCN TiNbCN	extraction 0.5 M H_2SO_4/0.1% Disperbyk-2012 + centrifugation	1.8 ms	TOF	no	characterisation (NP)	NP size distribution mass per NP distribution	STEM	90
petroleum products	Fe_3O_4	dilution (o-xylene)	100 µs	Q	He	characterisation (NP) quantitative (NP) quantitative (DE)	NP mean size NP size distribution NP mass concentration DE mass concentration	ICP-OES TEM	57
asphaltene solutions	Mo- Fe-	dilution (o-xylene)	100 µs	Q	no	characterisation (NP) quantitative (NP) quantitative (DE)	NP mean size NP size distribution NP mass concentration DE mass concentration	ICP-MS	91
tattoo inks	Al_2O_3 TiO_2 Cu-	-	5 ms	Q	He	characterisation (NP)	NP mean size NP size distribution	TEM DLS AF4- MALS	92
	Ti- Al- Cr- Cu- Zn- Pb-	-	5 ms	Q	He	characterisation (NP) quantitative (NP)	NP mean size NP number concentration NP mass concentration	ICP-MS	93
homeopathic medicine	Cu	-	-	Q	-	qualitative (NP)	-	DLS NTA SEM-EDS	94

* M: nanoparticle with composition M. M-: nanoparticle containing element M

Table 4 Scenario 2.1: Laboratory tests involving pristine nanoparticles or products containing nanoparticles.

View Article Online
DOI: 10.1039/D1AY00761K

sample	nanoparticle composition*	sample preparation	dwell time	mass analyser	collision/ reaction cell gas	analytical information	measurands	complementary techniques	ref.
Release studies									
migration									
food containers	Ag-	migration: - 3% acetic acid - 50% ethanol	100 µs	Q	no	qualitative (NP)	-	ICP-MS SEM-EDS	95
	Ag-	migration: - 3% acetic acid - 10% ethanol	3 ms	Q	no	characterisation (NP) quantitative (NP) quantitative (DE)	NP mean size NP mass concentration DE mass concentration	ICP-MS TEM-EDS	9
	Ag-	migration: - water - 3% acetic acid - 10% ethanol - 90% ethanol	10 ms	Q	no	characterisation (NP) quantitative (NP) qualitative (DE)	NP mean size NP size distribution NP number concentration -	ICP-MS SEM-EDS	9
	Ag-	migration: - water - 3% acetic acid - 10% ethanol	3 ms	Q	no	characterisation (NP) quantitative (NP)	NP mean size NP size distribution NP number concentration	ICP-MS TEM-EDS	9
	clays (Al-)	migration: - 3% acetic acid - 10% ethanol	100 ms	Q	no	qualitative (NP)	-	ICP-MS SEM-EDS	9
	plastic polymers (C-)	water	200 µs	Q	no	qualitive (NP)	-	FESEM	85
food packaging films	Ag-	migration: - water - 3% acetic acid - 10% ethanol	5 ms	Q	no	characterisation (NP)	NP mean size NP size distribution	ICP-MS STEM-EDS	10
cookware	Al- Ti- Si-	migration in 3% acetic acid	3 ms	Q	H_2	characterisation (NP) quantitative (NP)	NP mean size NP number concentration	ICP-MS SEM-EDS	
consumer products									
baby products	Ag-	leaching in artificial saliva	3 ms	Q	no	characterisation (NP) quantitative (NP)	NP mean size NP size distribution NP number concentration	ICP-MS TEM-EDS	9
toothbrush	Ag-	leaching in tap water	3 ms	Q	no	characterisation (NP) quantitative (NP)	NP mean size NP size distribution NP number concentration NP mass concentration	ICP-MS TEM-EDS	1
dermal transfer from surfaces (keyboard and painted surface)	Ag- Cu-	wiping test (artificial sweat) + water extraction	100 µs	Q	no He	characterisation (NP) quantitative (NP)	NP mean size NP number concentration NP mass concentration	ICP-MS SEM-EDS TEM-EDS	10
plaster	Ag-	water extraction + filtration + CPE	10 ms	Q	no	quantitative (NP)	mass concentration NP	ICP-OES TXRF SEM-EDS	104
textiles	TiO_2	leaching in water	100 µs	Q	no	characterisation (NP) quantitative (NP)	NP mean size NP size distribution NP number concentration NP mass concentration	ICP-MS TEM-EDS	1
	Ag	leaching under washing conditions	5 ms	Q	no	characterisation (NP) quantitative (NP)	NP mean size NP size distribution NP mass concentration	ICP-MS SEM TEM-EDS XANES	106
washing machine effluent	Ag	-	4 ms 1 ms	DF	no	characterisation (NP) quantitative (NP)	NP mean size NP number concentration	ISE TEM-EDS NTA	107
industrial materials									

CNT polymer nanocomposite	CNT (trace Y)	leaching in water + surfactant stabilization	100 µs	Q	no	quantitative (NP)	NP number concentration	XPS ATR-FTIR FESEM	108
pigmented polyethyelene	Fe_2O_3	leaching in: - 0.05% SDS - water - hard EPA water - SRNOM migration in: - water - 3% acetic acid - 10% ethanol	5 ms	Q	H_2	characterisation (NP) quantitative (NP)	NP mean size NP number concentration	ICP-MS TEM AUC FTIR	109
ZnO doped polymers	ZnO	migration to: - orange juice - chicken meat + Tris-HCl extraction	3 ms	Q	no	characterisation (NP) quantitative (NP)	NP mean size NP size distribution NP number concentration NP mass concentration	FAAS TEM-EDS FTIR DLS	[illegible]
antifouling paint	Cu_2O	leaching in freshwater from painted surface	100 µs	Q	no	characterisation (NP)	NP size distribution	DLS XRD XPS SEM-EDS TEM-EDS	111
paint	TiO_2	leaching in rainwater/snow from painted surface + filtration	50 µs	DF	no	characterisation (NP) quantitative (NP)	NP mean size NP size distribution NP number concentration NP mass concentration	ICP-MS	1 2
	TiO_2	leaching in water from painted surface	100 µs	Q	no	-	-	SEM-EDS TEM HRTEM XRD UV-Vis XPS XRD	1 3
printed circuits	Ag	leaching in water	100 µs	Q	no	characterisation (NP)	NP mean size	SEM AFM AF4-ICP-MS	[illegible]
photovoltaic cells	Ag- Al- Cd- Mo- Se- Zn-	leaching in: - model freshwater - model seawater - model acidic rainwater	30 ms	Q	no	qualitative (NP)	-	ICP-MS	115
wood	Cu-	leaching in water	-	Q	no	characterisation (NP) quantitative (NP)	NP mean size NP size distribution NP number concentration	AAS ICP-OES SEM-EDS ATR-FTIR	1 6
leather	Ag	leaching in water	50 µs	Q	no	qualitative (NP)	-	XPS FESEM	[illegible]
paper	multielement	collection of airborne particles in filter + suspension in DMEM	-	Q	no	qualitative (NP)	-	SEM-EDS TEM-EDS	118
environmental samples									
road dust	Pt-	leaching in stormwater runoff	5 ms	Q	He	characterisation (NP) quantitative (NP)	NP mean size NP size distribution NP mass concentration	ICP-MS	116
mine tailings	Th- U-	leaching in different media + filtration	50 µs	DF	no	characterisation (NP) quantitative (NP) quantitative (DE)	NP mean size NP size distribution NP number concentration DE mass concentration	ICP-MS	120
Fate studies									
food simulants									
water acetic acid (3%) ethanol (10%)	Ag (spiked)	-	3 ms	Q	no	characterisation (NP) quantitative (NP)	NP mean size NP number concentration NP mass concentration	TEM AF4-MALS	121
water acetic acid (3%)	Ag (spiked)	-	3 ms	Q	no	characterisation (NP) quantitative (NP)	NP size distribution NP number concentration	ICP-MS	122

View Article Online
DOI: 10.1039/D1AY00761K

ethanol (10-50%) olive oil milk						quantitative (DE)	NP mass concentration DE mass concentration		
in vitro digestion									
gastric fluid	Au Ag ZnO CeO_2 (spiked)	gastric step	50 µs	Q	no	characterisation (NP) quantitative (NP) quantitative (DE)	NP mean size NP number concentration DE mass concentration	SEM	123
digestion fluids	Ag (spiked)	3-steps in vitro-human gastro-intestinal digestion	-	Q	no	characterisation (NP) quantitative (NP)	NP mean size NP size distribution NP number concentration	SEM-EDS TEM DLS	124
chicken meat (spiked)	Ag (spiked)	3-steps in vitro-human gastro-intestinal digestion	10 ms	Q	no	characterisation (NP) quantitative (NP) quantitative (DE)	NP mean size NP number concentration DE mass concentration	ICP-MS TEM-EDS	125
orange juice chicken meat	ZnO	3-steps in vitro-human gastro-intestinal digestion	3 ms	Q	no	characterisation (NP) quantitative (NP)	NP mean size NP size distribution NP number concentration NP mass concentration	FAAS TEM-EDS FTIR DLS	170
laundry process									
washing solutions	Ag (spiked)	-	3 ms	Q	no	characterisation (NP) quantitative (NP) quantitative (DE)	NP mean size NP size distribution NP number concentration DE mass concentration	STEM-EDS	126
waters									
synthetic moderately hard water + NOM	Pt (spiked)	-	50 µs	Q	no	characterisation (NP) quantitative (NP)	NP mean size NP size distribution NP number concentration	-	127
	Au@Ag (spiked)	-	100 µs	Q	no	characterisation (NP) quantitative (NP)	NP mean size NP size distribution NP number concentration	-	128
ozonized water	Ag (spiked)	-	5 ms	Q	no	characterisation (NP) quantitative (NP)	NP mean size NP size distribution NP number concentration	ICP-OES DLS	129
lake water	Ag (spiked)	-	5 ms	Q	no	characterisation (NP) quantitative (NP)	NP mean size NP size distribution NP number concentration	ICP-MS AF4-UV-vis	130
	Ag (lake spike)	-	5 ms	Q	no	characterisation (NP) quantitative (NP) quantitative (DE)	NP size distribution NP mass concentration DE mass concentration	ICP-MS	131
	Ag (lake spike)	-	10 ms	Q	no	characterisation (NP) quantitative (NP)	NP mean size NP size distribution NP number concentration NP mass concentration	ICP-MS CPE+ICP-MS AF4-ICP-MS	132
	Ag (lake spike)	-	50 µs	DF	no	characterisation (NP) quantitative (NP) quantitative (DE)	NP mean size NP size distribution NP number concentration DE mass concentration	ICP-MS DGT+ICP-MS	133
river water	Ag Ag_2S (spiked)	CPE	500 µs	Q	He	characterisation (NP)	NP mean size NP size distribution	HAADF-STEM-EDX	134
	Ag CeO_2 Fe_2O_3 (spiked)	digestion ($Na_4P_2O_7$)	50 µs	Q	no	characterisation (NP)	NP mean size NP size distribution	ICP-OES AF4-ICP-MS	135
	TiO_2 ZnO (spiked)	-	100 µs	Q	no	characterisation (NP) quantitative (NP) quantitative (DE)	NP mean size NP size distribution NP number concentration NP mass concentration DE mass concentration	-	136
	Au Ag (spiked)	fractions collected from HDC	3 ms	Q	no	characterisation (NP) quantitative (NP)	NP mean size NP number concentration	DLS AUC	137

fresh waters	Ag	-	10 ms	Q	no	characterisation (NP) quantitative (NP)	NP mean size NP mass concentration	AF4-ICP-MS	138
synthetic seawater	Au (spiked)	-	3 ms	Q	no	characterisation NP	size distribution	AF4-UV-vis DLS	139
seawater	Ag Ag_2S AgCl (spiked)	CPE	500 µs	Q	He	characterisation (NP) quantitative (NP)	NP mean size NP size distribution NP number concentration	ICP-MS TEM-EDS	140
seawater	Ag (spiked)	-	10 ms	Q	no	characterisation (NP) quantitative (NP)	NP mean size NP number concentration NP mass concentration	TEM	141
seawater	Ag (spiked)	-	10 ms	Q	no	characterisation (NP)	NP mean size NP size distribution	-	142
waste water treatments									
synthetic wastewater	Ag (spiked)	SPE (Chelex-100)	100 µs	Q	no	characterisation (NP) quantitative (NP)	NP mean size NP size distribution NP mass concentration	NTA	143
	TiO_2 CeO_2 (spiked)	-	-	Q	no	qualitative (NP) qualitative (DE)	-	ICP-MS	144
	Fe + adsorbed Cd(II)	-	3 ms	Q	H_2 (MS/MS)	characterisation (NP) quantitative (NP)	NP mean size NP size distribution NP mass concentration	ICP-MS XRD	145
wastewater	Ag (spiked)	-	500 µs	Q	no	characterisation (NP)	NP size distribution	EDM-HSI DLS TEM	146
wastewater	Ag (spiked)	-	1 ms 100 µs	Q	no	characterisation (NP) quantitative (NP) quantitative (DE)	NP mean size NP number concentration DE mass concentration	TEM TOF-SIMS XPS UV-vis	147
wastewater	TiO_2 Ag (spiked)	-	3 ms	Q	no	characterisation NP	average size	ICP-MS STEM-EDS	148
wastewater river water	Au (spiked)	-	3 ms	Q	no	characterisation (NP)	NP mean size NP size distribution	-	149
wastewater river water	Ag (spiked)	centrifugation	10 ms	Q	no	characterisation (NP)	NP mean size NP size distribution	TEM-EDS DLS HDC-RI AF4-UV-vis-MALS-RI	150
wastewater river water	Ag (spiked)	HDC online separation	100 µs	Q	no	characterisation (NP) quantitative (NP)	NP mean size NP number concentration	HDC-ICP-MS	151
activated sludge	CNT (trace Y) (spiked)	centrifugation + ultrafiltration	10 ms	Q	no	quantitative (NP)	NP mass concentration	ICP-MS TEM-EDS	152
activated sludge	Ag	settling	100 µs	Q	no	characterisation (NP) quantitative (NP)	NP mean size NP size distribution NP mass concentration	-	153
biofilm reactor	Ag (spiked)	settling	100 µs	Q	no	characterisation (NP) quantitative (NP) quantitative (DE)	NP mean size NP mass concentration DE mass concentration	ICP-MS TEM-EDS	154
biofilm reactor	Ag (spiked)	settling	100 µs	Q	no	characterisation (NP) quantitative (NP) quantitative (DE)	NP mean size NP mass concentration DE mass concentration	ICP-MS TEM-EDS	155
drinking water treatments									
fresh water	Ag Au TiO_2 CeO_2 ZnO (spiked)	-	100 µs	Q	no	characterisation (NP) quantitative (NP)	NP mean size NP size distribution NP mass concentration	TEM-EDS	156

View Article Online
DOI: 10.1039/D1AY00761K

soils and sediments									
soil	Ag ZnO TiO_2 CeO_2 (spiked)	water extraction + centrifugation + filtration	10 ms	Q	no	characterisation (NP) quantitative (NP)	NP mean size NP size distribution NP mass concentration	SEM-EDS	156
	Ag (spiked)	water extraction + filtration + CPE	10 ms	Q	no	quantitative (NP)	mass concentration NP	ICP-OES TXRF SEM-EDS	104
	Ag (spiked)	- water extraction + centrifugation + filtration - extraction (DTPA 5mM) + centrifugation + filtration	10 ms	Q	no	qualitative (NP)	-	ICP-OES	157
	Ag (spiked)	extraction (2.5 mM $Na_4P_2O_7$)	50 µs	Q	no	characterisation (NP) quantitative (NP) quantitative (DE)	NP mean size NP number concentration NP mass concentration DE mass concentration	DLS TEM	103
	Ag (spiked)	extraction (2.5 mM $Na_4P_2O_7$) + settling	50 µs	Q	no	characterisation (NP) quantitative (NP)	NP mean size NP number concentration	ICP-MS	158
	Ag (spiked)	water extraction + centrifugation + filtration	50 µs	Q	no	characterisation (NP) quantitative (NP)	NP mean size NP mass concentration	ICP-MS ISE TEM-EDS DLS	100
soil colloids	CuO (spiked)	-	5 ms 100 µs	Q	H_2	characterisation (NP) quantitative (NP)	NP mean size NP number concentration	DLS	101
soil sediment	Au (spiked)	water extraction + centrifugation	10 ms	Q	no	characterisation (NP)	NP mean size NP size distribution	ICP-MS AF4-MALS-UV-ICP-MS DLS	102
soil sediment	Ag (spiked)	extraction (2.5 mM $Na_4P_2O_7$) + settling	3 ms	Q	no	characterisation (NP) quantitative (NP)	NP mean size NP number concentration	-	103
sediment column	aged Ag (spiked)	extraction (different media) + centrifugation (+ filtration)	5 ms	Q	no	qualitative (NP)	(presence of aggregates)	ICP-MS ICP-OES ETAAS TEM SEM-EDS HDC-ICP-MS	104
sand column	Au (spiked)	-	3 ms	Q	no	characterisation (NP)	NP size distribution	SEM	165
biological fluids									
artificial sweat	Ag (spiked)	-	100 µs	Q	no	characterisation (NP)	NP mean size	DLS UV-vis XAS SEM-EDS	166
plasma cellular blood fractions	Fe_3O_4 (spiked)	-	100 µs	Q	H_2	characterisation (NP)	NP mean size NP size distribution	TEM AF4-UV-MALS-ICP-MS	167

* M: nanoparticle with composition M. M-: nanoparticle containing element M

View Article Online
DOI: 10.1039/D1AY00761K

Table 5 Scenario 2.2: *In vitro*, *in vivo* and *ex vivo* (eco)toxicological tests.

sample	nanoparticle composition*	sample preparation	dwell time	mass analyser	collision/ reaction cell gas	analytical information	measurands	complementary techniques	ref.
***in vitro* studies**									
fungi									
Aspergillus flavus Aspergillus parasiticus Aspergillus carbonarius Aspergillus niger Aspergillus ochraceus Aspergillus steynii Aspergillus westerdijkiae Penicillium verrucosum	Ag (spiked)	-	3 ms	Q	no	characterisation (NP) quantitative (NP)	NP mean size NP size distribution NP number concentration NP mass concentration	TEM DLS	168
bacteria									
Pseudomonas aeruginosa Staphylococcus aureus	Ag (spiked)	-	5 ms	Q	no	characterisation (NP) quantitative (NP)	NP size distribution NP number concentration NP mass concentration	TEM-EDS XRD FTIR	169
Staphylococcus aureus Escherichia coli	Te (internalized)	bacteria lysis + centrifugation	5 ms	Q	no	characterisation (NP) quantitative (NP)	NP mean size NP size distribution NP number concentration	TEM XRD	[illegible]
river bacterial community	TiO_2 ZnO Ag (spiked)	-	100 µs	Q	no	characterisation (NP) quantitative (NP) quantitative (DE)	NP mean size NP size distribution NP number concentration NP mass concentration DE mass concentration	DLS	1 1
algae									
Chlamydomonas reinhardtii	Ag (spiked)	ultracentrifugation	0.5 ms	Q	no	characterisation (NP) quantitative (NP) quantitative (DE)	NP mean size NP mass concentration DE mass concentration	ICP-MS	172
Raphidocelis subcapitata	Cr- (biosynthesis)	filtration	50 µs	Q	no	characterisation (NP) quantitative (NP) quantitative (DE)	NP size distribution NP number concentration DE mass concentration	AAS TEM NTA	1 3
cells									
human umbilical vein endothelial cells	Au (spiked)	TMAH digestion	10 ms	Q	no	characterisation (NP) quantitative (NP)	NP mean size NP size distribution NP mass concentration	FIB-SEM flow citometry confocal microscopy	[illegible]
human macrophages and exosomes	Au (spiked)	ultracentrifugation + lysis	5 ms	Q	no	characterisation (NP) quantitative (NP)	NP mean size NP number concentration	TEM NTA flow cytometry confocal microscopy	175
human breast cancer cells	Au (spiked)	TMAH digestion	5 ms	Q	no	characterisation (NP) quantitative (NP)	NP mean size NP number concentration	ICP-MS	58
human epithelial colorectal adenocarcinoma cells human colon adenocarcinoma mucus secreting cells	Ag (spiked)	lysis	3 ms	Q	no	characterisation (NP) quantitative (NP) quantitative (DE)	NP mean size NP size distribution NP number concentration NP mass concentration	ICP-MS DLS TEM-EDS confocal microscopy	176

View Article Online
DOI: 10.1039/D1AY00761K

mouse embryonic stem cells	Ag Ag_2S (spiked)	-	3 ms	Q	no	characterisation (NP) quantitative (NP)	NP mean size NP size distribution NP number concentration NP mass concentration	ICP-MS TEM DLS	177
mouse neuroblastoma cells	TiO_2 Ag (spiked)	lysis	3 ms	Q	no	characterisation (NP) quantitative (NP)	NP mean size NP number concentration	ICP-MS LA-ICP-MS TEM DLS	178
trout liver cells	TiO_2 (spiked)	lysis	100 µs	Q	no	characterisation (NP) quantitative (NP) quantitative (DE)	NP mean size NP size distribution NP number concentration NP mass concentration DE mass concentration	ICP-MS TEM-EDS DLS confocal microscopy	179
***in vivo* studies**									
plants									
tomato	Au (spiked)	enzymatic digestion (macerozyme R-10)	100 µs	Q	no	characterisation (NP) quantitative (NP) quantitative (DE)	NP mean size NP size distribution NP mass concentration DE mass concentration	TEM DLS	180
tomato pumpkin soybean cucumber	CeO_2 (spiked)	enzymatic digestion (macerozyme R-10)	100 µs	Q	no	characterisation (NP) quantitative (NP) quantitative (DE)	NP mean size NP size distribution NP number concentration DE mass concentration	ICP-MS TEM	181
thale cress	Ag (spiked)	enzymatic digestion (macerozyme R-10)	50 µs	Q	no	characterisation (NP)	NP mean size NP size distribution	ICP-MS TEM	182
garden cress white mustard	Pt (spiked)	enzymatic digestion (macerozyme R-10) + filtration	100 µs	Q	no	characterisation (NP) quantitative (NP) quantitative (DE)	NP mean size NP size distribution NP number concentration DE mass concentration	ICP-MS	183
thale cress	Ag Cu ZnO (spiked)	enzymatic digestion (macerozyme R-10)	3 ms	Q	no	qualitative (NP)	-	ICP-MS SEM-EDS TEM-EDS DLS	184
cucumber wheat	Ag_2S (spiked)	enzymatic digestion (macerozyme R-10)	3 ms	Q	no	characterisation (NP) quantitative (NP)	NP size distribution NP number concentration	DLS SEM-EDS XAS	185
white mustard	Pd (spiked)	enzymatic digestion (macerozyme R-10)	100 µs	Q	no	characterisation (NP) quantitative (NP)	NP mean size NP size distribution NP number concentration	ICP-MS TEM	186
lettuce	Ag (spiked)	enzymatic digestion (macerozyme R-10)	10 ms	Q	no	characterisation (NP) quantitative (NP) quantitative (DE)	NP size distribution NP mass concentration DE mass concentration	ICP-OES XAS	187
	ZnO (spiked)	enzymatic digestion (macerozyme R-10)	100 µs	Q	no	characterisation (NP) quantitative (NP) quantitative (DE)	NP mean size NP size distribution NP number concentration DE mass concentration	ICP-MS HPLC-ICP-MS HPLC-QTOF-MS HPLC-FT-Orbitrap-MS	188
	CuO $Cu(OH)_2$ (spiked)	methanol extraction (50%)	100 µs	Q	no	characterisation (NP) quantitative (NP)	NP mean size NP size distribution NP number concentration	ICP-MS TEM	189
lettuce kale collard green	CuO (spiked)	enzymatic digestion (macerozyme R-10)	100 µs	Q	no	characterisation (NP) quantitative (NP) quantitative (DE)	NP mean size NP size distribution NP mass concentration DE mass concentration	FESEM TEM	190

wheat	Ag (spiked)	enzymatic digestion (macerozyme R-10)	100 µs	Q	no	characterisation (NP) quantitative (NP) quantitative (DE)	NP mean size NP size distribution NP mass concentration DE mass concentration	ICP-MS TEM DLS	191
	Ag Au (spiked)	enzymatic digestion (macerozyme R-10)	100 µs	Q	no	characterisation (NP) quantitative (NP) quantitative (DE)	NP size distribution NP mass concentration DE mass concentration	TEM	192
rice	TiO_2 (spiked)	enzymatic digestion (macerozyme R-10)	100 µs	Q	no	characterisation (NP) quantitative (NP)	NP size distribution NP number concentration	ICP-OES DLS STEM-EDS	193
rice soybean	Ag (spiked)	enzymatic digestion (macerozyme R-10)	50 µs	Q	no	characterisation (NP) quantitative (DE)	NP size distribution DE mass concentration	TEM-EDS	194
radish	CeO_2 CuO (spiked)	gastrointestinal digestion	100 µs	Q	no	characterisation (NP) quantitative (NP) quantitative (DE)	NP mean size NP size distribution NP mass concentration DE mass concentration	ICP-MS	195
	TiO_2 (spiked)	enzymatic digestion (macerozyme R-10)	100 µs	Q	O_2/H_2 (MS/MS)	characterisation (NP) quantitative (NP)	NP mean size NP size distribution NP number concentration NP mass concentration	ICP-MS	196
	CeO_2 (spiked)	enzymatic digestion (macerozyme R-10) + filtration	100 µs	Q	no	characterisation (NP) quantitative (NP)	NP mean size NP size distribution NP mass concentration	ICP-MS LA-ICP-MS	197
soil organisms									
Lumbriculus variegatus	Ag Au (spiked)	TMAH digestion	10 ms	Q	no	characterisation (NP) quantitative (NP)	NP mean size NP size distribution NP number concentration NP mass concentration	ICP-MS	198
Lumbriculus variegatus	Ag (spiked)	water extraction + centrifugation+ filtration	-	Q	no	characterisation (NP)	NP mean size NP size distribution	ICP-OES TEM DLS AF4-ICP-MS	199
Lumbriculus rubellus	Ag (spiked)	enzymatic digestion (collagenase+hyaluronidase+proteinase K)+centrifugation	3 ms	Q	no	characterisation (NP) quantitative (NP) quantitative (DE)	NP mean size NP size distribution NP number concentration NP mass concentration DE mass concentration	ICP-MS FESEM-EDS DLS	200
Caenorhabditis elegans	Au (spiked)	TMAH digestion	10 ms	Q	no	characterisation (NP) quantitative (NP)	NP size distribution NP number concentration	ICP-MS SEM-EDS TEM DLS ICP-MS	201
aquatic organisms									
Daphnia magna	Ag Au (spiked)	TMAH digestion	10 ms	Q	no	characterisation (NP) quantitative (NP)	NP mean size NP size distribution NP number concentration NP mass concentration	ICP-MS	198
	Ag nanowire (spiked)	collection of hemolymph	10 ms	Q	no	characterisation (NP) quantitative (NP) quantitative (DE)	NP mean size NP size distribution NP number concentration NP mass concentration DE mass concentration	ICP-MS SEM TEM	202
mussel	TiO_2 (spiked)	enzymatic digestion (proteinase K)	3 ms	Q	no	characterisation (NP) quantitative (NP)	NP mean size NP size distribution NP mass concentration	ICP-MS TEM	203
zebra fish (liver, intestine, gills)	Au Ag (spiked)	TMAH digestion+filtration	1 ms	Q	no	characterisation (NP) quantitative (NP)	NP mean size NP mass concentration	TEM	204
zebra fish (intestine, liver, gills, brain)	CeO_2 TiO_2 (spiked)	enzymatic digestion (proteinase K) + H_2O_2 digestion	3 ms	Q	no	characterisation (NP) quantitative (NP) quantitative (DE)	NP mean size NP number concentration NP mass concentration DE mass concentration	ICP-MS TEM DLS	205

View Article Online
DOI: 10.1039/D1AY00761K

trout (liver)	Ag (spiked)	TMAH digestion	3 ms	Q	He	characterisation (NP) quantitative (NP) quantitative (DE)	NP mean size NP size distribution NP number concentration NP mass concentration DE mass concentration		54
rat tissues									
spleen	Au (spiked)	TMAH digestion	3 ms	Q	no	characterisation (NP) quantitative (NP)	NP mean size NP size distribution NP mass concentration	-	206
	TiO_2 (spiked)	enzymatic digestion (proteinase K)	3 ms	Q	NH_3	characterisation (NP) quantitative (NP)	NP mean size NP size distribution NP mass concentration	SEM-EDS TEM	207
liver	Au (spiked)	lysis + centrifugation	10 ms	Q	no	characterisation (NP)	NP size distribution	TEM HPLC-ICP-MS	208
	SiO_2 (spiked)	enzymatic digestion (proteinase K)	3 ms	Q	CH_4	characterisation (NP)	NP mean size	ICP-MS TEM	209
liver lung	CeO_2 TiO_2 (spiked)	enzymatic digestion (proteinase K)	3 ms	Q	no	characterisation (NP) quantitative (NP)	NP size distribution NP mass concentration	ICP-MS DLS TEM	210
lung kidney blood	TiO_2 nanorods (spiked)	HCl/HNO_3 digestion+filtration	-	Q	-	qualitative NP		TEM SEM-EDS DLS	211
foetus, resorption, placenta, lung, liver, spleen, kidney, mammary gland	Ag (spiked)	TMAH digestion	100 µs	Q	no	characterisation (NP) quantitative (NP) quantitative (DE)	NP mean size NP size distribution NP number concentration NP mass concentration DE mass concentration	TEM-EDS	212
stomach, intestinal content, liver, spleen, kidney, lungs, blood	Ag (spiked)	enzymatic digestion (proteinase K)	3 ms	Q	no	characterisation (NP) quantitative (NP) quantitative (DE)	NP mean size NP mass concentration DE mass concentration	AAS TEM DLS	213
chicken tissues									
liver yolk	Ag (spiked)	enzymatic digestion (proteinase K)	2 ms	DF	no	characterisation (NP) quantitative (NP)	NP size distribution NP number concentration NP mass concentration	AAS SEM-EDS	214
***ex vivo* studies**									
human placenta	Ag (spiked)	enzymatic digestion (proteinase K)	3 ms	Q	no	characterisation (NP) quantitative (NP) quantitative (DE)	NP mean size NP size distribution NP number concentration NP mass concentration DE mass concentration	TEM DLS	215

* M: nanoparticle with composition M. M-: nanoparticle containing element M

View Article Online
DOI: 10.1039/D1AY00761K

Table 6 Scenario 3.1: Analysis of foods.

sample	nanoparticle composition*	sample preparation	dwell time	mass analysers	collision/ reaction cell gas	analytical information	measurands	complementary techniques	ref.
confectionery									
cakes candy chewing gum	TiO_2	H_2O_2 digestion	3 ms	Q	no	characterisation (NP)	NP size distribution	ICP-MS AF4-ICP-MS	216
chewing gum	TiO_2	water extraction	10 ms	Q	NH_3 (MS/MS)	characterisation (NP) quantitative (NP)	NP size distribution NP number concentration		217
silver pearls	Ag	water extraction	3 ms	Q	no	characterisation (NP) quantitative (NP)	NP mean size NP size distribution NP number concentration NP mass concentration	ICP-MS TEM-EDS HAADF-STEM	218
silver pearls decoration dusting powder	Ag Al Au	water extraction + centrifugation	5 ms	Q	no	qualitative (NP)		ICP-MS	74
custard cream candies pearls confectionery masses	TiO_2		100 µs	Q	no	qualitative (NP)		TEM-EDS CLS	219
candies	TiO_2	water extraction + filtration	100 µs	Q	no	characterisation (NP) quantitative (NP) quantitative (DE)	NP mean size NP size distribution NP number concentration DE mass concentration	AF4-MALS-ICP MS DLS	70
candies	TiO_2	centrifugation	100 µs	Q	no	characterisation (NP)	NP size distribution	SEM	220
silver coated chocolate and pearls	Ag	ethanol wetting + dispersion in 0.05% BSA	3 ms	Q	no	characterisation (NP) quantitative (NP)	NP mean size NP size distribution NP number concentration NP mass concentration	TEM	73
meat									
game meat	Pb	enzymatic digestion (proteinase K)	5 ms	Q	no	characterisation (NP) quantitative (NP) quantitative (DE)	NP mean size NP size distribution NP number concentration NP mass concentration DE mass concentration	ICP-MS	221
miscellaneous									
noodles	Al-	enzymatic digestion (α-amylase)	3 ms	Q	no	characterisation (NP) quantitative (DE)	NP mean size NP size distribution DE mass concentration	ICP-MS	222
drinks chocolate coffee chewing gum silver pearls	Ti- Si- Ag-	water extraction + filtration	100 µs	Q	He	characterisation (NP) quantitative (DE)	NP mean size DE mass concentration	ICP-MS DLS AF4-MALS-ICP MS	223
surimi sticks	TiO_2	enzymatic digestion (pancreatin and lipase)	100 µs	Q	He	characterisation (NP) quantitative (NP) quantitative (DE)	NP mean size NP size distribution NP number concentration DE mass concentration	ICP-MS TEM	224

* M: nanoparticle with composition M. M-: nanoparticle containing element M

View Article Online
DOI: 10.1039/D1AY00761K

Table 7 Scenario 3.2: Analysis of environmental samples.

sample	nanoparticle composition*	sample preparation	dwell time	mass analyser	collision/ reaction cell gas	analytical information	measurands	complementary techniques	ref.
soils, sediments and sludges									
soil	Fe-	water extraction + centrifugation	3 ms	Q	NH_3	characterisation (NP)	NP mean size NP size distribution	ICP-MS NTA DLS TEM AF4-UV-ICP-MS	225
mine tailings	$FeAsO_4 \cdot 2H_2O$ (scorodite)	water extraction + centrifugation	5 ms	Q	no	characterisation (NP)	NP size distribution NP mass distribution	ICP-MS EXAFS XAS TEM-EDS	2[illegible]
lake sediment	Ag-	water extraction + centrifugation + filtration	50 µs	DF	no	characterisation (NP) quantitative (NP) quantitative (DE)	NP mean size NP size distribution NP mass concentration DE mass concentration	ICP-MS	2[illegible]7
	Ag- Ti-	extraction (TMAH)	50 µs	Q	no	characterisation (NP) quantitative (NP)	NP mean size NP size distribution NP number concentration NP mass concentration	ICP-MS	2[illegible]
road runoff sediment	Cu- Zn- Zr- Cd- Ce- Pt- Pb-	surfactant extraction + centrifugation	5 ms	Q	H_2+He	characterisation (NP) quantitative (NP) quantitative (DE)	NP mean mass NP size distribution NP mass distribution NP mass concentration DE mass concentration	ICP-MS	[illegible]
sewage sludge	Ti-	digestion (HNO_3+H_2O_2) + filtration	3-10 ms	Q	no	characterisation (NP) quantitative (NP)	NP mean size NP size distribution NP number concentration NP mass concentration	ICP-MS	2[illegible]0
	Ti- Fe- Zn-	extraction (acetic acid) and centrifugation	100 µs	Q	n.r.	characterisation (NP) quantitative (NP) quantitative (DE)	NP mean size NP mass concentration DE mass concentration	ICP-MS FESEM-EDS TEM-EDS LDA	231
	Ti-	extraction (sodium pyrophosphate) + centrifugation	-	TOF	no	characterisation (NP) quantitative (NP)	NP mass distribution NP number concentration	ICP-MS TEM	2[illegible]
waters									
fresh waters	Ti-	filtration	50 µs	Q	no	characterisation (NP) quantitative (NP)	NP mean size NP size distribution NP number concentration NP mass concentration	ICP-MS TEM-EDS	56
	TiO_2	filtration	50 µs	Q	no	characterisation (NP) quantitative (NP) quantitative (DE)	NP mean size NP number concentration DE mass concentration	SEM-EDS FESEM	2[illegible]
	Ti-	-	10 ms	Q	no	quantitative (NP)	NP number concentration	ICP-MS ICP-OES SEM-EDS	2[illegible]4
	Ti-	centrifugation	4 ms 3ms	Q TOF	NH_3+He (MS/MS) no	characterisation (NP) quantitative (NP)	NP size distribution NP number concentration	TEM	2[illegible]
	Ti-	-	50 µs	DF	no	characterisation (NP) quantitative (NP)	NP mean size NP size distribution NP number concentration NP mass concentration	-	[illegible]
	Ti-	-	3 ms	Q	no	quantitative (NP)	NP number concentration	ICP-MS ICP-OES	236
	Ti-	filtration	10 ms	Q	no	characterisation (NP) quantitative (NP) quantitative (DE)	NP size distribution NP number concentration NP mass concentration DE mass concentration	CPE/TEM-EDS	237

	Ti-	filtration	100 µs	Q	no	characterisation (NP) quantitative (NP)	NP mean size NP size distribution NP number concentration	ICP-MS ICP-AES TEM-EDS HPLC-UV	238
	Ag- Ti-	-	50 µs	Q	no	characterisation quantitative (NP)	NP mean size NP size distribution NP number concentration NP mass concentration	ICP-MS	228
	Ag	filtration	50 µs	Q	no	characterisation (NP) quantitative (NP) quantitative (DE)	NP mean size NP number concentration DE mass concentration	-	239
	Ag	filtration	1 ms	DF	no	characterisation (NP) quantitative (NP) quantitative (DE)	NP mean size NP number concentration NP mass concentration DE mass concentration	ICP-MS ICP-AES IC	240
	Ag-	cloud point extraction	100 µs	Q	no	characterisation (NP) quantitative (NP)	NP size distribution NP mass concentration	ICP-MS ETAAS	241
	Ag- Ti- Ce-	-	3 ms	Q	no	characterisation (NP) quantitative (NP)	NP mean size NP size distribution NP number concentration NP mass concentration	-	3
	Ag- Ti- Au-	-	100 µs	Q	no	characterisation (NP) quantitative (NP) quantitative (DE)	NP mean size NP size distribution NP number concentration DE mass concentration	FESEM-EDS	2
	Ce- Zn-	-	100 µs	Q	no	characterisation (NP) quantitative (NP) quantitative (DE)	NP mean size NP size distribution NP number concentration DE mass concentration	-	243
	Ti- Ce-	filtration	1 ms	DF	no	characterisation (NP) quantitative (NP)	NP size distribution NP number concentration	ICP-MS ICP-AES FESEM-EDS IC	244
river water rainwater	Ce- La-	-	50 µs	DF TOF	no	characterisation (NP) quantitative (NP) quantitative (DE)	NP mean size NP size distribution NP number concentration NP mass concentration DE mass concentration	-	245
	Zn-	ion exchange (on line)	50 µs	DF	no	characterisation (NP) quantitative (NP) quantitative (DE)	NP mean size NP mean mass NP mass distribution NP number concentration DE mass concentration	TEM-EDS	5
seawater	Ag- Ti- Cu- Zn-	-	100 µs	Q	no	characterisation (NP) quantitative (NP)	NP mean size NP size distribution NP number concentration	ICP-MS	246
sea water fresh water	Ag- Ti- Ce-	filtration	100 µs	Q	no	characterisation (NP) quantitative (NP)	NP mean size NP size distribution NP number concentration NP mass concentration	-	247
wastewater	Ag-	filtration	5 µs	Q	no	characterisation (NP)	NP size distribution	ICP-MS ICP-OES	248
	Ag-	settling	20 ms	Q	no	quantitative (NP) quantitative (DE)	NP mass concentration DE mass concentration	-	249
	Ag-	filtration	100 µs	Q	no	characterisation (NP) quantitative (NP) quantitative (DE)	NP mean size NP size distribution NP mass concentration DE mass concentration	-	2
	Ag- Ti- Ce-	filtration	100 µs	DF	no	quantitative (NP)	NP number concentration	-	251
wastewater river water	Zn-	cation exchange separation	0.5 ms	Q	no	characterisation (NP) quantitative (NP) quantitative (DE)	NP mean size NP mass concentration DE mass concentration	-	252
wastewater river water	Zn-	settling and filtration	100 µs 3 ms	Q TOF	no H_2+He	characterisation (NP) quantitative (NP)	NP mean size NP size distribution NP number concentration	ICP-OES	253

View Article Online
DOI: 10.1039/D1AY00761K

						quantitative (DE)	NP mass concentration DE mass concentration		
wastewater river water lake water	Ag-	-	3 ms	Q	no	characterisation (NP) quantitative (NP)	NP mean size NP size distribution NP mass concentration	CPE+ETAAS	254
tap water	Ag- Ti- Pb- Sn- Cu- Fe-	-	10 ms	Q	n.r.	characterisation (NP) quantitative (NP) quantitative (DE)	NP size distribution NP mass concentration DE mass concentration	TEM-EDS	255
	Ag-	cloud point extraction	100 µs	Q	no	characterisation (NP) quantitative (NP)	NP mean size NP size distribution NP mass concentration	ETAAS	256
various types of waters	Ag-	-	0.5 ms	Q	no	characterisation (NP) quantitative (NP) quantitative (DE)	NP mean size NP size distribution NP number concentration NP mass concentration DE mass concentration	-	257
throughfall water	Cu-	-	100 µs	Q	no	characterisation (NP)	NP mean size	ICP-MS DLS AF4-MALS-ICP-MS	258
acid mine drainage	Fe- Cu-	-	100 µs	Q	NH_3	characterisation (NP) quantitative (NP)	NP size distribution NP number concentration	ICP-OES STEM-EDS IC	259
landfill leachates	Ti-	filtration + surfactant stabilization (0.1% NovaChem 100)	3 ms	Q	NH_3	characterisation (NP) quantitative (NP)	NP size distribution NP number concentration	ICP-OES SEM-EDS STEM-EDS DLS	260
miscellaneous									
cigarette smoke	As-	electrostatic trapping	100 µs	Q	no	qualitative (NP)		ICP-MS HPLC-ICP-MS	261
gas condensate	Hg-	dilution with THF	100 µs	Q	no	characterisation (NP) quantitative (NP) quantitative (DE)	NP mean size NP size distribution NP number concentration NP mass concentration DE mass concentration	ICP-MS STEM-EDS AF4-UV-MALS-ICP-MS	262

* M: nanoparticle with composition M. M-: nanoparticle containing element M
n.r.: not reported.

View Article Online
DOI: 10.1039/D1AY00761K

Table 8 Scenario 3.3: Analysis of biological samples.

sample	nanoparticle composition*	sample preparation	dwell time	mass analyser	collision/ reaction cell gas	analytical information	measurands	complementary techniques	ref.
microorganisms									
yeast	Se	enzymatic digestion (protease)	5 ms 100 µs	Q	H_2	characterisation (NP)	NP mean size NP size distribution	ICP-MS SEC-ICP-MS TEM-EDS	263
aquatic organisms									
molluscs	Ag-	enzymatic digestion (pancreatin/lipase)	50 µs	Q	no	characterisation (NP) quantitative (NP)	NP mean size NP size distribution NP number concentration	ICP-MS SEM	264
	Ti-	enzymatic digestion (pancreatin/lipase)	100 µs	Q	no	characterisation (NP) quantitative (NP)	NP mean size NP size distribution NP number concentration	ICP-MS DLS	265
	Ag- Ti- Cu- Zn-	enzymatic digestion (pancreatin/lipase)	100 µs	Q	no	characterisation (NP) quantitative (NP)	NP mean size NP size distribution NP number concentration NP mass concentration	ICP-MS	246
	20 elements	alkaline digestion (TMAH) + filtration	3 ms	Q	no	characterisation (NP) quantitative (NP)	NP mean size NP size distribution NP mass concentration	ICP-MS	266
various (plankton, crustaceans, molluscs, fish)	Ag- Ti-	alkaline digestion (TMAH)	50 µs	Q	no	characterisation (NP) quantitative (NP)	NP mean size NP size distribution NP number concentration NP mass concentration	ICP-MS	22[illegible]
human fluids and tissues									
blood	Ag	-	5 ms	Q	no	characterisation (NP) quantitative (NP) quantitative (DE)	NP mean hydrodynamic diameter NP mean mass per particle NP number concentration NP mass concentration DE mass concentration	HDC-SP-ICP-MS µXRF µXANES	267
urine	Ag- Ti-	-	100 µs	Q	no	characterisation (NP) quantitative (NP)	NP mean size NP size distribution NP number concentration	ICP-MS	268
hip fluid	Co- Cr-	enzymatic digestion (proteinase K)	3 ms	Q	no	characterisation (NP)	NP mean size NP size distribution	ICP-MS AF4-UV-MALS AF4-ICP-MS	[illegible]
periprosthetic tissue	Ti- Ta- Co- Cr- Mo- Al- V-	-	3 ms	Q	no	characterisation (NP) quantitative (NP)	NP mean size NP size distribution NP number concentration	ICP-MS SEM	270
liver spleen kidney intestine	TiO_2 SiO_2	enzymatic digestion (proteinase K)	2 ms 100 µs	DF Q	no H_2	characterisation (NP) quantitative (NP)	NP mean size NP size distribution NP mass concentration	ICP-MS SEM-EDS	271
liver spleen	TiO_2	enzymatic digestion (proteinase K)	2 ms	DF	no	characterisation (NP) quantitative (NP)	NP size distribution NP number concentration NP mass concentration	ICP-MS SEM-EDS	272
exhaled breath condensate	SiO_2	-	3 ms	Q	He	qualitative (NP)	-	TEM-EDS	273
miscellaneous									

View Article Online
DOI: 10.1039/D1AY00761K

gunshot residue wash from shooter's hand	Sb-Ba-Pb-	- washing with water - swabbing+water extraction	30 µs	Q	no	qualitative (NP)	-	274

* M: nanoparticle with composition M. M-: nanoparticle containing element M

View Article Online
DOI: 10.1039/D1AY00761K

Scenario 0: Analysis of pristine nanoparticles

The analysis of pristine nanoparticles is regarded as the least complex scenario, since there is no matrix in which they are contained. Engineered nanomaterials commonly produced at laboratories for research or industrial purposes,[61,63–72,75,76] but also commercial suspensions,[60,62,73,74] have been considered in this section. Table 2 summarizes the applications of SP-ICP-MS to the analysis of such pristine nanoparticles. In any case, the main aim of the analysis is focused on the characterisation of the nanoparticles, although the effect on size of different factors (stability,[60] kinetics,[61] use of specific reagents[67,76]) along their synthesis have also been studied by some authors.

Pure nanoparticles of metallic Au,[63–65] Ag,[60,61,63] Pd and Ni,[68] as well as TiO_2,[71] have been analysed by SP-ICP-MS. The nanoparticles were usually obtained by chemical synthesis, although they were also produced by milling.[60] Most of the nanoparticles were available as suspensions, however, those presented as powders had to be prepared as stable suspensions, requiring convenient dilutions in all cases. Only in the work by Lahtinen et al.[76] nanoparticles had to be extracted with water, because they were obtained by reduction of tetrachloroaurate adsorbed onto 3-D filters.

In relation to the analytical information delivered, size distributions and mean/median sizes were typically reported, although mass[61,68] and number concentration[64,68] were also considered when samples were originally presented as suspensions. In this scenario, characterisation was not only limited to sizing. Kalomista et al.[65] were able to provide information about the shape of the nanomaterial, differentiating between spherical nanoparticles and nanorods of Au by comparing the signal-time profiles of the peaks recorded. Merrifield et al.[62] characterised and quantified Au-Ag core-shell nanoparticles, whereas Keri et al.,[63] following a similar methodology to Kalomista,[65] were able to distinguish between Au-Ag alloyed and core-shell nanoparticles, providing average Au:Ag molar ratios.

The analysis by SP-ICP-MS of composite particles consisting of polymer[66] or silica[72] particles containing metallic nanoparticles allowed to obtain the mass of Au or Pt per particle, respectively, as well as the corresponding distributions and the number of metallic nanoparticles per composite particle when their size was known. Complex nanomaterials, like up-conversion nanoparticles ($NaYF_4$ and $NaGdF_4$ doped with Yb or Er), could also be characterised by decreasing the element mass per particle detection limit; this could be done by reducing the resolution of the quadrupole and hence increasing the transmission of ions.[70]

Although carbon nanotubes are not directly detectable by SP-ICP-MS, their metal impurities have been used as proxies for their detection. In that way, the yttrium contained in nanotubes allowed their detection,[73,74] although the concentration was underestimated due to the difficulties of detecting nanotubes with low loads of yttrium.

The characterisation of pristine nanoparticle by SP-ICP-MS has been complemented by electron microscopy techniques for size and shape characterisation[57,61,64,65,68–70,73,74] and XRD[68,69,72,75] for confirmation of their nature through their crystalline structure.

Scenario 1: Analysis of consumer and industrial products containing nanoparticles

Owing to their specific properties at the nanoscale level, nanoparticles are currently contained in numerous consumer and industrial products. The nano-enhanced products analysed by SP-ICP-MS are summarized in Table 3; they consist of consumer, mainly cosmetics,[53,77–85] and industrial products, including food additives[43,46,89] and other materials, like steel,[90] petroleum products[57,91] or tattoo inks.[92,93]

Nanoparticles in cosmetics are mainly focused on sunscreens,[77–79,84] in which TiO2 is the most frequent nanocomponent due to its photocatalytical properties, although ZnO has also been studied in this type of products.[80,81] TiO_2 was the target analyte in other cosmetics and personal care products, like toothpastes,[82,83] lip balms,[82,84] creams[84] and shampoos.[84] Aluminium oxide and silver nanoparticles in toothpastes[83] and moisturizing creams,[53] respectively, have also been measured by SP-ICP-MS, as well as plastic microparticles added as abrasives in exfoliant creams.[85] Sample preparation of cosmetics always requires their dispersion in ethanol or water, in most cases by adding a surfactant, although a previous defatting step with hexane is typical for sunscreens and lip balms.[79,82,84] When refractory nanoparticles like TiO_2 or Al_2O_3 are involved, a previous matrix digestion with hydrogen peroxide has been applied.[83] Other consumer products considered have been antibacterial sprays containing silver nanoparticles,[86–88] although the occurrence of other elements like Sn or Zn in these products has also been checked.[88]

TiO_2 and metallic Ag are approved food additives, labelled as E171 and E174, respectively. Raw samples of E171[46,89] and E174[43] have been characterised by SP-ICP-MS in combination with other techniques to obtain information about the nanoparticulate fraction in these materials. In the case of steels,[90] the aim of the analysis was the characterisation of refractory particles of titanium and niobium carbonitrides, whereas in petroleum products (crude and fuel oil,[57] and asphaltene solutions[91]) was the detection of iron and molybdenum containing particles. In a similar way, tattoo inks[92,93] were analysed to study the occurrence of nanoparticulate Al, Ti, Cu, Cr, Zn and Pb from the pigments used in their fabrication, or the presence of copper nanoparticles in homeopathic medicines.[94]

View Article Online
DOI: 10.1039/D1AY00761K

Given the nature of the materials considered and their commercial purpose, many of the studies were placed under the European Commission regulation and its definition of nanomaterial.[43,46,79,81,83,84,93] The principal objective of the use of SP-ICP-MS was therefore focused on the characterisation of the nanoparticle fraction, being the mean size and the particle size distribution the main measurands of concern.

Although concentration is not a serious constrain in this scenario, a common limitation when using SP-ICP-MS is the detection of the smallest fraction of the nanoparticles present with these samples. This can lead to partial histograms since complete size distributions are not always obtained. This was the case for titanium in some cosmetics[77–79,82] and food additives,[46] as well as for silver.[43,53,86,87] For microplastics,[85] the sizes of detectable particles were restricted at both size range limits. At lower size range, it is restricted due to the inherent limitations of carbon detection by ICP-MS, and at the upper size range due to low nebulization efficiency of large particles, being limited to sizes from 1 up to 5 µm.

Scenario 2.1: Laboratory tests involving nanoparticles or products containing nanoparticles

The applications developed under scenario 2.1, summarized in Table 4, include laboratory tests under controlled conditions, involving pristine nanoparticle or products containing nanoparticles. Laboratory tests with materials originally containing nanoparticles are devoted to studying their release into aqueous media under selected conditions, whereas the study of the fate and behaviour of nanoparticles in different media, or along different relevant processes, requires the addition of pristine nanoparticles to the samples of concern.

Release studies. The risk assessment of consumer and industrial products containing engineered nanoparticles involves knowing the human and environmental exposure to the nanoparticles released from such products along their whole life cycle. These release studies are usually performed at laboratory scale under controlled simulation conditions.

Direct human exposure to engineered nanoparticles and/or their transformation products might arise from the ingestion of foods stored in containers bearing nanoparticles (e.g., Ag, nanoclays). Migration test from existing regulations for conventional analytes, based on the use of model food simulants (acetic acid, ethanol), have been applied to plastic food containers[95–99] and packaging films,[100] as well as to cookware.[101] The procedures are straightforward; after incubation of the samples at selected temperatures during fixed time periods, simulants are diluted conveniently and analysed by SP-ICP-MS. In addition to plastic containers, polymers doped with Fe_2O_3[109] and ZnO[110] have also been studied by using these migration tests. In the case of baby products containing silver nanoparticles, release studies were performed by leaching in artificial saliva to simulate the exposure route for children.[98] In a similar way, silver release from toothbrushes was studied by leaching in tap water.[102] The dermal exposure from surfaces containing nanoparticles was simulated through wiping tests by using artificial sweat, followed by the extraction with water of the nanoparticles from the wipes.[103] Water extraction has also been applied to study the release of Ag nanoparticles from antibacterial plasters[104] or TiO_2 from textiles.[105]

Environmental exposure to engineered nanoparticles from nano-enhanced products is related to their release and transformations that they undergo during their life cycle. Most commonly, materials like wood,[116] leather[117] or polymers[108,109] have been subjected to direct leaching in water, whereas for paints[111,113] or conductive inks,[114] the release from painted surfaces or printed circuits have been considered, respectively. More realistic studies have involved the use of different model waters to study the leaching of metal bearing particles under end-of-life conditions from photovoltaic cells,[115] or the leaching of TiO_2 particles from painted surfaces by snow and rainwater under weathering conditions.[112] Mitrano et al.[106] studied the life cycle of nano-enhanced textiles subjected to different aging and washing processes to understand the release and transformation of the silver nanoparticles from the textiles. The release of metal containing particles from environmental samples, like road dust[119] and mine tailings,[120] has also been studied by leaching in different media as a source of environmental pollution.

Regarding the composition of the nanoparticles, silver[95–98,100,102–104,106,107,114,115,117] and titanium[101,105,112,113] are the most frequently studied, although zinc[110] and copper[103,111,116] have also been considered. Multielement monitoring has also been performed, as in the case of photovoltaic cells,[115] cookware[101] or the emission of particles from paper printing and shredding.[118] The release of carbon nanotubes from polymer nanocomposites was followed by monitoring the yttrium present in the nanotubes,[108] as it was described for pristine carbon nanotubes in scenario 0.[73,74] Detection of plastic microparticles released from food containers has also been possible by using the carbon-13 isotope.[85]

Although SP-ICP-MS allows to obtain detailed quantitative information about nanoparticle size and concentration, the technique has been used in some release studies only to confirm the presence of the nanoparticles in the food simulants[85,95,99] or the leaching media,[115,117,118] as well as of dissolved forms of the element monitored.[97] In these cases, the recorded time scans (Fig. 2.a) allow to obtain the qualitative information required, once the adequate metrological criteria have been applied.[44] In many other studies, detailed information about mean/median sizes, size distributions and number/mass concentration of the nanoparticles released were reported, although the profiles of the size distributions revealed that the nanoparticle distribution had been partially recorded due to the attainable size limits of detection, hence underestimating the actual concentrations and overestimating mean sizes.

Fate studies. Whereas the release studies discussed above involve consumer and industrial products, fate studies are mostly based on the use of pristine and well-characterised nanoparticles, commercially available or synthesized at the laboratory, although aged nanoparticles have also been used.[164] The nanoparticles are spiked in the matrix of interest and the samples analysed directly or after undergoing the simulated process under study (e.g., gastrointestinal digestion, laundry, wastewater treatment, environmental exposure). The main advantage of these controlled experiments is that both size and concentration

of the spiked nanoparticles can be selected as desired. Although concentration is not a serious limitation for SP-ICP-MS, allowing even to work at realistic environmental concentrations,[135,138,141] attainable size LODs can be a critical drawback when using SP-ICP-MS with real samples, as it has been discussed above and it will be shown again in relation to scenario 3.

Fate studies performed with spiked Ag nanoparticles in food simulants complement the migration tests of silver from food containers discussed above, allowing to obtain information about the oxidation of silver nanoparticles to dissolved forms.[121,122] In relation to the potential human exposure to engineered nanoparticles through ingestion, the behaviours of Ag,[123,124] but also of Au,[123] CeO_2[123] and ZnO[110,123] nanoparticles along *in vitro* gastrointestinal digestions have been studied by SP-ICP-MS through the direct spiking of the digestion fluids[123,124] or foods submitted to the *in vitro* digestions.[110,125] With respect to the dermal exposure to consumer products containing Ag nanoparticles, laboratory experiments with artificial sweat have allowed to detect changes in size of the nanoparticles.[166] The stability of iron oxide nanoparticles in Ferumoxytol, an intravenous preparation for treatment of the anaemia, was studied in human plasma and cellular blood fractions.[167] In relation to the life cycle of silver nano-enhanced textiles and their environmental implications, the fate and behaviour of pristine Ag nanoparticles in the washing solutions during the laundry process has also been studied.[126]

Environmental scenarios for studying the fate of nanoparticles by SP-ICP-MS have included different types of real and synthetic surface waters (lake,[130–133] river,[134–137] sea[140–142]) and wastewaters,[143–150,275] as well as soils[104,156–161] and sediments.[162,163] Whereas spiked water samples were usually analysed directly or after dilution, soil analysis required the extraction and the separation of the nanoparticles from the soil matrix. This was done by using water or other extractants, like sodium pyrophosphate,[158,159,163] followed by centrifugation or/and filtration.

Apart from works devoted to demonstrate the capability of SP-ICP-MS for detecting specific nanoparticles in water[142,150] and soil[159,161,163] samples, fate experiments focus mainly on studying the stability[129,143] and transformations (dissolution/ oxidation,[128,138] aggregation[127,135]...) of nanoparticles under laboratory controlled conditions, although experiments adding nanoparticles into natural aquifers have also been performed.[131–133] Special attention has been paid to the fate of nanoparticles in relation to drinking and wastewater treatments. The stability of Ag nanoparticles under ozonisation conditions[129] and the removal of different engineered nanoparticle through coagulation processes[155] and wastewater treatments[151–154] have been studied. Soil studies have focused on the interaction of the nanoparticles with soil components, that control their transformations as well as their retention and mobility.[157,162,164,165]

Most studies with environmental samples have focused on Ag nanoparticles,[104,121–126,129–135,137–143,146–148,150,152–160,275,163,164,166] as well as their transformation products, Ag_2S and AgCl.[134,140] Other nanoparticles studied include TiO_2,[136,144,148,155,156] ZnO,[136,155,156] CeO_2,[135,144,155,156] CuO,[161] Fe_2O_3,[135] Pt[127] and Au.[137,149,155,165] Less common nanoparticles like core-shell Au@Ag nanoparticles[128] and carbon nanotubes[151] have also been considered. The influence of the coating[104,129,130,138,141,142,146,157,162,163] and the size[123,126,149,150,155,159,163,165,166,275] of the spiked nanoparticles on the transformations studied have also been considered.

Fate studies focus on the transformations of the nanoparticles in relation to their potential toxicity.[130–132,136,138,141,149,155,164] In general, the mean/median size and size distributions are the most frequent measurands. These measurands are related to the stability of the nanoparticles, but also to their aggregation[110,122–129,131,133,136,138,139,141,145,148,152,157,158,162–164,166] and dissolution.[138,143,144,147,151] For this reason, the concentration of the dissolved element has also been considered in different studies.[122,123,125,126,131,133,136,144,147,153,154,158] To confirm the formation of aggregates, electron microscopy techniques (SEM, TEM),[110,123–125,141,147,151,158,164] DLS[110,124,129,139,158,162,166] or NTA[143] have been used as complementary techniques.

Scenario 2.2: *In vitro*, *in vivo* and *ex vivo* (eco)toxicological tests

Risk assessment of nanomaterials must be based on exposure information but also on their toxicological behaviour in humans, animals and the environment. Hence, *in vitro*, *in vivo* and *ex vivo* (eco)toxicological essays worth studying in order to assess these behaviours and effects on living organisms. However, unravelling the mechanisms of action of nanoparticles for the correct interpretation of (eco)toxicity data requires the availability of detailed analytical information from characterising and quantifying nanoparticles and their transformation products in biological media.[34] In this context, SP-ICP-MS has proved to be a valuable technique in recent years, as it is summarized in Table 5. As in the case of the fate studies discussed above, (eco)toxicological test use mostly pristine and well-characterised nanoparticles, commercially available or synthesized at laboratory, allowing to select their size and coating, as well as their concentration levels.

***In vitro* studies.** Bacteria, fungi and algae have been microorganisms used to assess the uptake, biotransformation and ecotoxicity of nanoparticles under laboratory-controlled conditions, in a similar way that it has been done with different types of cells for toxicity assessment.

Because many *in vitro* studies were performed with in-lab synthesised nanoparticles, SP-ICP-MS has been used in combination with other techniques only for characterisation of these pristine nanoparticles.[168,169] The uptake of Te nanoparticles by *Staphylococcus aureus* and *Escherichia coli* was studied by the direct addition of spherical nanoparticles into the culture medium. Their biotransformation to nanorods when they were incorporated into the bacterial strains was confirmed by TEM and XRD, whereas SP-ICP-MS was applied after bacteria lysis to determine the number of particles per bacteria and to infer dimensional information of the rod-shaped Te nanoparticles.[170] The effect of TiO_2, ZnO and Ag nanoparticles on a river bacterial community was studied by mixing river water with artificial treated wastewater containing added nanoparticles. After three days of exposure, water samples were analysed by SP-ICP-MS

to determine the mean size and size distributions, as well as the concentration of nanoparticles and dissolved species.[171]

Algae are commonly used in ecotoxicity testing. In this context, the dissolution of Ag nanoparticles and the bioavailability of silver to the model green alga *Chlamydomonas reinhardtii* was studied in a wastewater matrix,[172] using SP-ICP-MS for monitoring the aggregation and dissolution of the nanoparticles. Speciation studies with chromium (III) and (VI) in ISO 8692 algal medium showed the formation of Cr-bearing nanoparticles, detected by SP-ICP-MS, which could contribute to the ecotoxicity of chromium to *Raphidocelis subcapitata*.[173]

The risk assessment of nanoparticles in living beings involves the proper evaluation of their behaviour at cellular level by *in vitro* assays. Within this framework, SP-ICP-MS has been used in a number of studies with human cell lines (umbilical vein endothelium,[174] macrophages and exosomes,[175] breast cancer,[58] human epithelial colorectal adenocarcinoma and colon adenocarcinoma mucus secreting cells[176]) but also mouse (embryonic stem[177] and neuroblastoma[178]) and liver trout[179] cells. The uptake of nanoparticles by cells was demonstrated to be dependent on their concentration in the media,[174] exposure time and cell line.[58] SP-ICP-MS allowed to study their biotransformations,[176] as well as their dissolution and agglomeration[176] within the cells. Moreover, the release of internalised nanoparticles by macrophages through exosomes could also be confirmed.[175]

Au nanoparticles have been more frequently used in these *in vitro* studies with cells,[58,174,175] although Ag,[176–178] Ag_2S[177] and TiO_2[178,179] have also been investigated. After exposure in the culture media containing the nanoparticles, cells were separated by centrifugation and lysed[175,176,178,179] or digested with TMAH[58,174] as a previous step to the analysis by SP-ICP-MS.

***In vivo* studies.** Release of engineered nanoparticles to the environment may end up and accumulate in edible plants, which is a potential pathway to human exposure. SP-ICP-MS has been used to study the uptake of nanoparticles by different types of plants in suitable growing media (hydroponic solutions[185,187,192] and soils[180–184,186,188,191,193–197]) containing known concentrations of nanoparticles of selected compositions and sizes. Edible plants like tomato, pumpkin, soybean, cucumber, thale cress, garden cress, white mustard, lettuce, kale, collard green, wheat, rice, soybean and radish have been selected for these experiments. Most of uptake studies have involved Ag nanoparticles,[182,184,187,191,192,194] but also Ag_2S,[185] Cu,[184] $CuO/Cu(OH)_2$,[189,190,195] ZnO,[184,188] CeO_2,[181,195,197] TiO_2,[193,196] Au,[180,192] Pd[186] and Pt.[183] By analysing different parts of the plants (roots, leaves, fruits), the uptake of nanoparticles through the roots and their translocation to other parts as intact particles or dissolved has been followed.[183,196] In addition to the uptake of nanoparticles through the roots, the foliar exposure has been also assessed for Ag[194] and CuO[189,190] nanoparticles. In the case of silver, the transformation of Ag nanoparticles after foliar exposure to ionic silver was reported.

In most cases, plant tissues were enzymatically digested by using macerozyme R-10, an enzyme mixture able to break down vegetal cell walls maintaining nanoparticles intact, as confirmed by several authors.[182,190] To avoid dissolution of $CuO/Cu(OH)_2$ nanoparticles, Laughton et al.[189] proposed the use of methanol for extraction of the nanoparticles from lettuce leaves as an alternative to the enzymatic digestion.

The assessment of the nanoparticle ecotoxicity in aquatic and terrestrial environments is based on the use of model organisms. In this context, the bioaccumulation of Ag[198–200] and Au[198,201] nanoparticles in spiked sediments and soils has been studied in the earthworms *Lumbriculus variegatus*,[198,199] *Lumbriculus rubellus*[200] and *Caenorhabditis elegans*.[201] Homogenates of the whole organisms were submitted to enzymatic[200] or alkaline[198,201] digestions, as well as to water extraction[199] prior to SP-ICP-MS analysis.

In relation to ecotoxicity studies in aquatic environments, the uptake of Ag[198,202] and Au[198] nanoparticles by *Daphnia magna* was studied by analysing the haemolymph of the daphnids,[202] as well as whole organisms after alkaline digestion with TMAH.[198] In the case of mussels, Gallochio et al.[203] suggested the *in vivo* formation of TiO_2 nanoparticles after their exposure to both ionic and particulate titanium. Zebra fish[204,205] and trout[54] have also been used as target species for ecotoxicological studies with Ag, Au, TiO_2 and CeO_2 nanoparticles. The bioaccumulation of these nanoparticles was assessed by analysing different organs of the fishes (liver, intestine, gills, brain) by SP-ICP-MS after their digestion with TMAH or proteinase K.

Rats has been used extensively as model mammals for the toxicity assessment of nanomaterials. Different nanoparticles have been administered in a number of ways (oral gavage,[213,207] intravenous injection,[206] intratracheal instillation,[210] nose inhalation[212] or intraperitoneal injection[208]) and their bioaccumulation and distribution in tissues were investigated by SP-ICP-MS. Van der Zande et al.[213] reported the detection of silver nanoparticles in all the tissues studied after oral gavage, although the target organs were liver and spleen. Usually, samples were subjected to digestion with TMAH or proteinase K prior to SP-ICP-MS. Gallochio et al.[214] evaluated the oral administration of PVP-stabilized 20 nm Ag nanoparticles to chickens, detecting 16 nm nanoparticles in liver, but only ionic silver in egg yolks.

***Ex vivo* studies.** Experiments involving human tissues are scarce, nonetheless Vidmar et al.[215] conducted an *ex vivo* study involving human placentas obtained from pregnancies after caesarean section. The SP-ICP-MS analysis of the perfusion experiment confirmed the translocation and accumulation of Ag nanoparticles, although it could not be confirmed if the Ag-containing particles detected in the foetal circulation were translocated pristine Ag nanoparticles or Ag-bearing particles formed from dissolved silver that crossed the placental barrier.

Scenario 3.1: Analysis of foods

A number of inorganic substances are approved as food additives by different regulations. Whereas metallic aluminium (E173), silver (E174) and gold (E175) are used to colour the external coating of confectionery, TiO_2 (E171) is added to provide a whitening effect, and SiO_2 (E551) as anticaking agent. All these additives have been re-evaluated recently by the European Food Safety Authority in relation to their safety, recommending that information about particle size and percentage (in number) of

particles in the nanoscale should be included in their specifications when present in powder forms. Thus, as it has been seen in scenario 1 with E171 and E174 additives, regulatory requirements are the main driving factors for monitoring these elements by SP-ICP-MS, along with studying their occurrence as nanoparticles in foods. Table 6 summarises the applications of SP-ICP-MS in relation with food analysis.

TiO_2 has been studied in different confectionery products, such as candies,[79,216,219,220,223] chewing gum,[216,217,223] pastry products[219] or cakes,[216] but also in drinks[223] and surimi sticks.[224] These samples were typically subjected to water extraction, followed by centrifugation or filtration,[79,217,219,220] although Peters et al.[216] proposed the digestion with hydrogen peroxide to release the particles from the coating of the products. For the analysis of surimi sticks, samples underwent enzymatic digestion with pancreatin and lipase.[224] The occurrence of particulate and dissolved aluminium in noodles was studied by Loeschner et al.,[222] after enzymatic digestion with α-amylase of the food products. Metallic silver, aluminium and gold are available as decorating powders or found as coatings of confectionery products.[43,44,218] In these cases, samples had to be dispersed or extracted with water, or adding albumin as stabilising agent.[43] A different issue was addressed by Kollander et al.,[221] who studied the presence of Pb nanoparticles from ammunition in meat of hunted wild animals. Samples from the shot areas were digested with proteinase K and analysed by SP-ICP-MS, detecting Pb nanoparticles.

Although some analysis only focused on detecting the presence of nanoparticles in the samples,[44,219] most of them covered their size characterization and the determination of number and mass concentrations as well. Moreover, most works included the determination of the total content of the elements under study in their analysis schemes, as well as considering the use of electron microscopy techniques[43,218–220,224] or AF4 separations[79,216,223] to verify or complement the results obtained by SP-ICP-MS.

Scenario 3.2: Analysis of environmental samples

The widespread use of engineered nanomaterials in consumer products has increased their potential risk of environmental contamination, and consequently, the need and demand of analysis of environmental samples (waters, soils, sediments, sludges...) to provide reliable field information about their actual occurrence. On the other hand, SP-ICP-MS is also a suitable technique for monitoring naturally occurring or incidental nanomaterials.[32] In fact, an still unresolved challenge in this scenario is the discrimination between engineered and natural occurring nanomaterials, which will be discussed below.

Table 7 summarizes different environmental samples analysed by SP-ICP-MS. Most cases refer only to the detection of nanoparticles containing the monitored element because the chemical composition of the particles was not available. Thus, the size information reported was based on assuming a specific composition (e.g., metallic Ag, TiO_2) and a spherical shape. When the authors did not confirm the composition of the nanoparticles by an alternative technique, nanoparticles in Table 7 are referred as nanoparticles containing a specific element (e.g., Ag-, Ti-, Ce- instead of Ag, TiO_2, CeO_2).

In most studies, total element concentrations were determined by ICP-MS or other atomic spectrometry techniques (ICP-OES, AAS) to obtain complementary information of the samples. The use of complementary techniques, like TEM/FESEM or EXAF/XAS, for confirming the presence of nanoparticles or aggregates and obtaining information about morphology, size and composition of the particles was limited to samples containing particles at high enough concentrations.[55,56,242,244,255,259,225,226,231–234,237,238]

Soils, wastes, sediments and sludges. Solid environmental samples analysed by SP-ICP-MS include soils,[225] mine wastes,[226] sediments[227–229] and sludges from wastewater treatment plants.[230–232] In the latter case, these analyses were complemented by the analysis of the influent and the treated effluent of the plants,[230,231] or the analysis of the sediments of lake where discharges were carried out.[229] The nanoparticles of interest were diverse, comprising particles containing elements such as Ag,[227,228] As,[226] Ti,[228,230–232] Fe,[225,231] Zn,[229,231] Cu,[229] Pb,[229] Pt,[229] Cd,[229] Ce,[229] or Zr[229]. Sample preparation involved the extraction of the particulate matter with ultrapure water,[225–227] the addition of surfactants[229] or other reagents (sodium pyrophosphate,[232] acetic acid[231] or TMAH[228]); in the case of particles containing Ti, stronger procedures based on microwave acid digestion have also been applied.[230] These treatments were followed by a separation step consisting of centrifugation, filtration, or both sequentially, prior to the analysis of the corresponding supernatant or filtrate.

In relation to the information reported, only Gomez-Gonzalez et al.[226] determined by EXAFS and XAS the nature of the As-containing particles detected by SP-ICP-MS in mine tailings ($FeAsO_4 \cdot 2H_2O$, scorodite), providing real size information confirmed by TEM. Due to the unknown nature of the particles detected, Baur et al.[229] reported mean mass per particle and mass per particle distributions instead of information as equivalent size, which was the characterisation information typically reported, along with particle mass and number concentrations, as well as dissolved element concentrations.

Waters. Different types of waters have been analysed by SP-ICP-MS, including fresh waters from lakes, rivers and dams, as well as rain, sea, tap, pool and waste waters. The reasons for carrying out these analyses are diverse. The monitoring of titanium in river, lake and swimming pool waters is associated to the release of TiO_2 nanoparticles from sunscreens.[234–238] Silver has been monitored in different types of waters, although the most relevant studies are related to the removal of silver containing particles in wastewater treatment plants,[248–251,254] which has been also the case for Ti-,[251] Zn-[252,253] and Ce-containing particles.[251] In the case of cerium, CeO_2 nanoparticles can be released into the air by diesel emissions being detected in rain water[245] and other natural waters.[38,243–245,247,251] Tap waters have been analysed in relation to the release of incidental nanoparticles containing different metals from copper pipes.[255,256] Throughfall water from the wash-off of vine leaves treated with Cu-based fungicides has also been analysed by SP-ICP-MS in combination with other techniques to study the mobilization of Cu-containing particles.[258] The occurrence of Zn-,[246] Ag-,[246,247] Ti-,[246,247] Cu-[246] and Ce-[247] containing

particles[45] has also been monitored in seawaters. SP-ICP-MS was used to study acid mine drainage by monitoring Fe- and Cu-containing particles and the effects of water chemistry,[259] as well as the release of titanium from construction and demolition landfills by analysing their leachates.[260]

With respect to the preparation of water samples, the simplest procedures only involved the dilution of the sample, although settling, centrifugation or filtration were also applied when suspended matter was present.

In relation to the information reported, a reduced number of works provided qualitative information,[236,248,258,274] relying on time scans (Figure 2.a) to prove the presence of particles, whereas most of articles provided quantitative information, including mean/median particle sizes, particle size distributions and particle mass and number concentrations, despite that partial size distributions were obtained in some cases.[226,235,241,248,259] In this regard, although Rand and Ranville[259] have demonstrated the utility of SP-ICP-MS for detecting incidental nanoparticles in natural systems, they also recommended caution in the data treatment and their interpretation.

In an attempt to discriminate between anthropogenic engineered nanoparticles from natural ones, the measurement of element ratios has been proposed. This strategy assumes that engineered nanoparticles are high purity substances, containing a single major element, while natural nanoparticles have heterogeneous multielement compositions. The Ce/La ratio has been reported for identification of CeO_2 nanoparticles, [244,245,247] whereas for TiO_2 nanoparticles, the Ti/Al and Ti/V ratios have been considered. [232,234–236,238,244,247] Whereas SP-ICP-MS with quadrupole instruments is limited to the measurement of two isotopes in an individual particle, TOF instruments are able to record the whole mass spectrum from each particle. In this respect, a promising approach for discrimination of anthropogenic and natural particles was proposed by Praetorius et al.[276] based on the combination of single particle multielement analysis by SP-ICP-TOF-MS and machine learning data treatment.

Miscellaneous. The analysis of gaseous systems by SP-ICP-MS has been limited to condensates from cigarette smoke to study the presence of arsenic containing particles.[261] Condensates from cigarette smoke were accumulated in an electrostatic trapping device followed by washing with methanol. Whereas different inorganic and organoarsenic dissolved species were determined by HPLC-ICP-MS, no As containing particles were detected by SP-ICP-MS. Gas condensates from petroleum hydrocarbon samples were analysed by a number of techniques, including SP-ICP-MS, confirming the presence of Hg-containing nanoparticles by direct analysis of the samples diluted in THF.[262]

Scenario 3.3: Analysis of biological samples

The potential exposure of living organisms, including humans, to engineered nanoparticles has led to study their occurrence in such biological systems. Other applications include the detection of wear metal particles from prothesis in human fluids and tissues, as well as nanoparticles biosynthesised by microorganisms. Table 8 summarizes the application under this scenario involving biological samples originally containing nanoparticles. As in scenario 3.2, in most works total element concentrations were determined by ICP-MS and also electron microscopy techniques were applied to obtain complementary information.

Microorganisms. Nanoparticles synthesized by microorganisms from dissolved precursors can be analysed by SP-ICP-MS in a similar way than those internalized from culture media once the microorganisms have been selectively digested, as it has been seen in scenario 2.2. This was the case of selenium-rich yeast,[263] where biogenic-selenium nanoparticles where detected by SP-ICP-MS and confirmed by TEM-EDS, revealing the significance of nanoparticles in the speciation of metals and metalloids in biological systems.

Aquatic organisms. The analysis of aquatic organisms has included plankton,[228] crustaceans,[228] molluscs[228,246,264–266] and fishes.[228] In all cases, prior to SP-ICP-MS analysis, nanoparticles were extracted by digestion of the biological matrices. Enzymatic digestions included the use of pancreatin/lipase,[246,264,265] whereas alkaline digestions were based on the use of TMAH.[228,266] The most studied elements have been Ti[228,246,265] and Ag,[228,246,264] although nanoparticles containing Cu,[246] Zn[246] or different rare earth elements[266] have been also considered. In relation to the information reported, all the articles provided quantitative information of particle mass and number concentration, particle size distribution and mean size. Reported size detection limits and size distributions allowed to confirm that nanoparticle distribution were incomplete in some cases.[246,264,266] Moreover, and although SEM and DLS were used in some studies, these techniques did not provide conclusive information, hence the studies only confirmed the occurrence of particles containing the elements detected and not their specific nature.

Human body fluids and tissues. Although the monitoring of Ag-, Ti- and Si-bearing nanoparticles is supported by the potential exposure to Ag, TiO_2 and SiO_2 engineered nanoparticles,[268,271,272] human fluids and tissues have also been analysed in relation with the release of incidental nanoparticles containing different elements from metal prothesis[269,270] and their migration from wound dressings.[267] Moreover, exhaled breath condensates were analysed to detect the presence of respirable silica particles in quarry workers.[273] In this latter work, the combination of SP-ICP-MS and TEM-EDS allowed to confirm the presence of silica and silicate particles in the breath condensates. Post-mortem tissues (liver, spleen, kidney, intestine) from deceased persons were analysed after enzymatic digestion with proteinase K, providing detailed information about the SiO_2 and TiO_2 found in the tissues and confirmed by SEM-EDS.[271,272] On the other hand, periprosthetic tissues and hip fluids from arthroplasty patients were also analysed by SP-ICP-MS, confirming the presence of particles containing Co, Cr, Ti, V, Al, Ta and Mo and the importance of *in vivo* exposure assessments for realistic appraisal of metal toxicity and associated risks in arthroplasty.[269,270]

Urine[268] and blood[267] samples were analysed directly after dilution with 1% glycerol or ultrapure water, respectively. Whereas particles containing Ti and Ag were detected in urine,

View Article Online
DOI: 10.1039/D1AY00761K

only dissolved Ag was detected in blood from burned patients treated with wound dressings containing Ag nanoparticles.

SP-ICP-MS has also been used with forensic purposes for the direct analysis of gunshot residues.[274] Residues were sampled from the hands of shooters by washing with ultrapure water or swabbing (followed by water extraction from the swabs) to obtain the nanoparticle suspensions, which were analysed directly for screening the presence of Sb-, Ba- and Pb-bearing particles.

Instrumentation and data acquisition

As explained above, SP-ICP-MS was originally developed in commercial quadrupole mass spectrometers with data acquisition frequencies in the range of 1-100 Hz, by using dwell times in the millisecond range. The implementation of single particle detection in quadrupole instruments by manufacturers implied that higher acquisition frequencies became feasible by working at dwell times in the microsecond range, removing the settling time of the quadrupole between readings and improving the capability for transmission and storage of data. Although this new generation of instruments was commercially available since 2014, Tables 2 to 8 show that both ranges of dwell times are being currently used, mostly depending on the availability of instruments, with 45% and 55% of applications using microsecond and millisecond dwell times, respectively. In any case, the duration of the particle events limits the selection of dwell times. Dwell times longer than twice the duration of the events are recommended[17] when working at millisecond dwell times to record the particle events as pulses, whereas for microseconds, they should be shorter than half the duration of the events. Working at dwell times longer than 10 ms increases the number of events corresponding to two or more nanoparticles, whereas dwell times around the duration of a single nanoparticle event (300 µs–1 ms) makes difficult to confirm whether the recorded events correspond to one or more nanoparticles. In any case, an adequate dilution of the sample must be made, if needed, in accordance with the dwell time used, because it also affects to the number concentration linear range.[13] In spite of these constraints, dwell times in the range of 0.5–2 ms have been used in several works, compromising the quality of their results.

The feasibility of using microsecond dwell times with double focusing ICP-MS also depends on the instrument, with last generation instruments capable of working down to 10 µs.[11] In a similar way, a new design of TOF mass spectrometer with a temporal resolution of 33 µs became commercially available recently.[9] In either case, their less widespread use is reflected in the low number of applications found in tables 2-8. The main feature of TOF instruments lies in their simultaneous multi-element capability, recording nearly the whole mass spectrum within each reading. Although applications of SP-TOF-ICP-MS are still scarce, the technique offers unique performance for multi-element and isotope ratio analysis in individual nanoparticles, and for discerning between naturally occurring and engineered nanoparticles.[32] Although multielement SP-ICP-MS with quadrupole instruments has also been reported,[277] it is limited to monitoring up to two isotopes, and is not commercially available yet.

Apart from resolving spectral interferences, double focusing instruments provide better transmission efficiency and hence improved sensitivity with respect to quadrupole and TOF instruments, resulting in the lowest available size LODs.[77] The lower resolution of quadrupole ICP-MS is compensated by using single quadrupole instruments with collision/reaction cells (see Tables 2-8), as well as multipole instruments in MS/MS mode,[145,196,217,235] to reduce polyatomic interferences and improve size limits of detection for nanoparticles containing Ti, Fe, Si or Se. However, the collisions/interactions of the ion cloud generated by each particle with the collision/reaction gases increase the duration of the particle events, affecting the performance of the measurements.[278] In fact, the use of short dwell times instead of collision/reaction cell technologies has been proposed as an alternative for improving size LODs for silica particles.[279]

Sample preparation

When ICP-MS is used in single particle mode, the preservation of most of the properties of the nanoparticles is mandatory, hence sample treatments should be reduced to the minimum required. Apart from the extraction of the nanoparticles from solid samples, sample treatments prior to SP-ICP-MS measurements have been limited to clean-up procedures for removal of large particles or fats, the separation of nanoparticles from dissolved species and the preconcentration of the formers.

As it has been shown in the different scenarios discussed above, extraction of nanoparticles from solid samples can involve just the use of water or aqueous solutions containing surfactants, although 50% methanol has been proposed to avoid the dissolution of copper oxide nanoparticles.[189] However, for more refractory nanoparticles, like TiO_2, SiO_2 or CeO_2, more aggressive treatments based on the use of strong acids and/or hydrogen peroxide have been applied.[83,205,216,230] Nanoparticles from soils and sediments have been often extracted with tetrasodium pyrophosphate,[158,159,163] commonly used to disperse soil heteroaggregates. On the other hand, biological samples require the degradation of the organic matrix by using alkaline reagents, like TMAH, or enzymes. In this regard, enzymatic digestions of plant samples have relied exclusively on the use of macerozyme R-10, a mixture of cellulase, hemicellulase and pectinase, whereas for animal samples, proteinase K has been most often selected, although also mixtures of pancreatin/lipase[224] and amylase[222] have been used. In this regard, there is not a general agreement about the best digestion approach. For example, Loeschner et al.[206] reported that both TMAH and proteinase K provided similar size distributions for gold nanoparticles in animal tissues, although mass recoveries with proteinase K were not quantitative. In contrast, it was shown that enzymatic treatment with proteinase K was more suitable for silver nanoparticles in human placental tissue, as TMAH treatment appeared to change the nanoparticles, most likely by silver ion precipitation and/or nanoparticle aggregation.[280]

Once nanoparticles have been extracted from a solid sample, it is usual to separate the liquid phase containing the nanoparticles from the solid residue to remove large particles that may clog the nebulisers. This is also the case in release and fate studies involving solid materials as well as in the analysis of waters. Both filtration and centrifugation have been used for this purpose, although several authors have reported significant losses of nanoparticles in membrane filters.[126,159,163,245] Thus, filtration should be discouraged unless quantitative recoveries have been proved, therefore settling or centrifugation should be used on a routine basis if removal of large particles is needed. Other clean-up procedures involved the defatting of cosmetics by using hexane.[79,82,84]

The presence of dissolved species of the measured element has a negative effect on the size LODs, hence methods including their removal by ion exchange[55,252] or chelating resins[143] prior to SP-ICP-MS measurements have been reported.

Nanoparticle concentration is not a serious limiting factor for SP-ICP-MS in most scenarios due to its low limits of detection down to 100 particles per millilitre. When lower LODs are required, cloud point extraction has proved to be a valid approach for the isolation and concentration of nanoparticles, while preserving their core size and morphology.[104,132,140,241,256,281] Cloud point extraction involves the addition of a non-ionic surfactant (e.g., Triton X114) at concentrations over the critical micellar concentration, the incorporation of the nanoparticles in the micellar aggregates and the separation of the surfactant phase from the aqueous one by mild heating (ca. 40ºC). Besides the addition of a complexing agent allows the selective extraction of the nanoparticles in the presence of the corresponding cations.[282] Finally, a further dilution of the surfactant phase in a mixture of ethanol and water is required before SP-ICP-MS measurements.

As it has been discussed in the previous section, nanoparticle concentration of the measured suspensions should be low enough to be within the linear range, below 10^7-10^8 L^{-1} depending on the instrumental and acquisition conditions,[13] and hence the adequate dilution of the suspensions must be considered in each case.

Separation techniques coupled to SP-ICP-MS

Separation techniques like asymmetrical flow and centrifugal field flow fractionation, capillary electrophoresis, differential mobility analysis, hydrodynamic chromatography, as well as other chromatography modes (size exclusion, reverse phase, ion exchange) have been coupled to ICP-MS. In this situation, the ICP-MS instrument acts as an element specific detector of inorganic nanoparticles that are separated according to their size, density, surface properties or charge.[283] However, the coupling of an ICP-MS working in single particle mode allows to obtain additional information related to the homo/hetero-aggregation/agglomeration of primary inorganic nanoparticles as well as the element content in complex nanoparticles or nanocomposites, in addition to the information obtained directly through the separation itself.

Although methods based on the online coupling of SP-ICP-MS to HDC,[284] AF4,[285] capillary electrophoresis[286] and DMA[287] have been reported since 2012, most of them must be considered as proofs-of-concept because their applications to complex scenarios are still scarce or absent, as in the case of capillary electrophoresis and DMA.

The online coupling of HDC to SP-ICP-MS was first described by Pergantis et al.[284] for the simultaneous determination of nanoparticle size, number concentration and metal content, by using pristine Au nanoparticles. Subsequently, the capability of HDC-SP-ICP-MS to identify and characterize nanoparticle homoagglomerates in complex media by determining the mass and the hydrodynamic diameter of the separated particles was also demonstrated.[288]

Roman et al.[267] developed an algorithm to deconvolute the SP-ICP-MS signals of dissolved element and nanoparticles separated by HDC, providing information about the concentration of dissolved silver and the distribution of Ag nanoparticles in terms of hydrodynamic diameter, mass-derived diameter, number and mass concentration. The approach was suitable to study quantitatively the dynamics and kinetics of silver nanoparticles in complex biological fluids, including processes such as agglomeration, dissolution and formation of protein coronas. The method was applied to investigate the presence of Ag nanoparticles in the blood of burn patients treated with silver dressings, although only dissolved species were detected.

Under less complex conditions, HDC-SP-ICP-MS has been successfully applied to simultaneously determine both the hydrodynamic radius and the content of Au nanoparticles in liposomes used as carriers of Au nanoparticles.[289] It was possible to distinguish between subpopulations of liposomes with different hydrodynamic diameters and various nanoparticle loads. The application of HDC-SP-ICP-MS to the analysis of river and wastewaters under optimized conditions did not allow to detect silver nanoparticles in the samples, although Cu-containing nanoparticles could be identified.[275]

The feasibility of using AF4 online coupled with SP-ICP-MS to detect and quantify inorganic nanoparticles at environmentally relevant concentrations was firstly investigated by Huynh et al.[285] by using Ag and Ag-SiO_2 core shell nanoparticles. Later on, Hetzer et al.[100] used AF4-SP-ICP-MS to evaluate the migration behaviour of Ag nanoparticles from food packaging films with varying nanosilver content into three different food simulants (water, 3% acetic acid and 10% ethanol), verifying that both silver nanoparticles and silver nanoparticles/polymer heteroaggregates were released in water.

An alternative to online couplings is the analysis of the fractions collected from the effluents of HDC or AF4 by SP-ICP-MS. This was the approach followed by Proulx et al.,[137] who demonstrated the feasibility of using HDC offline coupled to SP-ICP-MS for detecting of 20 nm Ag nanoparticles spiked in a river water sample, as well as by Woo-Chun et al.[290] who analysed tap, river and waste waters spiked with 30, 60 and 100 nm silver nanoparticles. However, the nanoparticle concentrations used in both studies, in the range of mg L^{-1}, were well above those expected in the environment. In a simpler scenario, the content

View Article Online
DOI: 10.1039/D1AY00761K

of metal nanoparticles in composite particles consisting of Au nanoparticles embedded in polymeric particles was determined by using both asymmetrical flow and centrifugal field-flow fractionation.[66] Nanoplastics were separated according to their hydrodynamic diameter and buoyant mass, respectively, and the collected fractions analysed by SP-ICP-MS, confirming the presence of between 1 and more than 8 Au nanoparticles per plastic particle. Under more complex conditions, the SP-ICP-MS analysis of fractions collected from AF4 separations allowed to obtain complementary information about Ag nanoparticles in chicken meat digestates[291] and Al_2O_3 and TiO_2 nanoparticles in toothpaste.[83]

Techniques complementing SP-ICP-MS: Analytical platforms

As it has been highlighted through the previous sections, SP-ICP-MS has opened the way for analysing a variety of samples in different scenarios, allowing the detection of nanoparticles, the determination of their concentrations and their characterization to a certain level. However, SP-ICP-MS shows intrinsic limitations, mainly with respect to morphological characterization (size, shape, aggregation/agglomeration) and composition, therefore SP-ICP-MS is usually complemented by using additional techniques (see column "Complementary techniques" in tables 2-8), leading to advanced analytical platforms which are required for solving complex analytical problems. In the end, the size information provided by SP-ICP-MS has to be estimated from the content of the element directly measured in the particles together with their shape and composition, which must be determined by other complementary techniques; otherwise, these morphological parameters must be assumed and only an equivalent size could be reported. The first purpose of these complementary techniques is to provide additional information on nanoparticle size and shape, to supplement or validate the SP-ICP-MS information. In this way, dynamic light scattering, nanoparticle tracking analysis, and particularly electron microscopy are the most common techniques.

Due to its high spatial resolution, below 1 nm, TEM is one of the most powerful techniques to visualize nanoparticles, and then to obtain information not only about their size, but also shape and aggregation state. This technique is essential in the characterization of pristine nanoparticles (scenario 0), to verify the success of the synthesis of new nanoparticles and to confirm their properties. When more complex analytical scenarios are considered, SEM often substitutes TEM. Current SEM instruments, working with field-emission electron sources (FESEM), offer improved spatial resolutions, reaching competitive ranges for the determination of nanoparticle size and shape in complex samples with easier sample preparation than TEM. Moreover, FESEM provides images of larger sample areas, obtaining more representative size distributions. In any case, electron microscopy plays a significant role to evaluate shapes and possible aggregations of nanoparticles in scenarios 1 and 2, and even in scenario 3 if concentrations of nanoparticles are high enough.

On the other hand, unlike light scattering techniques, electron microscopy enables the determination of the chemical composition of the nanoparticles. Most SEM and TEM instruments include several detectors and are usually coupled to EDS, obtaining elemental composition of the nanoparticles for their identification, allowing the verification of their nature, but also studying their reactivity, stability and transformations. Although EDS is frequently coupled to TEM or SEM in any analytical scenario, other techniques like electron diffraction and electron energy-loss spectroscopy have also been considered to obtain structural information. The use of transmission electron microscopes working in scanning mode (STEM), [83,90,100,126,148,193,259,260,262] with high-angle annular dark-field detection,[46,134,218] allows to obtain Z-contrast images that can also add information about the chemical composition of the nanoparticles.

Even though XAS techniques do not provide information on nanoparticle morphology, they have also been considered in some works[166,182,185,187,226] because of the interest for improving the information about the composition of the nanoparticles in complex samples. Whereas XANES has been used to obtain information on the geometry and oxidation state of the elements,[106,267] EXAFS has done it on element coordination.[226] However, these techniques have been applied occasionally because of their limitations in sensitivity, data interpretation and availability of synchrotron radiation facilities. XRD is also a technique to be considered to obtain structural information of nanoparticles, although limited to pristine nanoparticles (scenario 0) or scenarios in which nanoparticle concentration is not a limitation (scenarios 1 and 2). Finally, the determination of the total element content in the samples under study is included in most works, to evaluate mass balances and recoveries, by using atomic spectrometry techniques (ICP-MS, ICP-OES, AAS) after a suitable digestion step.

SP-ICP-MS based immunoassay and hybridization methods

ICP-MS-based immunoassay methods for determination of biomolecules has gained increasing interest in recent years.[292] Immunoassays are based on the use of an antibody (or antigen) as a biorecognition agent of the analyte of interest, which acts as antigen (or antibody), respectively. Immunoassays are very widely used in clinical diagnostics, environmental and food safety, covering a range of analytes from small molecules to macromolecules. The high selectivity and affinity of an antibody against its antigen allows their specific binding in the presence of complex matrices (e.g., whole blood, serum, urine, foods). Most immunoassays require the labelling of the antibody (or the antigen) with easily detectable markers (e.g., radioisotopes, enzymes, small molecule light absorbers, fluorophores, nanoparticles). ICP-MS immunoassays are based on the use of elemental tags of metal ions, nanoparticles or metal containing polymers. Although element-tagged immunoassays were firstly

proposed in the 1970s,[293] it was not until the advent of ICP-MS that this methodology started to be relevant, largely due to its higher sensitivity in comparison with other atomic spectrometry techniques and its multiplexing capability.[294,295]

The use of metal nanoparticles as labels provides significant advantages, owing to their stability, biocompatibility, and easy conjugation to antibodies/antigens without modifying their binding properties. Moreover, when used in combination with an ICP-MS operated in single particle detection mode a further improvement in sensitivity is achieved. Whereas ICP-MS immunoassays are based on the conventional quantification of the tagging element, reaching detection limits in the range of 50-5000 pg mL^{-1}, these detection limits can be decreased to 1-15 pg mL^{-1} when SP-ICP-MS is used.[292] The improvement lies in the fact that the biomolecule concentration is related to the number concentration of nanoparticles determined by SP-ICP-MS and not to the total content of element measured by ICP-MS.

The first immunoassay based on SP-ICP-MS was reported in 2009. α-Fetoprotein was determined by a competitive immunoassay, using 45 nm Au nanoparticles as labels. A detection limit of 16 pg mL^{-1} was achieved, lower than using other immunoassay strategies.[296] Rabbit-anti-human immunoglobulin G was determined by a sandwich type immunoassay using 45 nm Au nanoparticles with detection limits of 100 pg mL^{-1}.[297] A self-validated homogeneous immunoassay was also proposed for the carcinoembryonic antigen quantification by monitoring both frequency and intensity of the gold nanoparticles used as labels. The method provided accurate results in human serum samples with detection limits in the pM level.[298] ZnSe quantum dots were used for tagging antibodies in a sandwich-type magnetic immunoassay for determination of carcinoembryonic antigen in human serum with a detection limit of 6 pg mL^{-1} by monitoring ^{64}Zn.[299] The determination of cytokeratin fragment antigen 21–1, carbohydrate antigen, and carcinoembryonic antigen was carried out by a simultaneous sandwich-type immunoassay using antibody-immobilized magnetic beads and Au, Ag and ZnSe nanoparticle labels, respectively.[300] The method was successfully applied to detect the three biomarkers in human lung cancer serum samples.

Besides immunoassay, SP-ICP-MS has also been applied in DNA hybridization and RNA methods.[301–304] A homogeneous DNA assay based on a target-induced hybridization chain reaction to achieve controlled spherical nucleic acid assembly has been reported. The strategy relies on the mediation of the hybridization chain reaction in the assembly of a nanogold core with oligonucleotide shell to generate controllable large Au nanoparticle aggregates and significant ^{197}Au counts as compared with the background of a simple dispersed Au nanoparticle. This homogeneous assay could determine DNA within the range of 5 fM to 10 pM.[302]

A rRNA detection platform was achieved by combining a sandwich type hybridization reaction with a single-molecule magnetic capture and SP-ICP-MS for the absolute and relative quantification of *E. coli* rRNA. This method was applied to the direct quantification of rRNA from dangerous human pathogens in milk samples with a detection limit of 10 fM.[304]

Table 9 summarises the SP-ICP-MS based immunoassay and hybridization methods developed up to date. Au nanoparticles have been more frequently used, although methods based on Ag and Pt nanoparticles have also been reported, as well as ZnS quantum dots. Quadrupole instruments have been used in all works, with dwell times in the range of milliseconds, but also at microseconds. In some cases, immunoassay and hybridization schemes use antibody-immobilised magnetic particles, that greatly improve the efficiency of the washing and separating steps of the captured antigens under a magnetic field.[298,302]

View Article Online
DOI: 10.1039/D1AY00761K

Table 9 SP-ICP-MS-based immunoassay and hybridization methods for the quantification of biomolecules.

analyte	sample	assay type	nanoparticle label	dwell time	LOD	ref.
α–fetoprotein	human serum	competitive immunoassay	Au (45 nm)	10 ms	16 pg mL^{-1}	296
rabbit-anti-human IgG	human serum	sandwich immunoassay	Au (45 nm)	10 ms	100 pg mL^{-1}	297
carcinoembryonic antigen	human serum	homogeneous immunoassay	Au (30 nm)	50 µs	210 pg mL^{-1} (1.2 pM)	298
	human serum	sandwich magnetic immunoassay	ZnSe (2.6 nm)	100 µs	6 pg mL^{-1}	299
cytokeratin fragment antigen carcinoembryonic antigen carbohydrate antigen	human serum	sandwich magnetic immunoassay	Au (29 nm) ZnSe (2.6 nm) Ag (14 nm)	100 µs	20 pg mL^{-1} 6 pg mL^{-1} 0.25 mU mL^{-1}	300
DNA	-	homogeneous DNA hybridization	Au (28 nm)	0.5 ms	1 pM	301
	human serum	homogeneous DNA hybridization chain reaction	Au (30 nm)	5 ms	3 fM	302
human immunodeficiency virus hepatitis B virus hepatitis C virus	human serum	multiplexed heterogeneous sandwich DNA hybridization	Au (25 nm) Ag (25 nm) Pt (20 nm)	0.5 ms	< 1 pM	303
E. coli RNA	milk	sandwich hybridization with magnetic particles	Au (30 nm)	-	10 fM	304

View Article Online
DOI: 10.1039/D1AY00761K

Conclusions

The features of SP-ICP-MS for the detection, quantification and characterization of nanoparticles have led to the development of this technique and its increasing application in many different fields under analytical scenarios of varying complexity, which have been comprehensively covered in this review. However, its implementation in commercial instruments by most ICP-MS manufacturers can be considered the key to its success. Despite the rapid evolution of SP-ICP-MS in the last ten years, in 2020 the number of publications related to fundamental aspects of the technique and the development of methods was still 1 out of 3 with respect to the number of publications dedicated to specific analytical applications. For this reason, by following Horlick's approach,[12] although SP-ICP-MS is on the way of becoming a mature technique, its characterization stage cannot be considered finished yet. Moreover, its progress towards maturity is currently hampered by other issues like the availability of validated methods and the traceability of their results. Both issues are conditioned by the availability of reference materials, which are currently restricted to pristine nanoparticles of specific compositions, whereas matrix reference materials are still not available due long-term stability problems.[19] This situation entails using nanoparticle suspensions supplied from a reduced number of manufacturers as standards for calibrations and quality control. Furthermore, since standards for only a small number of nanoparticle compositions are available, indirect calibrations based on the determination of the nebulisation efficiency and the use of dissolved standards are applied routinely to obtain quantitative information. This approach requires that not only the element in dissolved and particulate forms behave in the ICP in the same way, but also the nebulisation for the standards and the samples. These two factors cannot be disregarded to obtain unbiased results, which is particularly challenging when dealing with complex matrices.

The analytical scenarios in which SP-ICP-MS is more frequently applied are those related to studies about fate and (eco)toxicity under controlled laboratory conditions involving the use of pristine nanoparticles (type 2 scenarios). The main reason is that both size and concentration of the nanoparticles added can be selected according to the experiment design and the detection capability, although there is an increasing trend to perform these studies at realistic concentrations. In any case, the most complex challenge for SP-ICP-MS is the analysis of samples originally containing nanoparticles, namely foods and environmental and biological samples (scenarios type 3), because of the complexity of the matrices and the low concentrations expected, but also nano-enhanced products (scenario 1). The main drawback with these samples is that the nature of the particles is unknown in many cases. Consequently, only masses of element per particle or equivalent sizes (assuming an expected composition and shape) can be reported, unless complementary techniques are used to obtain such information. An additional difficulty with this samples arises when part of the particle size distribution is missed due to the attainable size LODs. In such cases, nanoparticle concentrations will be underestimated and mean sizes overestimated. Hence, results should include these limitations, only reporting the occurrence of particles in the sample over a certain (equivalent) size and number concentration, considering SP-ICP-MS as a screening technique instead of a fully quantitative one. On the other hand, particles are not the only targets of SP-ICP-MS, its capability for the simultaneous quantification of dissolved elements has also been exploited in many of the applications involving nanoparticles prone to oxidation or dissolution, like those made of Ag, CuO or ZnO.

Although SP-ICP-MS is mostly involved in methods for the analysis of samples containing nanoparticles, the technique is also suitable for being used in methods where nanoparticles are not analytes but analytical tools. This is the case of immunoassay and hybridization methods for the analysis of biomolecules, where nanoparticles are used as elemental labels conjugated to antibodies and oligonucleotides. By selecting the adequate nanoparticles, SP-ICP-MS can provide better limits of detection for these bioassays due to its high sensitivity in terms of number concentration. The applications of SP-ICP-MS in immuno- and hybridization assays are still scarce but show very promising results.

Author contributions

Eduardo Bolea: Writing - Review & Editing; Maria S. Jimenez: Writing - Original Draft; Josefina Perez-Arantegui: Writing - Original Draft; Juan C. Vidal: Investigation, Writing - Original Draft, Mariam Bakir: Investigation, Writing - Original Draft; Khaoula Ben-Jeddou: Investigation, Writing - Original Draft; Ana C. Gimenez-Ingalaturre: Investigation, Writing - Original Draft; David Ojeda: Investigation, Writing - Original Draft, Celia Trujillo: Investigation, Writing - Original Draft; Francisco Laborda: Conceptualization, Supervision, Visualization, Writing - Review & Editing.

Conflicts of interest

There are no conflicts to declare.

View Article Online
DOI: 10.1039/D1AY00761K

Acknowledgements

This work was supported by the Spanish Ministry of Science, Innovation and Universities and the European Regional Development Fund, project RTI2018-096111-B-I00 (MICINN/FEDER).

K. B.-J. thanks funding from the EU Horizon 2020 programme under the Marie Sklowdowska-Curie grant agreement no. 801586.

A.C.G. thanks the Government of Aragón (DGA) for a predoctoral contract.

C.T. thanks the University of Zaragoza for a predoctoral contract.

List of acronyms

AAS	atomic absorption spectrometry
AES	Auger electron spectroscopy
AFM	atomic force microscopy
AF4	asymmetric flow field flow fractionation
ATR-FTIR	attenuated total reflectance-Fourier transform infrared spectroscopy
AUC	analytical ultracentrifugation
BSA	bovine serum albumin
CE	capillary electrophoresis
CFFF	centrifugal field flow fractionation
CLS	centrifugal liquid sedimentation
CNT	carbon nanotube
CPE	cloud point extraction
DE	dissolved element
DF	double focussing
DGT	diffusive gradient in thin film
DLS	dynamic light scattering
DMA	differential mobility analysis
EDM-HSI	enhanced darkfield microscopy-hyperspectral imaging
EDS	energy dispersive X-ray spectroscopy
ETAAS	electrothermal atomic absorption spectrometry
EXAFS	extended X-ray absorption fine structure
FAAS	flame atomic absorption spectrometry
FESEM	field-emission scanning electron microscopy
FIBSEM	focused ion beam scanning electron microscopy
FTIR	Fourier transform infrared spectroscopy
HAADF	high-angle annular dark-field
HDC	hydrodynamic chromatography
HIM	helium ion microscopy
HPLC	high performance liquid chromatography
HRTEM	high resolution transmission electron microscopy
IC	ion chromatography
ICP-MS	inductively coupled plasms-mass spectrometry
ICP-OES	inductively coupled plasma-optical emission spectrometry
ISE	ion selective electrode potentiometry
LA	laser ablation
LDA	laser diffraction analysis
LOD	limit of detection
MALS	multiangle light scattering
NOM	natural organic matter
NP	nanoparticle
NTA	nanoparticle tracking analysis
Q	quadrupole
RI	refractive index
SAM	scanning Auger mapping
SDS	sodium dodecylsulphate
SEC	size exclusion chromatography
SEM	scanning electron microscopy
SIMS	secondary-ion mass spectrometry
SMPS	scanning mobility particle sizer
SP-ICP-MS	single particle-inductively coupled plasma-mass spectrometry
STEM	scanning transmission electron microscopy
TEM	transmission electron microscopy
TMAH	tetramethyl ammonium hydroxide
TOF	time of flight
TXRF	total reflection X-ray fluorescence
UV-vis	ultraviolet visible absorption
XANES	X-ray absorption near edge structure
XAS	X-ray absorption spectroscopy
XPS	X-ray photoelectron spectroscopy
XRD	X-ray diffraction

References

1 M. D. Montaño, J. W. Olesik, A. G. Barber, K. Challis and J. F. Ranville, *Anal. Bioanal. Chem.*, 2016, **408**, 5053–5074.
2 C. Degueldre and P.-Y. Favarger, *Colloids Surfaces A Physicochem. Eng. Asp.*, 2003, **217**, 137–142.
3 C. Degueldre and P.-Y. Favarger, *Talanta*, 2004, **62**, 1051–1054.
4 C. Degueldre, P.-Y. Favarger and C. Bitea, *Anal. Chim. Acta*, 2004, **518**, 137–142.
5 C. Degueldre, P.-Y. Favarger, R. Rossé and S. Wold, *Talanta*, 2006, **68**, 623–628.
6 C. Degueldre, P. Favarger and S. Wold, *Anal. Chim. Acta*, 2006, **555**, 263–268.
7 F. Laborda, J. Jiménez-Lamana, E. Bolea and J. R. Castillo, *J. Anal. At. Spectrom.*, 2011, **26**, 1362–1371.
8 H. E. Pace, N. J. Rogers, C. Jarolimek, V. A. Coleman, C. P. Higgins and J. F. Ranville, *Anal. Chem.*, 2011, **83**, 9361–9369.
9 O. Borovinskaya, B. Hattendorf, M. Tanner, S. Gschwind and D. Günther, *J. Anal. At. Spectrom.*, 2013, **28**, 226–233.
10 A. Hineman and C. Stephan, *J. Anal. At. Spectrom.*, 2014, **29**, 1252–1257.
11 P. Shaw and A. Donard, *J. Anal. At. Spectrom.*, 2016, **31**, 1234–1242.
12 G. Horlick, *J. Anal. At. Spectrom.*, 1994, **9**, 593–597.
13 I. Abad-Álvaro, E. Peña-Vázquez, E. Bolea, P. Bermejo-Barrera, J. R. Castillo and F. Laborda, *Anal. Bioanal. Chem.*, 2016, **408**, 5089–5097.
14 V. Geertsen, E. Barruet, F. Gobeaux, J.-L. Lacour and O. Taché, *Anal. Chem.*, 2018, **90**, 9742–9750.
15 F. Laborda, E. Bolea and J. Jiménez-Lamana, *Anal. Chem.*, 2014, **86**, 2270–2278.
16 F. Laborda, E. Bolea and J. Jiménez-Lamana, *Trends Environ. Anal. Chem.*, 2016, **9**, 15–23.
17 F. Laborda, A. C. Gimenez-Ingalaturre, E. Bolea and J. R.

Castillo, *Spectrochim. Acta Part B At. Spectrosc.*, 2020, **169**, 105883.

18 D. Mozhayeva and C. Engelhard, *J. Anal. At. Spectrom.*, 2020, **35**, 1740–1783.

19 F. Laborda, A. C. Gimenez-Ingalaturre and E. Bolea, in *Analysis and Characterisation of Metal-Based Nanomaterials*, eds. R. Milacic, J. Scancar, J. Vidmar and H. Goenaga-Infante, Elsevier, 1st editio., 2021.

20 ISO/TC 229, *ISO/TS 80004-2:2015 Nanotechnologies — Vocabulary — Part 2: Nano-objects*, 2015.

21 F. Laborda, C. Trujillo and R. Lobinski, *Talanta*, 2021, **221**, 121486.

22 A. Kéri, A. Sápi, D. Ungor, D. Sebők, E. Csapó, Z. Kónya and G. Galbács, *J. Anal. At. Spectrom.*, 2020, **35**, 1139–1147.

23 N. Joo and H. B. Lim, *Bull. Korean Chem. Soc.*, 2019, **40**, 1087–1092.

24 H.-A. Kim, B.-T. Lee, S.-Y. Na, K.-W. Kim, J. F. Ranville, S.-O. Kim, E. Jo and I.-C. Eom, *Chemosphere*, 2017, **171**, 468–475.

25 N. D. Donahue, E. R. Francek, E. Kiyotake, E. E. Thomas, W. Yang, L. Wang, M. S. Detamore and S. Wilhelm, *Anal. Bioanal. Chem.*, 2020, **412**, 5205–5216.

26 S. V. Jenkins, H. Qu, T. Mudalige, T. M. Ingle, R. Wang, F. Wang, P. C. Howard, J. Chen and Y. Zhang, *Biomaterials*, 2015, **51**, 226–237.

27 K. Flores, R. S. Turley, C. Valdes, Y. Ye, J. Cantu, J. A. Hernandez-Viezcas, J. G. Parsons and J. L. Gardea-Torresdey, *Appl. Spectrosc. Rev.*, 2019, **0**, 1–26.

28 L. C. Jones, E. Soffey and M. Kelinske, *Spectroscopy*, 2019, **34**, 10–20.

29 C. Stephan and R. Thomas, *Spectroscopy*, 2017, **32**, 12–25.

30 B. Meermann and V. Nischwitz, *J. Anal. At. Spectrom.*, 2018, **33**, 1432–1468.

31 R. M. Galazzi, K. Chacón-Madrid, D. C. Freitas, L. F. Costa and M. A. Z. Arruda, *Rapid Commun. Mass Spectrom.*, 2020, **34**.

32 M. D. Montaño, F. Von Der Kammer, C. W. Cuss and J. F. Ranville, *J. Anal. At. Spectrom.*, 2019, **34**, 1768–1772.

33 Z. Gajdosechova and Z. Mester, *Anal. Bioanal. Chem.*, 2019, 4277–4292.

34 F. Abdolahpur Monikh, L. Chupani, M. G. Vijver, M. Vancová and W. J. G. M. Peijnenburg, *Sci. Total Environ.*, 2019, **660**, 1283–1293.

35 G. E. Schaumann, A. Philippe, M. Bundschuh, G. Metreveli, S. Klitzke, D. Rakcheev, A. Grün, S. K. Kumahor, M. Kühn, T. Baumann, F. Lang, W. Manz, R. Schulz and H. Vogel, *Sci. Total Environ.*, 2015, **535**, 3–19.

36 M. Sargent, *J. Anal. At. Spectrom.*, 2020, **35**, 2479–2486.

37 T. P. J. Linsinger, Q. Chaudhry, V. Dehalu, P. Delahaut, a Dudkiewicz, R. Grombe, F. von der Kammer, E. H. Larsen, S. Legros, K. Loeschner, R. Peters, R. Ramsch, G. Roebben, K. Tiede and S. Weigel, *Food Chem.*, 2013, **138**, 1959–66.

38 R. J. B. Peters, G. van Bemmel, N. B. L. Milani, G. C. T. den Hertog, A. K. Undas, M. van der Lee and H. Bouwmeester, *Sci. Total Environ.*, 2018, **621**, 210–218.

39 M. Witzler, F. Küllmer, A. Hirtz and K. Günther, *J. Agric. Food Chem.*, 2016, **64**, 4165–4170.

40 R. J. B. Peters, Z. H. Rivera, G. van Bemmel, H. J. P. Marvin, S. Weigel and H. Bouwmeester, *Anal. Bioanal. Chem.*, 2014, **406**, 3875–3885.

41 P. Ruud JB, U. Anna K, M. Joost, B. Greet van, M. Sandra, B. Hans, N. Peter, S. Wobbe and L. Martijn K van der, *Curr. Trends Anal. Bioanal. Chem.*, 2018, **2**, 74–84.

42 M. Witzler, F. Küllmer and K. Günther, *Anal. Lett.*, 2018, **51**, 587–599.

43 N. Waegeneers, S. De Vos, E. Verleysen, A. Ruttens and J. Mast, *Materials (Basel).*, 2019, **12**, 2677.

44 F. Laborda, A. C. Gimenez-Ingalaturre, E. Bolea and J. R. Castillo, *Spectrochim. Acta Part B At. Spectrosc.*, 2019, **159**, 105654.

45 O. Geiss, I. Bianchi, C. Senaldi, G. Bucher, E. Verleysen, N. Waegeneers, F. Brassinne, J. Mast, K. Loeschner, J. Vidmar, F. Aureli, F. Cubadda, A. Raggi, F. Iacoponi, R. Peters, A. Undas, A. Müller, A. K. Meinhardt, E. Walz, V. Gräf and J. Barrero-Moreno, *Food Control*, 2021, **120**, 107550.

46 E. Verleysen, N. Waegeneers, F. Brassinne, S. De Vos, I. O. Jimenez, S. Mathioudaki and J. Mast, *Nanomaterials*, 2020, **10**, 592.

47 A. R. Montoro Bustos, K. P. Purushotham, A. Possolo, N. Farkas, A. E. Vladár, K. E. Murphy and M. R. Winchester, *Anal. Chem.*, 2018, **90**, 14376–14386.

48 R. Peters, Z. Herrera-Rivera, A. Undas, M. van der Lee, H. Marvin, H. Bouwmeester and S. Weigel, *J. Anal. At. Spectrom.*, 2015, **30**, 1274–1285.

49 S. Weigel, R. Peters, K. Loeschner, R. Grombe and T. P. J. Linsinger, *Anal. Bioanal. Chem.*, 2017, **409**, 4839–4848.

50 R. Peters, Z. Herrera-Rivera, A. Undas, M. Van Der Lee, H. Marvin, H. Bouwmeester and S. Weigel, *J. Anal. At. Spectrom.*, 2015, **30**, 1274–1285.

51 J. W. Olesik and P. J. Gray, *J. Anal. At. Spectrom.*, 2012, **27**, 1143–1155.

52 T. P. J. Linsinger, R. Peters and S. Weigel, *Anal. Bioanal. Chem.*, 2014, **406**, 3835–3843.

53 I. Rujido-Santos, L. Naveiro-Seijo, P. Herbello-Hermelo, M. del C. Barciela-Alonso, P. Bermejo-Barrera and A. Moreda-Piñeiro, *Talanta*, 2019, **197**, 530–538.

54 N. J. Clark, R. Clough, D. Boyle and R. D. Handy, *Environ. Sci. Nano*, 2019, **6**, 3388–3400.

55 L. Fréchette-Viens, M. Hadioui and K. J. Wilkinson, *Talanta*, 2019, **200**, 156–162.

56 S. Wu, S. Zhang, Y. Gong, L. Shi and B. Zhou, *J. Hazard. Mater.*, 2020, **382**, 121045.

57 J. Nelson, A. Saunders, L. Poirier, E. Rogel, C. Ovalles, T. Rea and F. Lopez-Linares, *J. Nanoparticle Res.*, 2020, **22**, 304.

58 J. Noireaux, R. Grall, M. Hullo, S. Chevillard, C. Oster, E. Brun, C. Sicard-Roselli, K. Loeschner and P. Fisicaro, *Separations*, 2019, **6**, 3.

59 F. Laborda and E. Bolea, in *Reference Module in Chemistry, Molecular Sciences and Chemical Engineering*, Elsevier, 2018, pp. 1–9.

60 J. D. Martin, L. Telgmann and C. D. Metcalfe, *Bull. Environ. Contam. Toxicol.*, 2017, **98**, 589–594.

61 H. Zhang, Y. Huang, J. Gu, A. Keller, Y. Qin, Y. Bian, K. Tang, X. Qu, R. Ji and L. Zhao, *New J. Chem.*, 2019, **43**, 3946–3955.

62 R. C. Merrifield, C. Stephan and J. R. Lead, *Talanta*, 2017, **162**, 130–134.

63 A. Kéri, I. Kálomista, D. Ungor, Á. Bélteki, E. Csapó, I. Dékány, T. Prohaska and G. Galbács, *Talanta*, 2018, **179**, 193–199.

64 J.-B. CHAO, J.-R. WANG and J.-Q. ZHANG, *Chinese J. Anal. Chem.*, 2020, **48**, 946–954.

65 I. Kálomista, A. Kéri, D. Ungor, E. Csapó, I. Dékány, T. Prohaska and G. Galbács, *J. Anal. At. Spectrom.*, 2017, **32**, 2455–2462.

66 A. Barber, S. Kly, M. G. Moffitt, L. Rand and J. F. Ranville, *Environ. Sci. Nano*, 2020, **7**, 514–524.

67 S. G. F. Eggermont, A. Rua-Ibarz, K. Tirez, X. Dominguez-

Benetton and J. Fransaer, *RSC Adv.*, 2019, **9**, 29902–29908.
68 R. P. Lamsal, M. S. E. Houache, A. Williams, E. Baranova, G. Jerkiewicz and D. Beauchemin, *Anal. Chim. Acta*, 2020, **1120**, 67–74.
69 K. Walbrück, F. Kuellmer, S. Witzleben and K. Guenther, *J. Nanomater.*, 2019, **2019**, 1–7.
70 S. Meyer, R. Gonzalez de Vega, X. Xu, Z. Du, P. A. Doble and D. Clases, *Anal. Chem.*, 2020, **92**, 15007–15016.
71 S. Salou, C. Cirtiu, D. Larivière and N. Fleury, *Anal. Bioanal. Chem.*, 2020, **412**, 1469–1481.
72 A. Sápi, A. Kéri, I. Kálomista, D. G. Dobó, A. Szamosvölgyi, K. L. Juhász, A. Kukovecz, Z. Kónya and G. Galbács, *J. Anal. At. Spectrom.*, 2017, **32**, 996–1003.
73 R. B. Reed, D. G. Goodwin, K. L. Marsh, S. S. Capracotta, C. P. Higgins, D. H. Fairbrother and J. F. Ranville, *Environ. Sci. Process. Impacts*, 2013, **15**, 204–213.
74 J. Wang, R. S. Lankone, R. B. Reed, D. H. Fairbrother and J. F. Ranville, *NanoImpact*, 2016, **1**, 65–72.
75 P. M. P. Danty, A. Mazel, B. Cormary, M. L. De Marco, J. Allouche, D. Flahaut, J. Jimenez-Lamana, S. Lacomme, M. H. Delville and G. L. Drisko, *Inorg. Chem.*, 2020, **59**, 6232–6241.
76 E. Lahtinen, E. Kukkonen, V. Kinnunen, M. Lahtinen, K. Kinnunen, S. Suvanto, A. Vaïsänen and M. Haukka, *ACS Omega*, 2019, **4**, 16891–16898.
77 M. Hadioui, G. Knapp, A. Azimzada, I. Jreije, L. Frechette-Viens and K. J. Wilkinson, *Anal. Chem.*, 2019, **91**, 13275–13284.
78 Y. Dan, H. Shi, C. Stephan and X. Liang, *Microchem. J.*, 2015, **122**, 119–126.
79 I. de la Calle, M. Menta, M. Klein, B. Maxit and F. Séby, *Spectrochim. Acta - Part B At. Spectrosc.*, 2018, **147**, 28–42.
80 P. J. Lu, S. W. Fang, W. L. Cheng, S. C. Huang, M. C. Huang and H. F. Cheng, *J. Food Drug Anal.*, 2018, **26**, 1192–1200.
81 B. Bocca, S. Caimi, O. Senofonte, A. Alimonti and F. Petrucci, *Sci. Total Environ.*, 2018, **630**, 922–930.
82 C. Adelantado, Á. Ríos and M. Zougagh, *Talanta*, 2020, **219**, 121385.
83 M. Correia, T. Uusimäki, A. Philippe and K. Loeschner, *Separations*, 2018, **5**, 1–25.
84 I. de la Calle, M. Menta, M. Klein and F. Séby, *Talanta*, 2017, **171**, 291–306.
85 F. Laborda, C. Trujillo and R. Lobinski, *Talanta*, 2021, **221**, 121486.
86 Y. Yang, L. Luo, H. P. Li, Q. Wang, Z. G. Yang, Z. P. Qu and R. Ding, *Talanta*, 2018, **182**, 156–163.
87 J. Therkorn, L. Calderón, B. Cartledge, N. Thomas, B. Majestic and G. Mainelis, *Environ. Sci. Nano*, 2018, **5**, 544–555.
88 S. Losert, A. Hess, G. Ilari, N. von Goetz and K. Hungerbuehler, *J. Nanoparticle Res.*, 2015, **17**, 293.
89 J. P. F. G. Helsper, R. J. B. Peters, M. E. M. van Bemmel, Z. E. H. Rivera, S. Wagner, F. von der Kammer, P. C. Tromp, T. Hofmann and S. Weigel, *Anal. Bioanal. Chem.*, 2016, **408**, 6679–6691.
90 A. Hegetschweiler, O. Borovinskaya, T. Staudt and T. Kraus, *Anal. Chem.*, 2019, **91**, 943–950.
91 J. Nelson, M. Yamanaka, F. Lopez-Linares, L. Poirier and E. Rogel, *Energy and Fuels*, 2017, **31**, 11971–11976.
92 B. Bocca, E. Sabbioni, I. Micetic, A. Alimonti and F. Petrucci, *J. Anal. At. Spectrom.*, 2017, **32**, 616–628.
93 B. Battistini, F. Petrucci, I. De Angelis, C. M. Failla and B. Bocca, *Chemosphere*, 2020, **245**, 125667.
94 M. Van Wassenhoven, M. Goyens, E. Capieaux, P. Devos and P. Dorfman, *Homeopathy*, 2019, **108**, 073–074.
95 Y. Echegoyen and C. Nerín, *Food Chem. Toxicol.*, 2013, **62C**, 16–22.
96 A. Mackevica, M. E. Olsson and S. F. Hansen, *J. Nanoparticle Res.*, 2016, **18**, 5.
97 K. Ramos, M. M. Gómez-Gómez, C. Cámara and L. Ramos, *Talanta*, 2016, **151**, 83–90.
98 R. Ding, P. Yang, Y. Yang, Z. Yang, L. Luo, H. Li and Q. Wang, *Food Addit. Contam. Part A*, 2018, **35**, 2052–2061.
99 Y. Echegoyen, S. Rodríguez and C. Nerín, *Food Addit. Contam. Part A*, 2016, **33**, 530–539.
100 B. Hetzer, A. Burcza, V. Gräf, E. Walz and R. Greiner, *Food Control*, 2017, **80**, 113–124.
101 S. Addo Ntim, S. Norris, K. Scott, T. A. Thomas and G. O. Noonan, *Food Control*, 2018, **87**, 31–39.
102 A. Mackevica, M. E. Olsson and S. F. Hansen, *J. Hazard. Mater.*, 2017, **322**, 270–275.
103 A. Mackevica, M. E. Olsson, P. D. Mines, L. R. Heggelund and S. F. Hansen, *NanoImpact*, 2018, **11**, 109–118.
104 L. Torrent, M. Iglesias, M. Hidalgo and E. Marguí, *J. Anal. At. Spectrom.*, 2018, **33**, 383–394.
105 A. Mackevica, M. E. Olsson and S. F. Hansen, *J. Nanoparticle Res.*, 2018, **20**, 6.
106 D. M. Mitrano, E. Lombi, Y. A. R. Dasilva and B. Nowack, *Environ. Sci. Technol.*, 2016, **50**, 5790–5799.
107 J. Farkas, H. Peter, P. Christian, J. A. Gallego Urrea, M. Hassellöv, J. Tuoriniemi, S. Gustafsson, E. Olsson, K. Hylland and K. V. Thomas, *Environ. Int.*, 2011, **37**, 1057–1062.
108 R. S. Lankone, J. Wang, J. F. Ranville and D. H. Fairbrother, *Environ. Sci. Nano*, 2017, **4**, 967–982.
109 N. Neubauer, L. Scifo, J. Navratilova, A. Gondikas, A. Mackevica, D. Borschneck, P. Chaurand, V. Vidal, J. Rose, F. von der Kammer and W. Wohlleben, *Environ. Sci. Technol.*, 2017, **51**, 11669–11680.
110 B. Gomez-Gomez, M. T. Perez-Corona and Y. Madrid, *Anal. Chim. Acta*, 2020, **1100**, 12–21.
111 A. S. Adeleye, E. A. Oranu, M. Tao and A. A. Keller, *Water Res.*, 2016, **102**, 374–382.
112 A. Azimzada, J. M. Farner, M. Hadioui, C. Liu-Kang, I. Jreije, N. Tufenkji and K. J. Wilkinson, *Environ. Sci. Nano*, 2020, **7**, 139–148.
113 M. T. Islam, A. Dominguez, R. S. Turley, H. Kim, K. A. Sultana, M. A. I. Shuvo, B. Alvarado-Tenorio, M. O. Montes, Y. Lin, J. Gardea-Torresdey and J. C. Noveron, *Sci. Total Environ.*, 2020, **704**, 135406.
114 D. P. Martin, N. L. Melby, S. M. Jordan, A. J. Bednar, A. J. Kennedy, M. E. Negrete, M. A. Chappell and A. R. Poda, *Chemosphere*, 2016, **162**, 222–227.
115 Y.-S. Zimmermann, A. Schäffer, P. F.-X. Corvini and M. Lenz, *Environ. Sci. Technol.*, 2013, **47**, 13151–13159.
116 R. S. Lankone, K. Challis, L. Pourzahedi, D. P. Durkin, Y. Bi, Y. Wang, M. A. Garland, F. Brown, K. Hristovski, R. L. Tanguay, P. Westerhoff, G. Lowry, L. M. Gilbertson, J. Ranville and D. H. Fairbrother, *Sci. Total Environ.*, 2019, **668**, 234–244.
117 M. C. Sportelli, R. A. Picca, F. Paladini, A. Mangone, L. C. Giannossa, C. Di Franco, A. L. Gallo, A. Valentini, A. Sannino, M. Pollini and N. Cioffi, *Nanomaterials*, 2017, **7**, 203.
118 N. Shin, K. Velmurugan, C. Su, A. K. Bauer and C. S. J. Tsai, *Environ. Sci. Process. Impacts*, 2019, **21**, 1342–1352.
119 K. Folens, T. Van Acker, E. Bolea-Fernandez, G. Cornelis, F. Vanhaecke, G. Du Laing and S. Rauch, *Sci. Total Environ.*, 2018, **615**, 849–856.
120 Z. Li, M. Hadioui and K. J. Wilkinson, *Environ. Pollut.*,

2019, **247**, 206–215.
121 S. Addo Ntim, T. A. Thomas and G. O. Noonan, *Food Addit. Contam. - Part A Chem. Anal. Control. Expo. Risk Assess.*, 2016, **33**, 905–912.
122 M. Jokar, M. Correia and K. Loeschner, *Food Control*, 2018, **89**, 77–85.
123 X. He, H. Zhang, H. Shi, W. Liu and E. Sahle-Demessie, *J. Am. Soc. Mass Spectrom.*, 2020, **31**, 2180–2190.
124 A. P. Walczak, R. Fokkink, R. Peters, P. Tromp, Z. E. Herrera Rivera, I. M. C. M. Rietjens, P. J. M. Hendriksen and H. Bouwmeester, *Nanotoxicology*, 2012, **7**, 1198–1210.
125 K. Ramos, L. Ramos and M. M. Gómez-Gómez, *Food Chem.*, 2017, **221**, 822–828.
126 D. M. Mitrano, Y. Arroyo Rojas Dasilva and B. Nowack, *Environ. Sci. Technol.*, 2015, **49**, 9665–9673.
127 M. Sikder, J. Wang, B. A. Poulin, M. M. Tfaily and M. Baalousha, *Environ. Sci. Nano*, 2020, **7**, 3318–3332.
128 R. C. Merrifield, C. Stephan and J. Lead, *Environ. Sci. Technol.*, 2017, **51**, 3206–3213.
129 L. Telgmann, M. T. K. Nguyen, L. Shen, V. Yargeau, H. Hintelmann and C. D. Metcalfe, *Anal. Bioanal. Chem.*, 2016, **408**, 5169–5177.
130 J. Jiménez-Lamana and V. I. Slaveykova, *Sci. Total Environ.*, 2016, **573**, 946–953.
131 D. C. Rearick, L. Telgmann, H. Hintelmann, P. C. Frost and M. A. Xenopoulos, *PLoS One*, 2018, **13**, 1–18.
132 L. M. Furtado, M. E. Hoque, D. M. Mitrano, J. F. Ranville, B. Cheever, P. C. Frost, M. A. Xenopoulos, H. Hintelmann and C. D. Metcalfe, *Environ. Chem.*, 2014, **11**, 419.
133 J. D. Martin, P. C. Frost, H. Hintelmann, K. Newman, M. J. Paterson, L. Hayhurst, M. D. Rennie, M. A. Xenopoulos, V. Yargeau and C. D. Metcalfe, *Environ. Sci. Technol.*, 2018, **52**, 11114–11122.
134 A. Urstoeger, A. Wimmer, R. Kaegi, S. Reiter and M. Schuster, *Environ. Sci. Technol.*, 2020, **54**, 12063–12071.
135 F. Loosli, J. Wang, M. Sikder, K. Afshinnia and M. Baalousha, *Sci. Total Environ.*, 2020, **715**, 136927.
136 N. Londono, A. R. Donovan, H. Shi, M. Geisler and Y. Liang, *Nanotoxicology*, 2017, **11**, 1140–1156.
137 K. Proulx and K. J. Wilkinson, *Environ. Chem.*, 2014, **11**, 392–401.
138 D. M. Mitrano, J. F. Ranville, A. Bednar, K. Kazor, A. S. Hering and C. P. Higgins, *Environ. Sci. Nano*, 2014, **1**, 248–259.
139 D. C. António, C. Cascio, Ž. Jakšić, D. Jurašin, D. M. Lyons, A. J. A. Nogueira, F. Rossi and L. Calzolai, *Mar. Environ. Res.*, 2015, **111**, 162–169.
140 A. Wimmer, A. Urstoeger, N. C. Funck, F. P. Adler, L. Lenz, M. Doeblinger and M. Schuster, *Water Res.*, 2020, **171**, 115399.
141 C. Toncelli, K. Mylona, I. Kalantzi, A. Tsiola, P. Pitta, M. Tsapakis and S. A. Pergantis, *Sci. Total Environ.*, 2017, **601–602**, 15–21.
142 C. Toncelli, K. Mylona, M. Tsapakis and S. A. Pergantis, *J. Anal. At. Spectrom.*, 2016, **31**, 1430–1439.
143 P. Cervantes-Avilés, Y. Huang and A. A. Keller, *Water Res.*, 2019, **166**, 115072.
144 T. Lange, P. Schneider, S. Schymura and K. Franke, *Water*, 2020, **12**, 2509.
145 J. Vidmar, P. Oprčkal, R. Milačič, A. Mladenovič and J. Ščančar, *Sci. Total Environ.*, 2018, **634**, 1259–1268.
146 T. Théoret and K. J. Wilkinson, *Anal. Methods*, 2017, **9**, 3920–3928.
147 M. Azodi, Y. Sultan and S. Ghoshal, *Environ. Sci. Technol.*, 2016, **50**, 13318–13327.
148 A. Georgantzopoulou, P. Almeida Carvalho, C. Vogelsang, M. Tilahun, K. Ndungu, A. M. Booth, K. V. Thomas and A. Macken, *Environ. Sci. Technol.*, 2018, **52**, 9431–9441.
149 C. Long, Z. Yang, Y. Yang, H. Li and Q. Wang, *J. Cent. South Univ.*, 2016, **23**, 1611–1617.
150 Y. jie Chang, Y. hsin Shih, C. H. Su and H. C. Ho, *J. Hazard. Mater.*, 2017, **322**, 95–104.
151 J. Kidd, Y. Bi, D. Hanigan, P. Herckes and P. Westerho, *Nanomaterials*, 2019, **9**, 1–14.
152 J. Tuoriniemi, M. D. Jürgens, M. Hassellöv and G. Cornelis, *Environ. Sci. Nano*, 2017, **4**, 1189–1197.
153 S. Alizadeh, S. Ghoshal and Y. Comeau, *Sci. Total Environ.*, 2019, **647**, 1199–1210.
154 S. Alizadeh, A. Abdul Rahim, B. Guo, J. Hawari, S. Ghoshal and Y. Comeau, *Environ. Sci. Technol.*, 2019, **53**, 9148–9159.
155 A. R. Donovan, C. D. Adams, Y. Ma, C. Stephan, T. Eichholz and H. Shi, *Chemosphere*, 2018, **195**, 531–541.
156 Y. Yang, X. Bi, P. Westerhoff, K. Hristovski and J. E. McLain, *Environ. Eng. Sci.*, 2014, **31**, 381–392.
157 L. Torrent, E. Marguí, I. Queralt, M. Hidalgo and M. Iglesias, *J. Environ. Sci. (China)*, 2019, **83**, 205–216.
158 A. H. Jesmer, J. R. Velicogna, D. M. Schwertfeger, R. P. Scroggins and J. I. Princz, *Environ. Toxicol. Chem.*, 2017, **36**, 2756–2765.
159 D. M. Schwertfeger, J. R. Velicogna, A. H. Jesmer, S. Saatcioglu, H. McShane, R. P. Scroggins and J. I. Princz, *Anal. Chem.*, 2017, **89**, 2505–2513.
160 D. Schwertfeger, J. Velicogna, A. Jesmer, H. McShane, R. Scroggins and J. Princz, *Environ. Chem.*, 2017, **14**, 123–133.
161 J. Navratilova, A. Praetorius, A. Gondikas, W. Fabienke, F. von der Kammer and T. Hofmann, *Int. J. Environ. Res. Public Health*, 2015, **12**, 15756–15768.
162 H. El Hadri, S. M. Louie and V. A. Hackley, *Environ. Sci. Nano*, 2018, **5**, 203–214.
163 L. Li, Q. Wang, Y. Yang, L. Luo, R. Ding, Z. G. Yang and H. P. Li, *Anal. Chem.*, 2019, **91**, 9442–9450.
164 L. Degenkolb, G. Metreveli, A. Philippe, A. Brandt, K. Leopold, L. Zehlike, H. J. Vogel, G. E. Schaumann, T. Baumann, M. Kaupenjohann, F. Lang, S. Kumahor and S. Klitzke, *Sci. Total Environ.*, 2018, **645**, 192–204.
165 S. Motellier, D. Locatelli and R. Bera, *Environ. Sci. Technol.*, 2019, **53**, 10714–10722.
166 D. M. Peloquin, E. J. Baumann and T. P. Luxton, *Chemosphere*, 2020, **249**, 126173.
167 K. C. Nwoko, A. Raab, L. Cheyne, D. Dawson, E. Krupp and J. Feldmann, *J. Chromatogr. B Anal. Technol. Biomed. Life Sci.*, 2019, **1124**, 356–365.
168 J. V. Gómez, A. Tarazona, F. Mateo, M. Jiménez and E. M. Mateo, *Food Control*, 2019, **101**, 58–68.
169 S. S. D. Kumar, N. N. Houreld, E. M. Kroukamp and H. Abrahamse, *J. Photochem. Photobiol. B Biol.*, 2018, **178**, 259–269.
170 B. Gomez-Gomez, M. Corte-Rodríguez, M. T. Perez-Corona, J. Bettmer, M. Montes-Bayón and Y. Madrid, *Anal. Chim. Acta*, 2020, **1128**, 116–128.
171 N. Londono, A. R. Donovan, H. Shi, M. Geisler and Y. Liang, *Chemosphere*, 2019, **230**, 567–577.
172 A. Azimzada, N. Tufenkji and K. J. Wilkinson, *Environ. Sci. Nano*, 2017, **4**, 1339–1349.
173 I. Aharchaou, J. S. Py, S. Cambier, J. L. Loizeau, G. Cornelis, P. Rousselle, E. Battaglia and D. A. L. Vignati, *Environ. Toxicol. Chem.*, 2018, **37**, 983–992.
174 H. Klingberg, L. B. Oddershede, K. Loeschner, E. H. Larsen, S. Loft and P. Møller, *Toxicol. Res.*, 2015, **4**, 655–666.

175 M. Logozzi, D. Mizzoni, B. Bocca, R. Di Raimo, F. Petrucci, S. Caimi, A. Alimonti, M. Falchi, F. Cappello, C. Campanella, C. C. Bavisotto, S. David, F. Bucchieri, D. F. Angelini, L. Battistini and S. Fais, *Eur. J. Pharm. Biopharm.*, 2019, **137**, 23–36.
176 A. Abdelkhaliq, M. van der Zande, A. K. Undas, R. J. B. Peters and H. Bouwmeester, *Nanotoxicology*, 2020, **14**, 111–126.
177 A. Abdelkhaliq, M. van der Zande, R. J. B. Peters and H. Bouwmeester, *Part. Fibre Toxicol.*, 2020, **17**, 11.
178 I.-L. Hsiao, F. S. Bierkandt, P. Reichardt, A. Luch, Y.-J. Huang, N. Jakubowski, J. Tentschert and A. Haase, *J. Nanobiotechnology*, 2016, **14**, 50.
179 T. Lammel, A. Mackevica, B. R. Johansson and J. Sturve, *Environ. Sci. Pollut. Res.*, 2019, **26**, 15354–15372.
180 Y. Dan, W. Zhang, R. Xue, X. Ma, C. Stephan and H. Shi, *Environ. Sci. Technol.*, 2015, **49**, 3007–3014.
181 Y. Dan, X. Ma, W. Zhang, K. Liu, C. Stephan and H. Shi, *Anal. Bioanal. Chem.*, 2016, 5157–5167.
182 D. Bao, Z. G. Oh and Z. Chen, *Front. Plant Sci.*, 2016, **7**, 1–8.
183 J. Jiménez-Lamana, J. Wojcieszek, M. Jakubiak, M. Asztemborska and J. Szpunar, *J. Anal. At. Spectrom.*, 2016, **31**, 2321–2329.
184 J. Nath, I. Dror, P. Landa, T. Vanek, I. Kaplan-Ashiri and B. Berkowitz, *Environ. Pollut.*, 2018, **242**, 1827–1837.
185 P. Wang, E. Lombi, S. Sun, K. G. Scheckel, A. Malysheva, B. A. McKenna, N. W. Menzies, F.-J. Zhao and P. M. Kopittke, *Environ. Sci. Nano*, 2017, **4**, 448–460.
186 K. Kińska, J. Jiménez-Lamana, J. Kowalska, B. Krasnodębska-Ostręga and J. Szpunar, *Sci. Total Environ.*, 2018, **615**, 1078–1085.
187 L. Torrent, M. Iglesias, E. Marguí, M. Hidalgo, D. Verdaguer, L. Llorens, A. Kodre, A. Kavčič and K. Vogel-Mikuš, *J. Hazard. Mater.*, 2020, **384**, 121201.
188 J. Wojcieszek, J. Jiménez-Lamana, K. Bierla, M. Asztemborska, L. Ruzik, M. Jarosz and J. Szpunar, *J. Anal. At. Spectrom.*, 2019, **34**, 683–693.
189 S. Laughton, A. Laycock, F. von der Kammer, T. Hofmann, E. A. Casman, S. M. Rodrigues and G. V. Lowry, *J. Nanoparticle Res.*, 2019, **21**, 174.
190 A. A. Keller, Y. Huang and J. Nelson, *J. Nanoparticle Res.*, 2018, **20**, 101.
191 F. Dang, Q. Wang, W. Cai, D. Zhou and B. Xing, *Nanotoxicology*, 2020, **14**, 654–666.
192 W. Y. Zhang, Q. Wang, M. Li, F. Dang and D. M. Zhou, *Nanotoxicology*, 2019, **13**, 1073–1086.
193 Y. Deng, E. J. Petersen, K. E. Challis, S. A. Rabb, R. D. Holbrook, J. F. Ranville, B. C. Nelson and B. Xing, *Environ. Sci. Technol.*, 2017, **51**, 10615–10623.
194 C. C. Li, F. Dang, M. Li, M. Zhu, H. Zhong, H. Hintelmann and D. M. Zhou, *Nanotoxicology*, 2017, **11**, 699–709.
195 M. Hayder, J. Wojcieszek, M. Asztemborska, Y. Zhou and L. Ruzik, *J. Sci. Food Agric.*, 2020, **100**, 4950–4958.
196 J. Wojcieszek, J. Jiménez-Lamana, L. Ruzik, M. Asztemborska, M. Jarosz and J. Szpunar, *Front. Environ. Sci.*, 2020, **8**, 1–12.
197 J. Wojcieszek, J. Jiménez-Lamana, K. Bierła, L. Ruzik, M. Asztemborska, M. Jarosz and J. Szpunar, *Sci. Total Environ.*, 2019, **683**, 284–292.
198 E. P. Gray, J. G. Coleman, A. J. Bednar, A. J. Kennedy, J. F. Ranville and C. P. Higgins, *Environ. Sci. Technol.*, 2013, **47**, 14315–14323.
199 J. G. Coleman, A. J. Kennedy, A. J. Bednar, J. F. Ranville, J. G. Laird, A. R. Harmon, C. A. Hayes, E. P. Gray, C. P. Higgins, G. Lotufo and J. A. Steevens, *Environ. Toxicol. Chem.*, 2013, **32**, 2069–2077.
200 S. Makama, R. Peters, A. Undas and N. W. van den Brink, *Environ. Chem.*, 2015, **12**, 643.
201 M. E. Johnson, S. K. Hanna, A. R. Montoro Bustos, C. M. Sims, L. C. C. Elliott, A. Lingayat, A. C. Johnston, B. Nikoobakht, J. T. Elliott, R. D. Holbrook, K. C. K. Scott, K. E. Murphy, E. J. Petersen, L. L. Yu and B. C. Nelson, *ACS Nano*, 2017, **11**, 526–540.
202 L. D. Scanlan, R. B. Reed, A. V. Loguinov, P. Antczak, A. Tagmount, S. Aloni, D. T. Nowinski, P. Luong, C. Tran, N. Karunaratne, D. Pham, X. X. Lin, F. Falciani, C. P. Higgins, J. F. Ranville, C. D. Vulpe and B. Gilbert, *ACS Nano*, 2013, **7**, 10681–10694.
203 F. Gallocchio, G. Biancotto, A. Moressa, F. Pascoli, T. Pretto, A. Toffan, G. Arcangeli, F. Montesi, R. Peters and A. Ricci, *Food Chem.*, 2020, **323**, 126841.
204 H. K. Sung, E. Jo, E. Kim, S. Yoo, J. Lee, P. Kim, Y. Kim and I.-C. Eom, *Chemosphere*, 2018, **209**, 815–822.
205 F. Abdolahpur Monikh, L. Chupani, E. Zusková, R. Peters, M. Vancová, M. G. Vijver, P. Porcal and W. J. G. M. Peijnenburg, *Environ. Sci. Technol.*, 2019, **53**, 946–953.
206 K. Loeschner, M. S. J. Brabrand, J. J. Sloth and E. H. Larsen, *Anal. Bioanal. Chem.*, 2014, **406**, 3845–3851.
207 R. Tassinari, F. Cubadda, G. Moracci, F. Aureli, M. D'Amato, M. Valeri, B. De Berardis, A. Raggi, A. Mantovani, D. Passeri, M. Rossi and F. Maranghi, *Nanotoxicology*, 2014, **8**, 654–662.
208 R. Álvarez-Fernández García, N. Fernández-Iglesias, C. López-Chaves, C. Sánchez-González, J. Llopis, M. Montes-Bayón and J. Bettmer, *J. Trace Elem. Med. Biol.*, 2019, **55**, 1–5.
209 F. Aureli, M. Ciprotti, M. D'Amato, E. do Nascimento da Silva, S. Nisi, D. Passeri, A. Sorbo, A. Raggi, M. Rossi and F. Cubadda, *Nanomaterials*, 2020, **10**, 888.
210 J. Modrzynska, T. Berthing, G. Ravn-Haren, K. Kling, A. Mortensen, R. R. Rasmussen, E. H. Larsen, A. T. Saber, U. Vogel and K. Loeschner, *PLoS One*, 2018, **13**, 1–22.
211 T. Horváth, A. Papp, N. Igaz, D. Kovács, G. Kozma, V. Trenka, L. Tiszlavicz, Z. Rázga, Z. Kónya, M. Kiricsi and T. Vezér, *Int. J. Nanomedicine*, 2018, **Volume 13**, 7061–7077.
212 L. Campagnolo, M. Massimiani, L. Vecchione, D. Piccirilli, N. Toschi, A. Magrini, E. Bonanno, M. Scimeca, L. Castagnozzi, G. Buonanno, L. Stabile, F. Cubadda, F. Aureli, P. H. B. Fokkens, W. G. Kreyling, F. R. Cassee and A. Pietroiusti, *Nanotoxicology*, 2017, **11**, 687–698.
213 M. van der Zande, R. J. Vandebriel, E. Van Doren, E. Kramer, Z. Herrera Rivera, C. S. Serrano-Rojero, E. R. Gremmer, J. Mast, R. J. B. Peters, P. C. H. Hollman, P. J. M. Hendriksen, H. J. P. Marvin, A. a C. M. Peijnenburg and H. Bouwmeester, *ACS Nano*, 2012, **6**, 7427–7442.
214 F. Gallocchio, G. Biancotto, V. Cibin, C. Losasso, S. Belluco, R. Peters, G. van Bemmel, C. Cascio, S. Weigel, P. Tromp, F. Gobbo, S. Catania and A. Ricci, *J. Agric. Food Chem.*, 2017, **65**, 3767–3774.
215 J. Vidmar, K. Loeschner, M. Correia, E. H. Larsen, P. Manser, A. Wichser, K. Boodhia, Z. S. Al-Ahmady, J. Ruiz, D. Astruc and T. Buerki-Thurnherr, *Nanoscale*, 2018, **10**, 11980–11991.
216 R. J. B. Peters, G. van Bemmel, Z. Herrera-Rivera, H. P. F. G. Helsper, H. J. P. Marvin, S. Weigel, P. C. Tromp, A. G. Oomen, A. G. Rietveld and H. Bouwmeester, *J. Agric. Food Chem.*, 2014, **62**, 6285–6293.
217 S. Candás-Zapico, D. J. Kutscher, M. Montes-Bayón and J. Bettmer, *Talanta*, 2018, **180**, 309–315.
218 E. Verleysen, E. Van Doren, N. Waegeneers, P. J. De

Temmerman, M. Abi Daoud Francisco and J. Mast, *J. Agric. Food Chem.*, 2015, **63**, 3570–3578.

219 O. Geiss, J. Ponti, C. Senaldi, I. Bianchi, D. Mehn, J. Barrero, D. Gilliland, R. Matissek and E. Anklam, *Food Addit. Contam. - Part A Chem. Anal. Control. Expo. Risk Assess.*, 2020, **37**, 239–253.

220 G. Bucher and F. Auger, *J. Anal. At. Spectrom.*, 2019, **34**, 1380–1386.

221 B. Kollander, F. Widemo, E. Ågren, E. H. Larsen and K. Loeschner, *Anal. Bioanal. Chem.*, 2017, **409**, 1877–1885.

222 K. Loeschner, M. Correia, C. López Chaves, I. Rokkjær and J. J. Sloth, *Food Addit. Contam. - Part A Chem. Anal. Control. Expo. Risk Assess.*, 2018, **35**, 86–93.

223 I. de la Calle, M. Menta, M. Klein and F. Séby, *Food Chem.*, 2018, **266**, 133–145.

224 M. V. Taboada-López, P. Herbello-Hermelo, R. Domínguez-González, P. Bermejo-Barrera and A. Moreda-Piñeiro, *Talanta*, 2019, **195**, 23–32.

225 C. Moens, N. Waegeneers, A. Fritzsche, P. Nobels and E. Smolders, *J. Chromatogr. A*, 2019, **1599**, 203–214.

226 M. A. Gomez-Gonzalez, E. Bolea, P. A. O'Day, J. Garcia-Guinea, F. Garrido and F. Laborda, *Anal. Bioanal. Chem.*, 2016, **408**, 5125–5135.

227 C. D. Metcalfe, T. Sultana, J. Martin, K. Newman, P. Helm, S. Kleywegt, L. Shen and V. Yargeau, *Environ. Monit. Assess.*, 2018, **190**, 555.

228 B. Xiao, Y. Zhang, X. Wang, M. Chen, B. Sun, T. Zhang and L. Zhu, *Environ. Sci. Nano*, 2019, **6**, 3431–3441.

229 S. Baur, T. Reemtsma, H.-J. Stärk and S. Wagner, *Chemosphere*, 2020, **246**, 125765.

230 S. P. Bitragunta, S. G. Palani, A. Gopala, S. K. Sarkar and V. R. Kandukuri, *Bull. Environ. Contam. Toxicol.*, 2017, **98**, 595–600.

231 F. Tou, Y. Yang, J. Feng, Z. Niu, H. Pan, Y. Qin, X. Guo, X. Meng, M. Liu and M. F. Hochella, *Environ. Sci. Technol.*, 2017, **51**, 4831–4840.

232 F. Loosli, J. Wang, S. Rothenberg, M. Bizimis, C. Winkler, O. Borovinskaya, L. Flamigni and M. Baalousha, *Environ. Sci. Nano*, 2019, **6**, 763–777.

233 D. T. Maiga, B. B. Mamba and T. A. M. Msagati, *Water Supply*, 2020, **20**, 516–528.

234 A. P. Gondikas, F. Von Der Kammer, R. B. Reed, S. Wagner, J. F. Ranville and T. Hofmann, *Environ. Sci. Technol.*, 2014, **48**, 5415–5422.

235 A. Gondikas, F. von der Kammer, R. Kaegi, O. Borovinskaya, E. Neubauer, J. Navratilova, A. Praetorius, G. Cornelis and T. Hofmann, *Environ. Sci. Nano*, 2018, **5**, 313–326.

236 R. B. Reed, D. P. Martin, A. J. Bednar, M. D. Montaño, P. Westerhoff and J. F. Ranville, *Environ. Sci. Nano*, 2017, **4**, 69–77.

237 A. K. Venkatesan, R. B. Reed, S. Lee, X. Bi, D. Hanigan, Y. Yang, J. F. Ranville, P. Herckes and P. Westerhoff, *Bull. Environ. Contam. Toxicol.*, 2018, **100**, 120–126.

238 L. N. Rand, Y. Bi, A. Poustie, A. J. Bednar, D. J. Hanigan, P. Westerhoff and J. F. Ranville, *Sci. Total Environ.*, 2020, **743**, 140845.

239 D. T. Maiga, H. Nyoni, B. B. Mamba and T. A. M. Msagati, *SN Appl. Sci.*, 2020, **2**, 326.

240 J.-L. Wang, E. Alasonati, M. Tharaud, A. Gelabert, P. Fisicaro and M. F. Benedetti, *Water Res.*, 2020, **176**, 115722.

241 A. Wimmer, A. Kalinnik and M. Schuster, *Water Res.*, 2018, **141**, 227–234.

242 A. R. Donovan, C. D. Adams, Y. Ma, C. Stephan, T. Eichholz and H. Shi, *Chemosphere*, 2016, **144**, 148–153.

243 A. R. Donovan, C. D. Adams, Y. Ma, C. Stephan, T. Eichholz and H. Shi, *Anal. Bioanal. Chem.*, 2016, **408**, 5137–5145.

244 K. Phalyvong, Y. Sivry, H. Pauwels, A. Gélabert, M. Tharaud, G. Wille, X. Bourrat and M. F. Benedetti, *Front. Environ. Sci.*, 2020, **8**, 1–14.

245 I. Jreije, A. Azimzada, M. Hadioui and K. J. Wilkinson, *Molecules*, 2020, **25**, 5516.

246 L. Xu, Z. Wang, J. Zhao, M. Lin and B. Xing, *Environ. Pollut.*, 2020, **260**, 114043.

247 J. Sanchís, J. Jiménez-Lamana, E. Abad, J. Szpunar and M. Farré, *Environ. Sci. Technol.*, 2020, **54**, 3969–3978.

248 R. Vogt, D. Mozhayeva, B. Steinhoff, A. Schardt, B. T. F. Spelz, A. Philippe, S. Kurtz, G. E. Schaumann, C. Engelhard, H. Schönherr, D. K. Lamatsch and J. Wanzenböck, *Sci. Total Environ.*, 2019, **696**, 134034.

249 D. M. Mitrano, E. K. Lesher, A. Bednar, J. Monserud, C. P. Higgins and J. F. Ranville, *Environ. Toxicol. Chem.*, 2012, **31**, 115–121.

250 P. Cervantes-Avilés, Y. Huang and A. A. Keller, *Water Res.*, 2019, **156**, 188–198.

251 J. Tuoriniemi, G. Cornelis and M. Hassellöv, *Anal. Chem.*, 2012, **84**, 3965–3972.

252 M. Hadioui, V. Merdzan and K. J. Wilkinson, *Environ. Sci. Technol.*, 2015, **49**, 6141–6148.

253 S. Bevers, M. D. Montaño, L. Rybicki, T. Hofmann, F. von der Kammer and J. F. Ranville, *Front. Environ. Sci.*, 2020, **8**, 84.

254 L. Li, M. Stoiber, A. Wimmer, Z. Xu, C. Lindenblatt, B. Helmreich and M. Schuster, *Environ. Sci. Technol.*, 2016, **50**, 6327–6333.

255 A. K. Venkatesan, B. T. Rodríguez, A. R. Marcotte, X. Bi, J. Schoepf, J. F. Ranville, P. Herckes and P. Westerhoff, *Environ. Sci. Water Res. Technol.*, 2018, **4**, 1923–1932.

256 A. Wimmer, J. Beyerl and M. Schuster, *Environ. Sci. Technol.*, 2019, **53**, 13293–13301.

257 M. GAJEC, E. KUKULSKA-ZAJĄC and A. KRÓL, *Appl. Ecol. Environ. Res.*, 2020, **18**, 5775–5788.

258 I. De la Calle, P. Pérez-Rodríguez, D. Soto-Gómez and J. E. López-Periago, *Microchem. J.*, 2017, **133**, 293–301.

259 L. N. Rand and J. F. Ranville, *Environ. Sci. Technol.*, 2019, **53**, 11214–11222.

260 R. Kaegi, A. Englert, A. Gondikas, B. Sinnet, F. von der Kammer and M. Burkhardt, *NanoImpact*, 2017, **8**, 73–79.

261 J. R. Huang, P. Li, J. H. Wen, X. Hu, Y. J. Chen, D. H. Yin and H. Z. Lian, *Spectrosc. Lett.*, 2018, **51**, 252–256.

262 D. Ruhland, K. Nwoko, M. Perez, J. Feldmann and E. M. Krupp, *Anal. Chem.*, 2019, **91**, 1164–1170.

263 J. Jiménez-Lamana, I. Abad-Álvaro, K. Bierla, F. Laborda, J. Szpunar and R. Lobinski, *J. Anal. At. Spectrom.*, 2018, **33**, 452–460.

264 M. V. Taboada-López, N. Alonso-Seijo, P. Herbello-Hermelo, P. Bermejo-Barrera and A. Moreda-Piñeiro, *Microchem. J.*, 2019, **148**, 652–660.

265 M. V. Taboada-López, S. Iglesias-López, P. Herbello-Hermelo, P. Bermejo-Barrera and A. Moreda-Piñeiro, *Anal. Chim. Acta*, 2018, **1018**, 16–25.

266 Q. Zhou, L. Liu, N. Liu, B. He, L. Hu and L. Wang, *Ecotoxicol. Environ. Saf.*, 2020, **198**, 110670.

267 M. Roman, C. Rigo, H. Castillo-Michel, I. Munivrana, V. Vindigni, I. Mičetić, F. Benetti, L. Manodori and W. R. L. Cairns, *Anal. Bioanal. Chem.*, 2016, **408**, 5109–5124.

268 K. Badalova, P. Herbello-Hermelo, P. Bermejo-Barrera and A. Moreda-Piñeiro, *J. Trace Elem. Med. Biol.*, 2019, **54**, 55–61.

269 K. Loeschner, C. F. Harrington, J.-L. Kearney, D. J.

Langton and E. H. Larsen, *Anal. Bioanal. Chem.*, 2015, 4541–4554.
270 J. Schoon, S. Geißler, J. Traeger, A. Luch, J. Tentschert, G. Perino, F. Schulze, G. N. Duda, C. Perka and A. Rakow, *Nanomedicine Nanotechnology, Biol. Med.*, 2017, **13**, 2415–2423.
271 R. J. B. Peters, A. G. Oomen, G. van Bemmel, L. van Vliet, A. K. Undas, S. Munniks, R. L. A. W. Bleys, P. C. Tromp, W. Brand and M. van der Lee, *Nanotoxicology*, 2020, **14**, 420–432.
272 M. B. Heringa, R. J. B. Peters, R. L. A. W. Bleys, M. K. van der Lee, P. C. Tromp, P. C. E. van Kesteren, J. C. H. van Eijkeren, A. K. Undas, A. G. Oomen and H. Bouwmeester, *Part. Fibre Toxicol.*, 2018, **15**, 15.
273 E. Leese, J. F. Staff, V. A. Carolan and J. Morton, *Ann. Work Expo. Heal.*, 2017, **61**, 902–906.
274 R. d. Heringer and J. F. Ranville, *Forensic Sci. Int.*, 2018, **288**, e20–e25.
275 K. Proulx, M. Hadioui and K. J. Wilkinson, *Anal. Bioanal. Chem.*, 2016, **408**, 5147–5155.
276 A. Praetorius, A. Gundlach-Graham, E. Goldberg, W. Fabienke, J. Navratilova, A. Gondikas, R. Kaegi, D. Günther, T. Hofmann and F. von der Kammer, *Environ. Sci. Nano*, 2017, **4**, 307–314.
277 M. D. Montaño, H. R. Badiei, S. Bazargan and J. F. Ranville, *Environ. Sci. Nano*, 2014, **1**, 338–346.
278 E. Bolea-Fernandez, D. Leite, A. Rua-Ibarz, T. Liu, G. Woods, M. Aramendia, M. Resano and F. Vanhaecke, *Anal. Chim. Acta*, 2019, **1077**, 95–106.
279 M. D. Montaño, B. J. Majestic, Å. K. Jämting, P. Westerhoff and J. F. Ranville, *Anal. Chem.*, 2016, **88**, 4733–4741.
280 J. Vidmar, T. Buerki-Thurnherr and K. Loeschner, *J. Anal. At. Spectrom.*, 2018, **33**, 752–761.
281 A. Urstoeger, A. Wimmer, R. Kaegi, S. Reiter and M. Schuster, *Environ. Sci. Technol.*, 2020, acs.est.0c02878.
282 J. Chao, J. Liu, S. Yu, Y. Feng, Z. Tan, R. Liu and Y. Yin, *Anal. Chem.*, 2011, **83**, 6875–6882.
283 F. Laborda, E. Bolea, G. Cepriá, M. T. Gómez, M. S. Jiménez, J. Pérez-Arantegui and J. R. Castillo, *Anal. Chim. Acta*, 2016, **904**, 10–32.
284 S. a Pergantis, T. L. Jones-Lepp and E. M. Heithmar, *Anal. Chem.*, 2012, **84**, 6454–6462.
285 K. A. Huynh, E. Siska, E. Heithmar, S. Tadjiki and S. A. Pergantis, *Anal. Chem.*, 2016, **88**, 4909–4916.
286 D. Mozhayeva, I. Strenge and C. Engelhard, *Anal. Chem.*, 2017, **89**, 7152–7159.
287 J. Tan, J. Liu, M. Li, H. El Hadri, V. A. Hackley and M. R. Zachariah, *Anal. Chem.*, 2016, **88**, 8548–8555.
288 D. Rakcheev, A. Philippe and G. E. Schaumann, *Anal. Chem.*, 2013, **85**, 10643–10647.
289 Y. U. Hachenberger, D. Rosenkranz, F. L. Kriegel, B. Krause, R. Matschaß, P. Reichardt, J. Tentschert, P. Laux, N. Jakubowski, U. Panne and A. Luch, *Materials (Basel).*, 2020, **13**, 1–14.
290 W.-C. Lee, B.-T. Lee, S. Lee, Y. S. Hwang, E. Jo, I.-C. Eom, S.-W. Lee and S.-O. Kim, *Microchem. J.*, 2016.
291 K. Loeschner, J. Navratilova, C. Købler, K. Mølhave, S. Wagner, F. von der Kammer and E. H. Larsen, *Anal. Bioanal. Chem.*, 2013, **405**, 8185–8195.
292 R. Liu, P. Wu, L. Yang, X. Hou and Y. Lv, *Mass Spectrom. Rev.*, 2014, **33**, 373–393.
293 M. CAIS, S. DANI, Y. EDEN, O. GANDOLFI, M. HORN, E. E. ISAACS, Y. JOSEPHY, Y. SAAR, E. SLOVIN and L. SNARSKY, *Nature*, 1977, **270**, 534–535.
294 C. Zhang, F. Wu, Y. Zhang, X. Wang and X. Zhang, *J. Anal. At. Spectrom.*, 2001, **16**, 1393–1396.
295 O. I. Ornatsky, R. Kinach, D. R. Bandura, X. Lou, S. D. Tanner, V. I. Baranov, M. Nitz and M. A. Winnik, *J. Anal. At. Spectrom.*, 2008, **23**, 463–469.
296 S. Hu, R. Liu, S. Zhang, Z. Huang, Z. Xing and X. Zhang, *J. Am. Soc. Mass Spectrom.*, 2009, **20**, 1096–103.
297 R. Liu, Z. Xing, Y. Lv, S. Zhang and X. Zhang, *Talanta*, 2010, **83**, 48–54.
298 Z. Huang, C. Wang, R. Liu, Y. Su and Y. Lv, *Anal. Chem.*, 2020, **92**, 2876–2881.
299 Y. Cao, G. Mo, J. Feng, X. He, L. Tang, C. Yu and B. Deng, *Anal. Chim. Acta*, 2018, **1028**, 22–31.
300 Y. Cao, J. Feng, L. Tang, G. Mo, W. Mo and B. Deng, *Spectrochim. Acta - Part B At. Spectrosc.*, 2020, **166**, 105797.
301 G. Han, Z. Xing, Y. Dong, S. Zhang and X. Zhang, *Angew. Chemie Int. Ed.*, 2011, **50**, 3462–3465.
302 B. Li, H. Tang, R. Yu and J. Jiang, *Anal. Chem.*, 2020, **92**, 2379–2382.
303 S. Zhang, G. Han, Z. Xing, S. Zhang and X. Zhang, *Anal. Chem.*, 2014, **86**, 3541–3547.
304 X. Xu, J. Chen, B. Li, L. Tang and J. Jiang, *Analyst*, 2019, **144**, 1725–1730.

View Article Online
DOI: 10.1039/D1AY00761K

The authors belong to the Group of Analytical Spectroscopy and Sensors (GEAS) of the University of Zaragoza. The main research area of the group lies in the development and application of analytical techniques and methods in Nanometrology for the detection, characterization and quantification of natural and engineered nanoparticles. The group has made significant contributions in single particle ICP-MS and flow field flow fractionation hyphenated to ICP-MS. The authors have a long experience in these techniques but also in hydrodynamic chromatography, electron microscopy, as well as X-ray and electroanalytical techniques, which leads to a broad analytical platform for solving complex problems involving nanoparticles and colloids. The group has more than 10 year of experience and 40 publications in this field of Analytical Nanometrology.

View Article Online
DOI: 10.1039/D1AY00761K

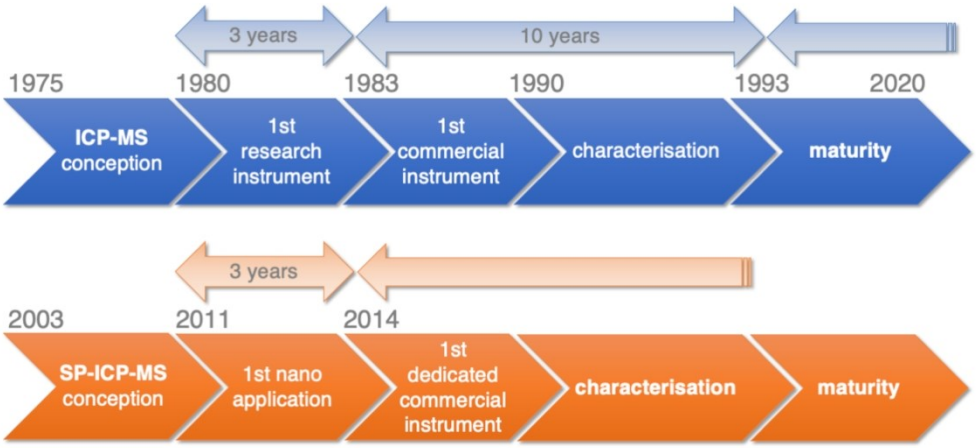

Fig. 1 Comparison of the evolution of SP-ICP-MS with respect to ICP-MS (adapted from Horlick[12]).

99x47mm (600 x 600 DPI)

View Article Online
DOI: 10.1039/D1AY00761K

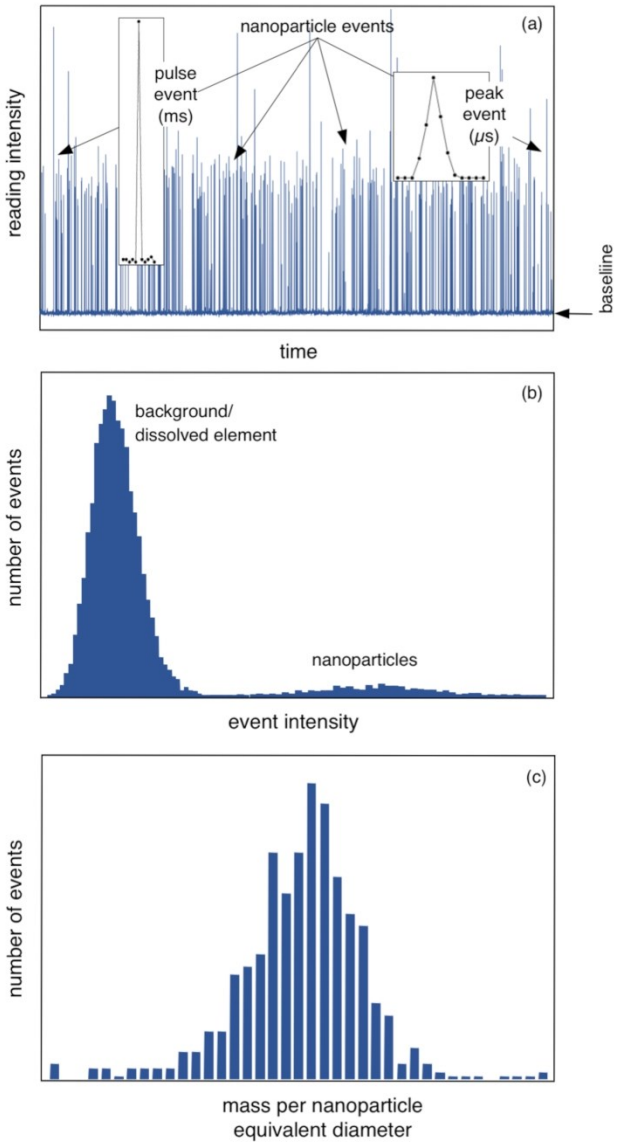

Fig. 2 (a) Time scan of suspension containing nanoparticles and dissolved forms of the same element. (b) Event intensity histogram of data from (a). (c) Mass per nanoparticle/size distribution of spherical nanoparticles calculated from the second intensity distribution in (b).

90x160mm (600 x 600 DPI)

View Article Online
DOI: 10.1039/D1AY00761K

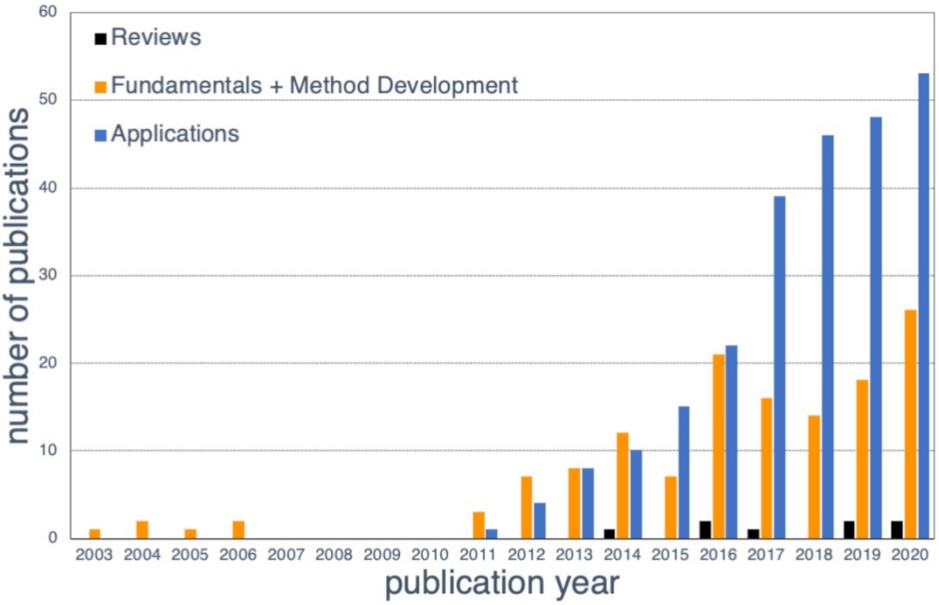

Fig. 3 Evolution of SP-ICP-MS publications related to Reviews, Fundamentals, Method Development and Applications.

99x63mm (600 x 600 DPI)

View Article Online
DOI: 10.1039/D1AY00761K

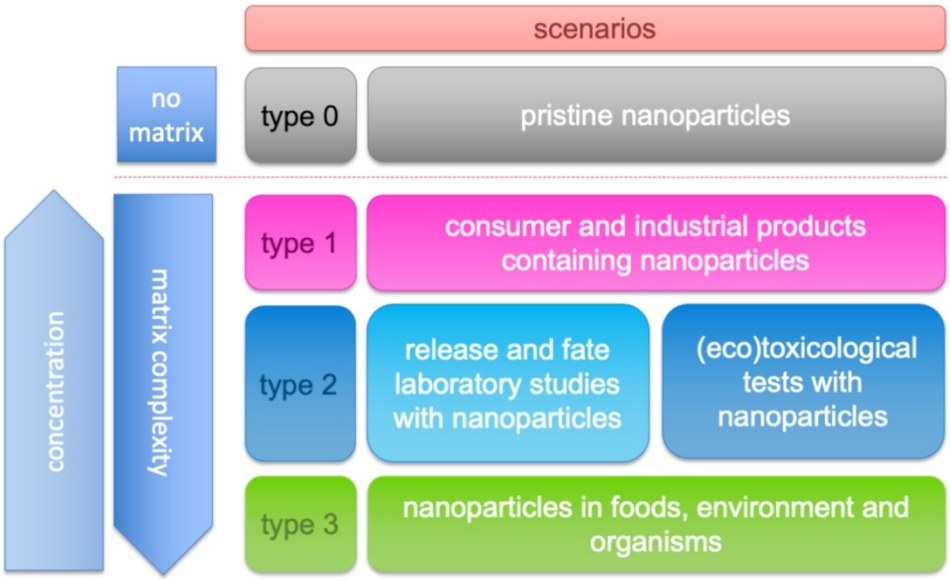

Fig. 4 Analytical scenarios related to nanoparticles (adapted from Laborda et al.[59]).

99x63mm (600 x 600 DPI)

View Article Online
DOI: 10.1039/D1AY00761K

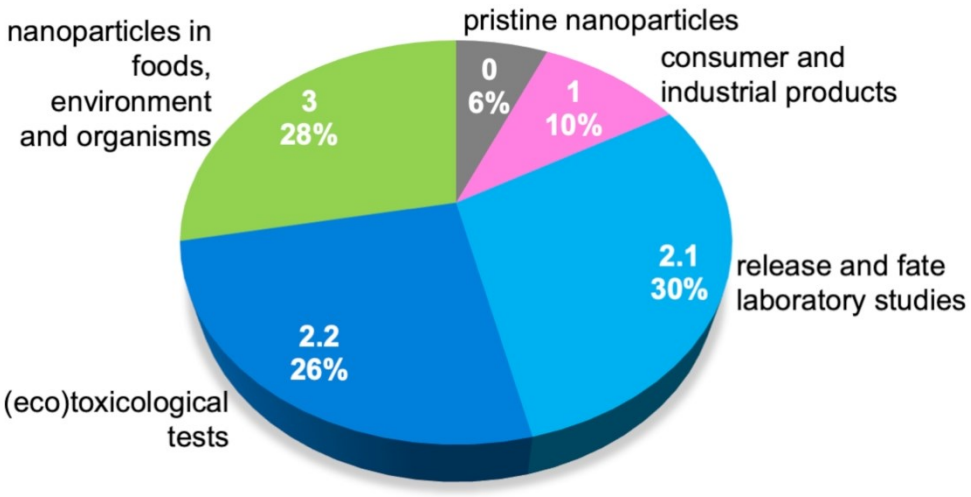

Fig. 5 Distribution of publications related to applications of SP-ICP-MS in different analytical scenarios.

99x56mm (600 x 600 DPI)

View Article Online
DOI: 10.1039/D1AY00761K

Real-world applications of single-particle ICP-MS are comprehensively and critically reviewed.

79x39mm (600 x 600 DPI)